REPORT NO.
UCB/EERC-87/21
DECEMBER 1987

EARTHQUAKE ENGINEERING RESEARCH CENTER

DYNAMIC RESERVOIR INTERACTION WITH MONTICELLO DAM

by

RAY W. CLOUGH
YUSOF GHANAAT
XIONG-FEI QIU

Report to the National Science Foundation

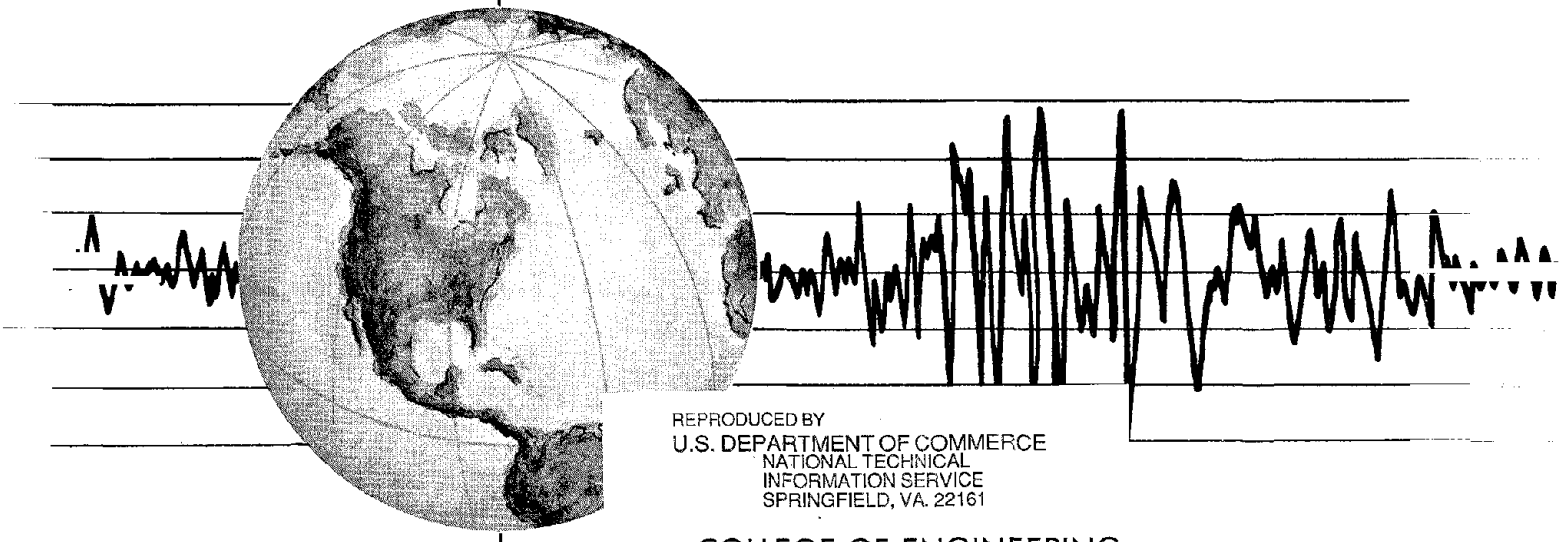

COLLEGE OF ENGINEERING

UNIVERSITY OF CALIFORNIA AT BERKELEY

For sale by the National Technical Information Service, National Bureau of Standards, U.S. Department of Commerce, Springfield, Virginia 22161

See back of report for up to date listing of EERC reports.

DYNAMIC RESERVOIR INTERACTION WITH MONTICELLO DAM

by

Ray W. Clough

Yusof Ghanaat

and

Xiong-Fei Qiu

A Report to the National Science Foundation
on research funded by Grant No. ECE-8512186

Report No. UCB/EERC-87/21
Earthquake Engineering Research Center
College of Engineering
University of California
Berkeley, California

December 1987

ABSTRACT

This study of arch dam-reservoir interaction is an outgrowth of a 4-year U. S. - China cooperative research project on "Interaction Effects in the Seismic Response of Arch Dams." Inconsistent comparisons were obtained in that project between measured and calculated dynamic reservoir pressures induced by shaking tests of arch dams, hence this study was planned to obtain improved understanding of the dynamic interaction mechanism. Monticello Dam, an arch dam in California designed by the U. S. Bureau of Reclamation, was chosen as the test system, and the research involved comparison of hydrodynamic pressures measured during vibration tests with results predicted analytically. A major question for this study was the significance of compressibility of the reservoir water with regard to the interaction forces applied to the dam by the reservoir, so analyses were done both including and neglecting compressibility.

Results of the study showed that hydrodynamic pressures measured at the face of the vibrating dam were in reasonable order-of-magnitude agreement with analytical results. Consideration of compressibility made little difference in this comparison, but it is recognized that the vibration frequencies of the dam and the reservoir differed enough that interaction effects would not be great.

In the final phase of the study, the response of Monticello Dam to an earthquake appropriate to that location was calculated by two computer programs: ADAP-II which neglects compressibility

and EACD-3D which includes it. Comparison of the results shows that reservoir compressibility had little effect on the calculated stresses in the dam if the reservoir boundaries are rigid, but use of the EACD-3D program assuming soft reservoir boundaries led to significant decreases of seismic stress.

TABLE OF CONTENTS

LIST OF TABLES

LIST OF FIGURES

Chapter 1

INTRODUCTION

1.1 Background

In 1981 a four year cooperative research program on "Dynamic Interaction Effects on Arch Dams" was initiated under the U.S. - China Protocol for Scientific and Technical Cooperation in Earthquake Studies. The cooperating institutions were the Scientific Research Institute for Water Conservancy and Hydroelectric Power and Tsinghua University, both of Beijing, China, and the Earthquake Engineering Research Center of the University of California at Berkeley. A major purpose of that investigation was to study the dynamic interaction between arch dams and their reservoirs. The experimental procedure was to excite the natural vibrations of selected arch dams using rotating mass shaking machines, and to measure the resulting hydrodynamic pressures induced in the reservoirs. These measured pressures were then compared with predicted values calculated by dynamic analysis of the reservoir-dam systems.

Two arch dams in China were studied in this way: Xiang Hong Dian (XHD), a gravity dam with cylindrically curved upstream face (1), and Quan Shui (QS), a doubly curved thin shell dam (2). Results of these studies, presented in reports as indicated in the list of References, show that the calculated hydrodynamic pressures agree reasonably well with the measured values for XHD Dam; however, the test data obtained from QS Dam are sig-

nificantly different from the calculated pressures for this doubly curved structure. A discussion of the comparative results for these two cases is presented in Reference (3).

Because the reason for the drastically differing results of the analytical correlation for this second dam was not known, it was decided that an additional research program should be carried out -- concentrating exclusively on the hydrodynamic interaction mechanism. The new research effort was intended to be done similarly to the first two, but in this case funding was requested only from the National Science Foundation to avoid the administrative complexity of a cooperative project. However, the Chinese institutions that had cooperated in the earlier studies were invited to participate in the third test as observers; in addition a Research Assistant from China was employed during the first years of the new project duration to assist with the analytical and field work.

1.2 Monticello Dam

The structure chosen for this third investigation is Monticello Dam, a doubly curved circular arch of uniform thickness along each arch ring. The dam was designed by the U. S. Bureau of Reclamation and construction was completed in 1957 (4). It is 304 ft high, has a crest length of 1,025 ft, the crest thickness is 12 ft and it reaches a maximum thickness of 86 ft at the deepest part of the dam; it is shown in aerial view in Fig. 1.1. This dam was selected partly because it is similar to QS Dam in size and it was hoped that the results might help explain the poor correlation of analysis with experiment obtained in that investigation. Other factors favoring the choice of Monticello Dam

were its location (only about 60 miles from Berkeley) and the fact that the dam already had been studied experimentally (5) and analytically (6) so that some advance knowledge of its dynamic properties was available. However, the previous studies had not dealt directly with the dynamic interaction of dam and reservoir, which is the subject of this new study.

1.3 Objectives

The first objective of this research program was to measure the hydrodynamic pressures induced in the reservoir during harmonic shaking of Monticello Dam, and to compare these results with analytical values obtained by mathematical simulation of the harmonic test procedure. The plan was to perform the calculations first assuming the reservoir water to be incompressible, and then to repeat the analysis taking account of the reservoir compressibility; it was hoped that comparison of these results would demonstrate the importance of compressibility in the dam-reservoir interaction mechanism and thus might explain the poor results obtained at QS Dam.

A second objective of the study was to examine the practical significance of the compressibility effect by calculating the dynamic response of Monticello Dam to an appropriate earthquake excitation -- both considering and neglecting the reservoir compressibility. Only if the compressibility of the liquid caused a significant change in the calculated earthquake stresses could it be considered an important factor in the seismic safety of the dam.

1.4 Report Organization

This report is organized in essentially the same sequence as

the work on the project was done. The analysis of the response of the dam to harmonic shaking is described first, including the predicted vibration properties, the harmonic crest displacements and the harmonic water pressures. This is followed by a brief description of the experimental equipment and test procedures, and also of the reduction techniques used to evaluate the test results. The next chapter presents a comparison of the measured harmonic response results with those predicted analytically. The following chapter briefly describes a new frequency domain computer program (EACD-3D) for taking account of reservoir compressibility in earthquake response analysis of arch dams, and an earthquake input selected for the analysis of Monticello Dam; and then makes a comparison of the stress results obtained when neglecting and when considering the compressibility of the reservoir water. Conclusions concerning the significance of reservoir interaction in the earthquake response analysis of arch dams are presented in the final chapter.

1.5 Acknowledgments

The authors had support and assistance from many individuals and organizations during the course of this investigation, and it was only with this support that it was possible to carry the work to its conclusion. First must be acknowledged the financial support of the National Science Foundation whose Research Grant No. ECE-86-44895 under the management of Dr. S. C. Liu made possible this rather elaborate investigation. The authors appreciate very much the support and encouragement given by Dr. Liu, both during this Monticello Dam research and also during the U. S. - China Cooperative Project that preceded it.

The mobilization of equipment used in the field investigation and the actual field measurement work was managed by Mr. Roy M. Stephens, Principal Development Engineer, and Mr. Richard Parsons, Principal Laboratory Mechanician, both of the University of California at Berkeley, Department of Civil Engineering. Also participating in the field work, as well as in the data reduction and some subsequent analytical studies were Research Assistants Abdulkarim Rinawi and Wu Bing of the Civil Engineering Department. The contributions of all these men were indispensable in the successful completion of the project.

As was mentioned above, the leaders for the Chinese side of the U. S. - China Cooperative Project that preceded this work were invited to act as observers during the field measurements on Monticello Dam. We were pleased that Dr. K. T. Zhang, Vice President of the Council of Tsinghua University, and Mr. Chen Huo-Qun of the Institute for Water Conservancy and Hydroelectric Power Research, both of Beijing, were able to come for this phase of the work. A third observer from China was Dr. Lu Guang-Ping, Director of the Anhui Water Resources Research Institute, Bengbu, Anhui; he also was involved in the studies on XHD Dam during the earlier cooperative research. The authors thank all of these observers for their valuable suggestions and discussion during the field investigation.

Finally we acknowledge with gratitude the permission to test Monticello Dam and the assistance in arranging to make the field measurements that was provided by all authorities responsible for the dam and its management. These include Mr. James N. Moore, Regional Director for the U. S. Bureau of Reclamation in Sacra-

mento and his predecessor Mr. L. F. Hancock, Acting Regional Director. Also involved were USBR engineers Howard Boggs and Clifford Quinton. Additional assistance at the dam site was provided by Darrell Rosenkild, Jay Shepard and Don Burby of the Solano County Irrigation District, as well as by Sammy Gonzalez, Facility Manager of the Lake Berryessa Recreational Area. The authors again express their thanks to all of the aforementioned persons.

Chapter 2

ANALYSIS OF HYDRODYNAMIC INTERACTION

2.1 ADAP Computer Program

The analysis of the dynamic behavior of Monticello Dam followed essentially the same procedures used in the studies of XHD and QS Dams (1,2). The vibration properties first were calculated by means of the basic ADAP program (7) including the incompressible liquid finite element subroutine RSVOIR (8) to model the reservoir interaction, as described in the XHD Dam report (1). Then the extended version of the program was used to calculate the displacement response of the dam and the reservoir hydrodynamic pressures due to the harmonic excitation; these analytical procedures also are described in (1).

2.2 Dam and Foundation Model

The geometry of Monticello Dam is shown by the plan and section views of Fig. 2.1. The mesh generator capability of ADAP was used to define the 56 finite elements that model the concrete arch; of these, 30 thick-shell elements represent the interior region and 26 3D shell elements form the interface region that makes contact with the foundation rock. A perspective view of the dam finite element mesh is shown in Fig. 2.2.

The foundation rock in the immediate vicinity of the dam was modeled by the ADAP Type 1 coarse foundation mesh (1,7); it was generated automatically by the ADAP program except for minor adjustment of the topography adjacent to the canyon rim. One

hundred and twelve (112) 8-node solid elements were used in this mesh, which was constructed using semicircular planes cut into the canyon wall in the direction normal to the dam-foundation contact surface. A perspective view of half the foundation model is shown in Fig. 2.3, in which it is seen that six nodes spaced equally around the semicircular planes define the boundary of the foundation model; these nodes are fixed in position because it is assumed that the rock beyond this region is rigid.

2.3 Reservoir Model

It is apparent in the aerial view of the dam and reservoir shown in Fig. 1.1 that the reservoir has a very irregular geometry, due to the rough topography of the valley in which it is located. The main features of this topography were modeled by the liquid finite element mesh, as shown by the plan and isometric views in Fig. 2.4. Four layers of-16 node isoparametric liquid finite elements in the upstream direction were used to construct the model, with the nodes matching those at the face of the dam; the total number of these elements was 224. In addition, a layer of 8 node curvilinear two-dimensional isoparametric elements (56 in number) was provided at the dam face to provide for convenient definition of the interface hydrodynamic pressures. The upstream boundary of the reservoir model was taken as a vertical rigid plane located about 900 ft from the dam face; similarly the reservoir bottom was assumed to be rigid. It will be noted that the reservoir model satisfies the customary modelling criterion of a length to depth ratio of three.

2.4 Analysis of Vibration Properties

To evaluate the vibration properties of the dam-reservoir

system, the standard ADAP eigenproblem solver was used. First the mass and stiffness properties of the dam and foundation rock elements were calculated by the ADAP subroutines. In this analysis, the concrete was modeled using the material properties adopted by the U. S. Bureau of Reclamation (6):

Modulus of Elasticity	$E = 5.1 \times 10^6$ psi
Poisson's Ratio	$\upsilon = 0.2$
Unit Weight	w = 150 pcf

For the rock, the modulus and Poisson's ratio were the same as for the concrete; but the mass of the rock was neglected as is customary in ADAP analyses.

For the reservoir, it was assumed that the surface level was at elevation 433 ft, as it was at the time of the 1966 test program (5), and the water was assumed to be incompressible. The pressures at internal nodes of the model were condensed out, leading to the formulation of added mass quantities for the interface nodes. These added masses were then combined with the concrete masses defined for the same nodes.

With the system completely defined by the dam-foundation stiffness matrix, and the dam-reservoir mass matrix, the resulting eigenproblem was solved to obtain the vibration mode shapes and frequencies. Three distinct cases were considered, depending on whether the reservoir and/or the foundation were included in the mathematical model; this resulted in three sets of frequencies as shown in Table 2.1. In the basic case "a", the dam alone was analyzed; in case "b", the additional flexibility of the foundation rock was included, leading to lowered frequencies; applying the added mass of the reservoir in case "c"

caused a further frequency reduction. Mode shapes also were calculated in these analyses, but they will be discussed later in comparison with the measured shapes.

2.5 Adjustment of Concrete Modulus

The calculated frequencies for the complete system (case "c") shown in Table 2.1 are significantly higher than those measured during the 1966 test program (shown in the last column of Table 2.1), and since the mass used in the analysis cannot be greatly in error it is evident that the modulus of elasticity adopted for the analysis is too large. To determine an appropriate adjustment, the modulus of elasticity required to give exact agreement between the calculated and the measured frequency was calculated for each mode, using a proportional adjustment as described in Reference (1) (p. 44). Then the average of the modulus values calculated for the first three modes ($E = 4.141 \times 10^6$ psi) was taken as the best estimate for the present analysis. Using this modulus and the 433 ft water level, frequencies were calculated for the first seven modes, as listed in the second column of Table 2.2. These compare very well with the 1966 measured values shown in column 4, as must be the case for the first three modes because they were the basis for choosing the modulus. It is believed that the large discrepancy in the results for Mode 5 is due to the fact that the measured frequency was not for Mode 5 (as will be discussed later).

Because it was expected that the reservoir would be at a lower level by the time when the 1986 test was to be done, another frequency analysis was performed for an assumed water level of 420 ft. Results of this analysis, shown in Col. 3 of

Table 2.2, indicate the expected increase of frequency with reduced reservoir interaction. As a matter of fact, however, surprisingly heavy rains fell during spring 1986, so that the actual water level at the time of the 1986 tests was 436 ft; consequently a subsequent analysis was done for this water level, with results as described in Chapter 5.

2.6 Forced Harmonic Response of Dam

The primary experimental objective of this research was to measure the hydrodynamic pressures induced during harmonic shaking tests of the dam, so an analytical simulation of the proposed shaking tests was performed to obtain estimates of the expected pressure data. In the analyses, the two shaking machine loads were positioned at finite element nodes on the dam crest and oriented in the radial direction; the node locations were chosen such that significant excitation would be provided in each of the lower mode shapes (see inset of Fig. 2.5). The force output applied by each of the two shakers, plotted as a function of excitation frequency for various eccentric weight combinations, is shown in Fig. 2.6 (9). The heavy solid line segments in this graph indicate the weight combinations intended to be used in this test so that relatively high forces could be achieved over the desired frequency range.

Applying the appropriate forces analytically by means of the FORCEVB subroutine developed in the cooperative research program (Ref. 1, p. 33), the response of the dam crest was calculated for the frequency range of the first six modes. The subroutine uses the mode-superposition procedure, and takes account of the three modes with frequencies closest to the excitation frequency; the

damping values measured in the 1966 tests (5) were specified for each mode. The resulting frequency response curves for crest nodes having the largest motions are shown in Fig. 2.5, calculated for the case with the reservoir level at 420 ft.

2.7 Forced Hydrodynamic Reservoir Pressures

Using the additional subroutine FVHYDRO, developed in the previous cooperative research (Ref. 1, p. 35), the hydrodynamic pressures at the face of the dam were calculated from the nodal displacements given by FORCEVB. First these pressures were determined using the pressure-acceleration coefficient matrix that was derived in evaluating the added mass matrix for an incompressible reservoir. Then the coefficient matrix was modified to account for the frequency effect at the specified excitation frequencies, and pressures at the face of the dam were again determined from the calculated face node accelerations.

Pressures calculated at the face of the dam due to excitation at the frequencies of the first four modes are shown in Fig. 2.7. These figures show that the compressible liquid (heavy solid lines) develops somewhat higher pressures at these frequencies than does the incompressible liquid (light solid lines). Corresponding results calculated at the finite element nodal section about 98 ft from the dam face are shown in Fig. 2.8. It must be emphasized that the plotting scale here is different from that in Fig. 2.7; the pressures are reduced by about two orders of magnitude at a distance of 98 ft. Study of these two figures tends to suggest that the influence of compressibility on the hydrodynamic pressures is relatively greater at some distance into the reservoir, as compared with the dam face

location.

By far the most significant information demonstrated by the results shown in Figs. 2.7 and 2.8 is the reduction of dynamic pressure by two orders of magnitude in a distance of 98 ft. Even more important than the distance is the fact that the reduced pressures are evaluated at the first liquid element node within the reservoir, thus the reduction appears to be an artifact of the finite element model rather than of the physical phenomenon. For this reason, detailed study of the calculated pressures within the reservoir is not considered to be meaningful; further comments on this point will be made in Chapter 4, in discussing the comparison of calculated and measured results. On the other hand, it must be remembered that the interaction effect of the reservoir on the dam is associated with pressures developed at the dam face, so reliable prediction of pressures within the reservoir is not of great practical significance.

2.8 Supplementary Analyses with Rigid Dam

In order to emphasize the influence of water compressibility on the dynamic behavior of the reservoir and to exclude the effects of dam deformations, an additional set of analyses was done in which it was assumed that the dam was rigid and was subjected to harmonic motion in the upstream-downstream direction. Thus, in these calculations it was assumed that every node at the face of the dam had identical harmonic motion in the specified direction.

The resulting variation with excitation frequency of the hydrodynamic pressure amplitude at the centerline base of the dam face (i.e. the pressure-frequency response curve) is shown in

Fig. 2.9. In this graph, the dynamic pressures are expressed as a ratio to the static pressure at the same point (which is the zero frequency pressure). The frequencies are expressed as ratios to the fundamental frequency of vertical wave propagation in a uniform depth reservoir extending to infinity. It will be noted in this graph that the first resonant frequency for the Monticello reservoir has a frequency ratio of about 1.3; this demonstrates that the effective (or average) depth of the V-shape channel is noticeably less than the maximum depth. For comparison the ratios representing the natural frequencies of the flexible dam with incompressible reservoir also have been marked in the figure. They are seen to be considerably lower than the first reservoir frequency with rigid dam, which suggests that interaction may be expected to have little effect on the behavior of the actual system in which flexibility is present in both dam and reservoir.

Chapter 3

EXPERIMENTAL EQUIPMENT AND PROCEDURES

3.1 General Comments

The experimental study of Monticello Dam-reservoir interaction was carried out by procedures similar to those used in the U. S. - China cooperative study (1,2). However, because the study in this case was focused exclusively on the dynamic reservoir pressures, much less effort was devoted to measurement of the dam vibrations and no measurements were made of the foundation rock motions. The shaking equipment used in this investigation was not the same as had been used in China (1,2), but it actually was the same pair of rotating mass shakers that had been used in the 1966 USBR study of Monticello Dam (5). These were two of the group of four shakers developed at the California Institute of Technology under direction of a committee of Earthquake Engineering Research Institute members (9), and this pair have been under the management of the College of Engineering, University of California at Berkeley since the early 1960's. However, a new digital electronic control unit was designed and built at the University of California in the early 1980's to provide greater convenience and precision in their operation.

3.2 Rotating Mass Shakers

The two U.C. harmonic shakers have a force capacity of 5,000 lb each and a test frequency range up to 10 Hz. The force developed as a function of frequency for each of various combina-

tions of eccentric weights is given by the curves of Fig. 2.7; the heavy line segments of the curves show the weight combinations actually used in the various frequency ranges during this Monticello test program. Based on the prior knowledge of the dam's lower mode shapes (5,6), the positions at which the shakers were bolted to the dam crest were selected as shown in Figs. 2.5 and 3.1. Using these locations, it was hoped that significant response would be developed in all of the dam's lower vibration modes, by using in-phase and out-of-phase operation for the symmetric and antisymmetric modes, respectively.

It may be worth noting that the d-c motor drives of these shaking machines experienced some failures during the test program, each of them burning out on separate occasions. The failures were due, in part, to trying to operate them at higher than the specified voltage; in addition, continued operation at high speeds during periods of very high air temperatures was a contributing factor. These failures caused important delays in the test schedule and eventually led to elimination of some less significant phases of the planned test program. However, because it was possible to borrow replacement motors and to arrange for expeditious repairs, the ultimate impact of the failures on the objectives of the test program was not severe.

3.3 Vibration Transducers

Even though the dynamic behavior of the dam was not of primary concern in this investigation, it was necessary to measure its vibratory response in order to validate the analysis of hydrodynamic pressures predicted due to the shaking tests. The transducers used in measuring the forced vibrations of the

dam were Statham Model A linear accelerometers with a maximum rating of 0.25g. A total of 15 stations for measuring accelerations in the radial direction were located at nearly equal arc distance intervals along the crest of the dam, as shown in Fig. 3.1. These stations were approximately at the contraction joints between the concrete monoliths; also they coincided with the nodes of the finite element mesh shown in Fig. 2.2. Because only 8 accelerometers were available, these were positioned initially at alternate stations (a,c,e....); then in a subsequent test sequence they were moved to the remaining stations (b,d,f....). The gage at station "g" was left in place during both test sequences to provide quantitative correlation between both sets of data.

Ambient vibrations also were measured during a preliminary data acquisition sequence in order to verify that the vibration mode shapes and frequencies had not changed materially since the 1966 investigation. For this purpose a set of 8 Ranger seismometers was deployed at alternate stations (a,c,e....) oriented in the radial direction. These were the same very sensitive instruments used to measure foundation motions in the previous tests in China, and they provided valid data from the ambient vibrations as hoped. Because their results showed no important differences from the data obtained during the forced vibration studies, the ambient test data were not utilized in this investigation, but the frequencies obtained from the ambient measurements are listed later, in Table 4.1.

3.4 Pressure Transducers

The dynamic pressure measurements were made during this

project with the same type of piezoelectric gages used in the China studies: Kistler Model 206 Piezotron low pressure, high sensitivity transducers. To provide waterproofing and to protect them from damage, the gages were encased in cylinders machined from blocks of stainless steel; to facilitate their positioning at the designated measurement points, the eight gages were assembled in two groups of four with the four cables of each group bundled together.

The stations at which dynamic pressures were measured are shown in Fig. 3.2; the plan positions are indicated in part "a" of the figure, while the vertical section through the center of the dam, shown in part "b", indicates their vertical positions. The four gages in each gage group were assembled with lengths of their cables differing by 50 ft increments so that when the gage with the longest cable was suspended at 250 ft elevation, the other three gages were at elevations of 300 ft, 350 ft and 400 ft, respectively, as indicated in the figure. The reservoir surface at the time of the test was 436 ft, so the deepest gage was at a depth of 186 ft during these measurements.

Gages located at the face of the dam were installed by merely suspending them from the dam crest at the stations shown in Fig. 3.2(a). To install the gages out in the reservoir, a cable was stretched between anchor points on the rocky ridges at each side of the reservoir; then a second cable was attached between the middle of this cable and the face of the dam. This fixed support cable system also is shown in Fig. 3.2(a). A boat was used to transport the gage group assemblies so that they could be attached to the support cables at the positions and

elevations shown in Fig. 3.2(b). Note that these pressure stations were located at nodal points of the liquid finite element reservoir model (Fig. 2.4) to facilitate correlation between the measured and calculated pressures.

3.5 Data Acquisition System

In contrast to the previous forced vibration tests done by the EERC (including those done during the cooperative tests in China), the vibration data obtained in this investigation were recorded in digital form. The recording system was controlled by an IBM PC-AT microcomputer, and the analog signals from the transducers were converted to digital form by means of a Keithley A/D converter. During this study, up to 16 channels of data could be recorded simultaneously; additional channels can be provided in the acquisition system in the future, if desired. A software package manages the acquisition procedure, processes the data as desired, and presents it in a specified format.

Another important part of the data acquisition equipment was a Rockland Spectrum Analyzer Model 512-18; this is the same unit that was brought to China for use on the cooperative dam studies (1,2). It was used "on line" during the Monticello tests to determine directly the amplitude of response for selected channels at each test frequency. By study of the variation of these amplitudes with successively changed frequencies, it was a simple matter to determine the peak response frequency for each mode of vibration, and the corresponding peak response amplitude.

The control system for the rotating mass shakers and all of the data acquisition units were housed in a portable field office structure that was parked at the center of the dam crest.

3.6 Test Procedure

Although the forced vibration measurement procedures were equivalent in principle to what had been done in the tests performed in China (1,2), many details were modified to take advantage of the digital recording system. Also, because the modal frequencies were known with reasonable accuracy, it was not necessary to record the forced vibration response over the entire frequency range. Instead a sequence of suitable frequencies was specified at a convenient frequency increment, usually 0.05 Hz or 0.025 Hz, ranging from below to above the expected modal frequency.

To carry out the test for each modal frequency, the shaking machine digital controller was set to the first frequency of the specified sequence and the Rockland frequency analyzer was connected to a transducer channel expected to show significant response in the mode under consideration. When the amplitude of the Rockland measurement stabilized at the selected frequency, indicating that the dam was responding fully to the shaker excitation, the IBM data acquisition system was turned on. Twenty two seconds of vibration data were recorded simultaneously from each of the transducer channels being monitored, at a rate of 50 samples per second. The shaking machines were then set to the next specified frequency and the process was repeated; the measurements continued in this way until all frequencies of a given modal sequence had been treated.

Frequency response data were obtained by this procedure for the first six modal frequencies identified in the 1966 USBR tests

(5), setting the shakers for in-phase or out-of-phase operation as required to produce the desired symmetric or antisymmetric mode shapes. As was noted earlier, there were not sufficient data recording channels to use all of the pressure and acceleration transducers at once, so the entire sequence of measurements was repeated until the desired pressures and accelerations had been recorded at all designated stations.

3.7 Data Reduction Procedure

The digital dynamic response data recorded from each transducer channel in this investigation represented the discrete values of the response quantity (acceleration or pressure) sampled at the rate of 50 readings per second from an analog signal varying harmonically at the frequency imposed by the shaking machines. For the purpose of this study, only the amplitude of each harmonic signal at the test frequency was of interest, so this was determined by taking the Discrete Fourier Transform of the digital data sequence. The transformation was performed by the data acquisition software, using a sequence of 1,024 discrete data points recorded at a time interval of 0.02 second; thus the period of the measured data was $T = 20.48$ seconds.

The results of the Fourier transformation were the amplitudes of 1,024 harmonics of the test signal, with a frequency increment $f = 1/T = 0.0488$ Hz. Of course, the bulk of the response energy was concentrated about the excitation frequency, but in general the excitation frequency did not correspond with any of the transformation harmonics. Hence it was necessary to apply a correction to account for the "leakage" of energy from the test frequency to the adjacent discrete transform

frequencies. The result of this reduction and correction procedure was a single amplitude value for the response quantity at each of the test frequencies. The data points connected by straight lines shown in Figs. 3.3 to 3.7 are the experimental frequency response curves obtained in this way for radial accelerations measured at selected points on the crest of the dam.

The purpose of the construction of these response curves was to determine the amplitude of response at the peak response frequency for each mode; using such data taken from all transducer stations it would then be possible to construct the mode shape corresponding to each peak frequency. However, it is clear that considerable judgment would be needed to identify the peak response frequency amplitude from these irregularly shaped response curves. For that reason it was decided to use a least squares procedure to fit a single degree of freedom (SDOF) response curve to the measured frequency response data as described in the following.

The amplitude of response V_i for a SDOF system excited at frequency $\bar{\omega}_i$ may be written:

$$V_i = \frac{P_0 / K}{\sqrt{(1-\beta_i^2)^2 + (2\xi\beta_i)^2}} \qquad (3.1)$$

where P_o/K = C is the response constant (to be calculated)

$\beta_i = \frac{\bar{\omega}_i}{\omega_o}$ is the ith exciting frequency ratio

ω_o = natural vibration frequency of system (estimated as peak response frequency

from the test data)

ξ = damping ratio (to be calculated)

Squaring both sides and rearranging, this can be written:

$$4V_i^2\beta_i^2\xi^2 - C^2 = - V_i^2 (1-\beta_i^2)^2$$

An equation like this can be written for each exciting frequency for which the response V_i has been measured. Thus a set of such equations can be written for all the test frequencies $\bar{\omega}_i$, where i = a, b, c,.... and arranged as follows:

$$\begin{bmatrix} 4V_a^2\beta_a^2 & -1 \\ 4V_b^2\beta_b^2 & -1 \\ 4V_c^2\beta_c^2 & -1 \\ \cdot & \cdot \\ \cdot & \cdot \end{bmatrix} \begin{Bmatrix} \xi^2 \\ C^2 \end{Bmatrix} = - \begin{bmatrix} V_a^2 (1-\beta_a^2)^2 \\ V_b^2 (1-\beta_b^2)^2 \\ V_c^2 (1-\beta_c^2)^2 \\ \cdot \\ \cdot \end{bmatrix} \tag{3.2}$$

This may be represented symbolically as:

$$\underline{A}\ \underline{x} = \underline{B} \tag{3.3}$$

Now, applying the least squares procedure to Eq. 3.3, it may be reduced to a pair of simultaneous equations for the two unknowns in $\underline{x}$:

$$\underline{A}^T\underline{A}\ \underline{x} = \underline{A}^T\underline{B} \tag{3.4}$$

Solving these equations then gives the least squares values of the damping ratio and the response constant (both quantities squared)

$$\underline{X} = \begin{Bmatrix} \xi^2 \\ C^2 \end{Bmatrix}$$

and using these, the peak response amplitude is given by

$$V_{max} \equiv V(\beta=1) = \frac{C}{2\xi} \tag{3.5}$$

This procedure was used to obtain a best fit estimate of the peak response associated with each of the measured data sets shown in Figs. 3.3 to 3.7. Data listed on each figure includes the estimated peak response frequency (which is assumed to be the true modal frequency), the damping ratio and the response constant obtained from the least squares fit, and finally the peak response given by Eq. 3.5. Also shown on each graph is a solid line curve which is a plot of Eq. 3.1 in which the derived damping ratio and response constant quantities have been introduced to obtain values of V_i for a sequence of specified values of β_i.

Thus the solid line curves on Figs. 3.3 to 3.7 are the best interpretation that can be made of the radial acceleration frequency response relationship measured at selected points on the crest of the dam for modes 1, 2, 3, 4 and 6. The peak value recorded on each figure is the measured acceleration response quantity due to harmonic excitation at the modal frequency indicated on the figure, and it is quantities such as these that are compared with the corresponding calculated results in Chapter 4.

3.8 Measured Pressure Frequency Response Results

Because there is no known information in the literature on measured hydrodynamic pressures in a reservoir induced by motions

of a dam retaining the reservoir, some of the pressure results obtained in this study are presented in Figs. 3.8, 3.9, 3.10 and 3.11. The data contained in these figures is not complete because some of the pressure gages became inactive due to water leakage during the latter stages of the experimental work, and unfortunately the test schedule did not allow time for making repairs. It is important to note that each of these response curves has been derived by making a least squares fit of a SDOF curve to the pressure values measured at each frequency, following the procedure described above for the acceleration curves.

Fig. 3.8 shows the pressure response curves for modes 1, 4 and 6, measured at elevation 400 ft at various distances from the dam face on the vertical plane through the midsection of the dam and reservoir. It will be noted in the curves for mode 1 that the peak response frequency is the same at all measured distances. On the other hand, a definite trend toward increasing frequency with increasing distance from the dam face is seen in the mode 6 data; whereas no consistent trend is evident in the fourth mode data. Similar results are presented in Fig. 3.9 for pressures measured at the 350 ft elevation. Again, the first mode shows no frequency shift with distance, the sixth mode shows increasing peak frequencies with distance, and the fourth mode results show erratic variations of frequency. No rationale has been found to explain these differing behavior patterns for the three modes, but it is possible that they relate in some way to resonances in the reservoir.

A similar study indicating the effect of position of the gage station across the dam face at the 300 ft elevation is shown

in Fig. 3.10. Again it is evident for the mode 1 excitation that essentially the same peak response frequency is found at all measurement positions across the dam face. However, in the third and fourth mode excitations, there is an apparent decrease of frequency toward the increasing station designations, and a comparable increase of frequency in the opposite direction. Again no explanation can be offered for this observed behavior.

Finally, Fig. 3.11 presents a similar study of the influence of vertical position on the pressure peak frequency for measurements made at the midsection of the dam face. In the curves for the third mode frequency, only the shallowest station (400 ft elevation) shows any appreciable difference of peak response frequency; at this level the frequency is slightly reduced. The analagous situation occurs in the curves for mode 4, for which the only noticeable depth effect is an increase of frequency at the deepest pressure station. Note that the net effect in both modes 3 and 4 is a trend toward increase of frequency with depth. The same trend may be observed in the results for mode 6 -- a fairly consistent increase of frequency with increasing depth. The significance of all the trends shown in Figs. 3.9, 3.10 and 3.11 remains to be determined, however they seem to be too consistent to merely result from experimental scatter.

Chapter 4

COMPARISON OF ANALYTICAL AND EXPERIMENTAL RESULTS

4.1 General Comments

As was noted earlier, the basic purpose of this investigation was to obtain improved understanding of the mechanism of dynamic interaction between an arch dam and its reservoir; the approach was to examine the interaction phenomenon analytically and experimentally, and to compare the results obtained both ways. In the ideal situation where the results from both procedures are equivalent, it may be concluded that the mathematical model of the interacting system is valid and that the computational technique is satisfactory. In this case the analytical approach may be used with confidence in calculating the response of the dam-reservoir system to arbitrary types of dynamic loading. On the other hand, differences between the two sets of results demonstrate that further research is needed before results of this type of analysis may be considered reliable.

In this chapter comparisons are made between the analytical and experimental results obtained for Monticello Dam. First are considered the results describing the behavior of the dam -- specifically the vibration frequencies, mode shapes and damping; these are of primary importance because the hydrodynamic behavior depends directly on the dam response. Then the reservoir response is studied, comparing the experimental measurements with the analytical calculations of hydrodynamic pressures induced by

harmonic shaking of the dam. Two types of analytical results are considered in these comparisons, based on whether the water in the reservoir is assumed to be incompressible or compressible. It was hoped that these dual comparisons would demonstrate whether the simpler assumption of incompressibility could be assumed to provide adequate analytical results.

4.2 Dam Vibration Frequencies

A preliminary comparison of analytical and experimental values of the dam vibration frequencies was discussed in Chapter 2, in which the modulus of elasticity of the concrete was adjusted to provide the best possible agreement between the calculated frequencies and those measured by the USBR in their 1966 test program (5). The results of that adjustment, presented in Table 2.2, gave the most reliable mathematical model of the dam-reservoir system that was available prior to the experimental studies done in this investigation.

The final results of the present frequency measurements, obtained as described in Chapter 3, are listed in column 2 of Table 4.1. It is apparent that these are quite similar to the 1966 test results shown in Table 2.2; however there are some slight differences, and also the reservoir was at a higher level in 1986 than it was in 1966. For these reasons, it was necessary to repeat the modulus of elasticity adjustment to obtain a refined value of the elasticity modulus for use in the present analytical studies. The adjustment was done as described previously, starting with the calculation of frequencies based on the present reservoir level (436.2 ft) and the previously determined modulus of elasticity (E_c = 4.141 x 10^6 psi). Results of these analyses

are listed in column 3 of Table 4.1, and it is evident that these frequencies are slightly smaller than the presently measured values of column 2. Hence the adjusted modulus of elasticity that would give exact frequency agreement with the measured results was calculated mode by mode, leading to the results listed in column 4. The average of the values for the first three modes was assumed to be the best approximation that could be obtained in the present study. This average value, E_c = 4.262 x 10^6 psi, was used to calculate the frequencies of the first seven modes of vibration of the dam-reservoir system, with results as listed in the fifth column of Table 4.1

It is evident that the frequencies calculated for the first three modes agree very well with the measured results, as is to be expected when the modulus of elasticity of the mathematical model is adjusted in this way. Moreover, good agreement was obtained for the fourth mode frequency, and the calculated values for the sixth and seventh modes agree reasonably well with the test data. Additional confidence in the experimental results is given by the frequencies for the first four modes, determined from ambient vibration data and listed in the last column of Table 4.1. These measured frequencies agree well both with the forced vibration results in the second column and with the calculated values in the fifth column.

It is important to note that no experimental value was obtained for the fifth mode frequency. Study of the calculated fifth mode shape (see Fig. 4.2) revealed that it involved reversal of displacement directions within the height of the dam; i.e., it is equivalent to a second cantilever mode. Unfor-

tunately, the excitation applied by the shakers at the dam crest did not provide enough energy in this mode to produce a measurable response. From a practical point of view, however, this omission is not important because this type of mode cannot make a very significant contribution to the earthquake response of the dam.

4.3 Vibration Mode Shapes

The same analyses that produce the frequencies discussed in the preceding section also provided the corresponding mode shapes. Plots of the calculated modal crest displacements are presented by the solid line curves in Fig. 4.1; for comparison, the measured crest displacements (determined as described in Chapter 3) are shown by the dashed lines. It must be noted, however, that these measured motions are not consistent with the calculated results. The calculated crest displacements are the vector sum of the upstream and the cross-channel components at each node, whereas the experimental motions were measured only in the radial direction (tangential motions were not measured). Thus, part of the apparent discrepancy between analysis and experiment in Fig. 4.1 is due to this cause, which is especially important for the higher modes in which considerable tangential motions occur. Note again that no experimental result was obtained for mode 5.

Although the measured mode shape data was obtained only at the dam crest, it is of interest to note the modal vibration patterns over the full height of the dam. These patterns help explain why the fifth vibration mode was not observed experimentally, as was mentioned above; also they provide some understand-

ing of the pressure distributions determined within the reservoir. The calculated mode shape results are presented in Fig. 4.2, parts "a" through "f" depicting modes 1 through 6 respectively. In each graph, the displacements are shown at three horizontal sections: elevations 456 ft, 400 ft and 350 ft. In addition, the displacement variation in the vertical direction is shown for each mode at the vertical section having the greatest crest displacement.

4.4 Modal Damping Ratios

As was described in Chapter 3, measured frequency response curves were obtained for each mode by fitting a SDOF curve to the response accelerations measured for each frequency. The results of this procedure were shown in Figs. 3.3 to 3.7, and the experimental peak response frequencies are listed in column 2 of Table 4.1. For comparison purposes, the forced vibration response of the dam crest due to harmonic crest excitation was calculated for each of the frequencies of the response curve, as described in Chapter 2. However, the true reservoir level and final adjusted value of the concrete modulus were used in these calculations. In addition, the damping ratio used in these calculations was adjusted so that the calculated amplitude of response (based on superposition of the designated mode with the two adjacent modes) matched the crest displacement measured at the same station. The measured displacement, converted from the peak acceleration given by the SDOF curve fit, is listed for each mode in column 3 of Table 4.2, and this is the amplitude that was matched by adjusting the damping ratio in the forced vibration response analysis. The station at which the displacements were

matched are shown in column 2 of the Table, and the damping ratios used to obtain the displacement amplitudes of column 3 are listed in column 5. For comparison purposes, the damping ratio derived from the SDOF curve fit procedure is shown in column 4. Although the two sets of damping ratios differ somewhat, for practical purposes they may be considered equivalent; it is unrealistic to think of damping ratios specified to less than a single percentage point.

A graphical comparison between the analytical and the experimental frequency response curves is shown in Fig. 4.3. Here the calculated displacement response values have been converted to an acceleration response curve (dashed lines) for direct comparison with the experimental smoothed SDOF curves shown previously in Figs. 3.3 to 3.7. As expected, the curves generally agree very well because the analysis is forced to match the test displacement amplitude at the peak response frequency. However, the difference between the calculated and the measured peak response frequencies that is evident for modes 4 and 6 in Table 4.1 is also clear here. In addition, because it was the displacement responses that were matched, a discrepancy is induced in the peak acceleration amplitudes by the differences in the frequencies at which the displacements were matched. It also may be noted that the breadth of the calculated and measured frequency response curves differ; by reference to Table 4.2 it is easy to see that the breadth is directly related to the damping ratio, as required by the SDOF half-power method of damping analysis.

4.5 Pressure Response Curves

Following the procedure used to derive the smoothed SDOF response curves from measured accelerations, similar smoothed curves were derived from pressure data measured at all reservoir stations -- both at the dam face and along the channel midsection within the reservoir. Peak values of the SDOF fitted curves then were taken to represent the measured pressures at the designated modal frequencies. Typical response curves for pressures measured at the dam face centerline at elevations 350 or 400 ft are shown in Fig. 4.4. Note that results are not shown for mode 2 because water leakage made the gage inoperable during that test.

The general resemblance of these pressure response curves to the acceleration response curves of Fig. 4.3 is evident, and it is not surprising because the pressures are induced directly by the accelerations of the dam face. The fact that the relative amplitude of the pressure curves from mode to mode is different from the relative amplitude of the acceleration curves is because the pressures and the accelerations were not determined at the same nodes on the dam face.

Because of the mathematical proportionality between pressure and acceleration at the dam face for the case of an incompressible liquid, the measured centerline pressures were normalized by dividing them by the acceleration measured at the dam crest for the same frequencies; the results of this normalizing procedure are shown in Fig. 4.5. Assuming that the accelerations at the pressure gage location are proportional to the measured crest

accelerations -- i.e., that the mode shape does not change with small changes of frequency -- these normalized curves demonstrate that the pressures are not directly proportional to the face accelerations. In other words, the deviation of the curves of Fig. 4.5 from a horizontal straight line demonstrates that the pressure-acceleration relationship is not frequency independent as is expected of an incompressible liquid and makes evident the presence of some form of compressibility effects. No specific compressibility mechanism has been postulated, but it is possible that a rational explanation may be discovered for the distinctly differing shapes of the various curves.

4.6 Distribution of Hydrodynamic Pressures at the Dam Face

The complete set of hydrodynamic pressure results obtained in this study of Monticello Dam are presented in Table 4.3 for the values obtained at the dam face, and in Table 4.4 for pressures determined along the reservoir midsection at various distances from the dam face. Results are listed separately for each of the five excitation frequencies that produced maximum modal responses, and are displayed in accordance with their reservoir nodal point location: depth and position across face or distance from face. The first value listed for each point is the hydrodynamic pressure calculated assuming the reservoir liquid to be incompressible; that is followed by the pressure calculated for the compressible liquid. At the nodes where hydrodynamic pressures were measured during the harmonic testing, the measured pressure result is listed third. It will be noted that the measurements were not obtained at many points at several of the test frequencies; this was due to malfunction of the pressure

gages caused by water leakage. Also it will be noted that, for reasons of completeness, pressures were calculated at stations more distant from the dam face than were attempted to be included in the measurement program.

For convenience, the pressure results at the dam face are discussed in this section; those along the reservoir midsection are discussed in the following section. The pressures at the dam face are depicted graphically in Fig. 4.6; parts "a" through "e" give values for modes 1 through 6, respectively, with mode 5 being omitted. Calculated results for the compressible liquid are shown by the "heavy" solid line curves while the "light" solid lines give the incompressible results; the measured values are indicated by the "x" symbols. In general, these graphs show that the assumed compressibility of the liquid has relatively little effect on the calculated results, although in most modes the calculated compressible pressures are slightly higher than the incompressible. Measured values for the first mode are somewhat lower than both types of calculated pressures; for the other modes the agreement is better on the average, but the experimental values tend to be erratic. These results do not provide any meaningful evidence as to whether or not compressibility of the liquid should be considered in analysis of dam-reservoir response to dynamic loads. However, it is of interest that the measured values generally are of the same order of magnitude as both sets of calculated results.

4.7 Distribution of Hydrodynamic Pressures along the Reservoir Midsection

As was noted in the preceding section, the calculated and

measured values of hydrodynamic pressures along the midsection of the reservoir are tabulated in Table 4.4. A graphical view of these results is presented in Fig. 4.7, with experimental values shown by the solid lines and calculated data by dashed lines. This graph demonstrates dramatically that the relatively good agreement between analysis and experiment observed at the dam face does not exist at any significant distance into the reservoir. Calculated values at a distance of 98 ft are at least two orders of magnitude smaller than the measured pressures at that distance, and similar comparisons apply to the 246 ft distance.

The plots of the measured pressure variation with distance show that they diminish as might be expected from a typical wave propagation phenomenon, whereas the analytical results merely drop almost to zero at the first finite element node away from the dam face. This indicates that the analytical procedure does not capture any significant wave propagation phenomenon, and it is interesting to note from the data in Table 4.4 that the consideration of compressibility in this model does not make a significant difference in the results.

The inability of the analysis to predict hydrodynamic pressures away from the dam face casts considerable doubt on the validity of the ADAP-II finite element reservoir model applied with the harmonic excitation analysis procedure. On the other hand, it is only the hydrodynamic pressures at the dam face that have any effect on the dynamic response of the dam, and since the calculated dam face pressures are reasonably consistent with the measured values, it may be concluded that this type of reservoir interaction analysis can be effective in the earthquake response

analysis of an arch dam. Further evidence on this point will be discussed in the next chapter of this report.

Chapter 5

EARTHQUAKE RESPONSE ANALYSIS

5.1 Background

The final phase of this investigation of arch dam-reservoir interaction was an analytical study of the stresses induced in Monticello Dam by the ground motions recorded from a selected earthquake applied at the boundary of the finite element foundation model. The purpose of this study was to compare the stresses calculated by the ADAP-II program, using an incompressible finite element reservoir model, with the results obtained by the program EACD-3D (10) recently developed by Professor A. K. Chopra. Both analyses were done for the reservoir at 420 ft elevation.

Professor Chopra's program uses a finite element model of the dam similar to the ADAP model, but allows for compressibility in the reservoir model. Thus it was hoped that this comparison would give direct evidence of the importance of liquid compressibility on the most significant aspect of the seismic response -- the stresses in the dam. It was recognized, of course, that other response quantities such as hydrodynamic pressure might be more sensitive to the influence of liquid compressibility. But the focus of this research effort has been on the question of seismic safety, so in this sense the liquid compressibility is important only with regard to its influence on the amplitude of seismic stresses in the dam.

In this chapter, the general features of the program EACD-3D will be described first, next the earthquake selected for this comparative study will be discussed, and finally the results obtained by the two computer programs (ADAP-II and EACD-3D) will be presented and compared.

5.2 Computer Program EACD-3D

As was mentioned above, the mathematical model employed in the EACD-3D program uses a finite element assemblage to represent the concrete arch and the block of foundation rock that is assumed to interact with the dam; these finite element models are essentially equivalent to those employed by the ADAP program. Also, in the region near the dam face, EACD-3D uses liquid finite elements to model the reservoir; these are similar to the liquid elements in ADAP-II, but they incorporate a finite rather than infinite modulus of compressibility. A major difference in EACD-3D, however, is that the reservoir beyond the finite element mesh is modeled as a prismatic body of water extending to infinity; this permits the pressure waves in the compressible water to radiate earthquake response energy away from the dam. Another major difference of EACD-3D is that the reservoir boundary is assumed to be a compressible medium which also can absorb wave energy from the reservoir. The stiffness property of the boundary is expressed by the wave reflection coefficient "α", and it may be selected to represent any expected foundation behavior, ranging from the total reflection of a rigid surface ($\alpha = 1.0$) to the condition of complete absorption with no reflection ($\alpha = 0$). Actual boundary conditions in the field, which may range from rock faces to a soft silt layer, would have reflection coeffi-

cients somewhere between these limiting values.

For reasons of computational efficiency, the dam, the foundation block and the reservoir are formulated as individual substructures; the dynamic behavior of each substructure is expressed in terms of generalized coordinates which are its vibration mode shapes. However, similar to the ADAP-II model, only the flexibility of foundation block is considered and its inertial and damping effects are ignored. In order to deal with compressibility in both the reservoir and its boundary region, a frequency domain procedure is used to evaluate the response of the coupled system of substructures to dynamic loads. A Fast Fourier Transform (FFT) subroutine is used first to express the earthquake excitation in terms of its harmonic components. Then the response of the system to each harmonic component is expressed by a transfer function which indicates the harmonic amplitude of a specified response quantity due to application of unit harmonic earthquake motions. The product of the transfer function and the harmonics of the earthquake input, taken frequency by frequency, then represents the frequency domain expression of the earthquake response. The final step of the analysis is the transformation of the response back to time domain, using an inverse FFT subroutine. Because EACD-3D is completely described in Reference 10, this brief description will suffice for the purposes of this report.

5.3 Earthquake Response Transfer Functions

In the frequency domain method of analysis, the physical properties of the system being analyzed are represented completely by the transfer functions. In the EACD-3D program, the

transfer functions express the harmonic response of a specified response quantity of the dam-foundation-reservoir model to harmonic excitation applied to the rigid boundary of the foundation block. An example of such a transfer function is shown in Fig. 5.1; this indicates the radial direction acceleration of the center of the dam crest due to unit acceleration of the foundation boundary in the upstream direction. The three curves indicate the effect of different assumed boundary reflection coefficients: full reflection, α = 1.0; very stiff boundary, α = 0.9; and rather soft silt boundary, α = 0.5. In this plot, the frequency is expressed as a ratio to the first mode frequency of the dam-foundation system without any reservoir. The frequencies of the dam-foundation system without reservoir calculated by EACD-3D are listed in column 2 of Table 5.1. From this it is apparent that a frequency ratio of 1.0 in Fig. 5.1 represents a frequency of 3.85 Hz. The corresponding frequencies calculated by ADAP are shown in the third column of Table 5.1; these show that the ADAP and the EACD-3D models are essentially equivalent. The first spike in the transfer functions, at a frequency ratio of about 0.86, represents the first mode of the dam-foundation-reservoir system with a frequency of about 3.31 Hz. This may be compared with the ADAP-II first mode frequency reported in Chapter 2 of 3.23 Hz, for the reservoir at 420 ft elevation.

The other spikes in the transfer functions of Fig. 5.1 represent the second symmetric mode of the dam-foundation-reservoir system and the frequencies of the infinite reservoir. Frequencies calculated by EACD-3D for the infinite prismatic reservoir are listed in Table 5.2. The second major spike, at a

frequency ratio of about 1.55, is equivalent to 5.97 Hz which compares very well with the first reservoir mode frequency in Table 5.2 of 6.02 Hz. Also the next major spike in Fig. 5.1, at a frequency ratio of about 3.33, or about 12.82 Hz, is reasonably close to the third infinite channel frequency of 14.19 Hz. It is important to note that the transfer function spikes for these reservoir resonances are very sharp when rigid reservoir boundaries are assumed ($\alpha = 1.0$), but that they are greatly attenuated even with a reflection coefficient as large as $\alpha = 0.9$, and are essentially eliminated by a soft boundary ($\alpha = 0.5$). Also it is important to note that boundary energy absorption has a relatively lesser effect on the fundamental resonance of the dam as represented by the spikes at the frequency ratio of 0.85.

Because the earthquake motions applied to the boundary of the foundation block have components acting in the vertical and the cross-channel directions as well as upstream, it was necessary to develop transfer functions for these additional components of seismic input. These functions are presented in Figs. 5.2 and 5.3 for the vertical and cross-channel excitations, respectively, in the same format used in Fig. 5.1. The curves in Fig. 5.2 exhibit spikes at the same frequencies seen in Fig. 5.1; this is to be expected because both the upstream and vertical motions excite the essentially symmetric modes of vibration of the system. On the other hand, the spikes in Fig. 5.3 represent essentially antisymmetric response modes; thus the first spike on this curve at a ratio of 1.00, or 3.85 Hz, corresponds to the second mode frequency of the dam-foundation-reservoir system, calculated by ADAP-II (Table 2.2) to have a frequency of 3.67 Hz.

The discrepancy between these values is associated partly with the dam-foundation model (see Table 5.1) and partly with the differences in reservoir modeling. The second major spike in Fig. 5.3 represents the first antisymmetric mode of the infinite reservoir; the much smaller peaks corresponding with the first and second symmetric reservoir modes also may be noted in this figure due to the fact that the system is not truly symmetric.

5.4 Earthquake Excitation

In order to judge the importance of the reservoir compressibility effect on the earthquake response of Monticello Dam, it was considered important to apply an earthquake that might be representative of the region where the dam is located. It was not the purpose of this investigation to evaluate the seismic safety of the dam, and therefore no seismicity study was made of the dam site and surrounding region. However, it seemed reasonable to assume that the frequency characteristics of an earthquake at Monticello would be similar to those of earthquakes recorded in other parts of the San Francisco Bay region. Accordingly, the earthquake selected as input for this analysis was the one recorded at Morgan Hill, California, in April 1984 (11). The peak acceleration contained in the record is 0.34 g, and this appears to be a reasonable estimate of the intensity of a major earthquake that might occur at Monticello Dam.

Figs. 5.4, 5.5 and 5.6 (reproduced from Reference 11) show the acceleration, velocity and displacement histories for the earthquake motions assumed to act on Monticello Dam in the upstream, vertical and cross-channel directions, respectively. Response spectra calculated from these input motions (also from

Reference 11) are shown in Figs. 5.7, 5.8 and 5.9, respectively, in the form of four-way log plots. The plots show the pseudo-spectral velocity (PSV), the pseudo-spectral acceleration (PSA) and the spectral displacement of the ground motion components when read against the appropriate log scales. Five different curves are presented showing the results for 0, 2, 5, 10 and 20 percent critical damping, with decreasing amplitude corresponding to increasing damping. Also shown by a dashed line on each figure is the Fourier amplitude spectrum of the input motion component; these are the result of Fast Fourier Transformation of the earthquake record, as discussed above.

5.5 Response to Earthquake Input

As was mentioned above, the response of Monticello Dam to the Morgan Hill Earthquake motions was calculated by both ADAP-II with its incompressible reservoir model, and by EACD-3D which accounts for reservoir compressibility. In both programs a form of mode superposition is used; in ADAP-II the vibration modes are those of the dam-foundation-reservoir system, in EACD-3D the modes are those of the dam-foundation system with empty reservoir. In ADAP-II, the reservoir boundary is assumed to be rigid; in EACD-3D three different boundary rigidity conditions were assumed expressed by reflection coefficients $\alpha = 1.0$ (rigid), $\alpha = 0.9$ and $\alpha = 0.5$ (very soft).

Both of these computer programs have the capability of calculating the static state of stress that exists before the earthquake occurs. The results of such an analysis considering the gravity load of the concrete and the hydrostatic pressure of the reservoir at 420 ft elevation are presented in the form of

stress contours in Fig. 5.10. The contour interval in these plots is 50 psi and negative values indicated compression. Plots a, b, c and d show arch direction stresses on the upstream and downstream faces, and cantilever direction stresses on the upstream and downstream faces, respectively. No specific significance is given to these results; they are shown in order to give a sense of scale to the dynamic earthquake stresses. In practice, the static and dynamic stresses would be combined, of course, to indicate tendencies toward cracking damage to the dam. They are not combined in this investigation in order to emphasize the fact that this is not intended to be an evaluation of the safety of Monticello Dam.

As noted, a total of four dynamic analyses were performed, one with ADAP-II and three with EACD-3D using three different reflection coefficients. Complete time history response results were obtained from all of these analyses, but a good basis for evaluation of the importance of reservoir compressibility and of boundary wave absorption is provided by comparison of the much simpler "envelope" stress contours for the four analyses. The envelope values are the largest value of each stress component obtained in each element of the finite element mesh during the entire history of the earthquake. Thus it is apparent that the contours do not show a concurrent state of stress -- the maximum values occur at different times at different locations. However, the tensile stress values in particular do show the tendency toward cracking damage of the dam, and comparison of these tensile envelope contours gives a significant indication of the influence of the various analytical assumptions. It must be noted

that all three components of earthquake motion were applied simultaneously, so these envelope values represent the full dynamic effect of the earthquake.

The tensile stress envelope contours obtained from these analyses are presented in Figs. 5.11, 5.12, 5.13 and 5.14. Each figure portrays only one component of stress on one face of the dam; the four plots displayed on each figure show the results obtained with ADAP-II first, and then with the three different reflection coefficients assumed in the EACD-3D analyses. Considering first Fig. 5.11, which shows arch direction stresses on the upstream face of the dam, it is apparent from the top two plots that ADAP and EACD with $\alpha = 1.0$ give quite similar results. The shapes of the contours differ somewhat, but the peak stress values and their locations are quite similar. This comparison indicates that for this particular dam and earthquake, and for this stress component, the water compressibility does not have any significant effect. Comparing the second and third plots, it is seen that the softer boundary (with $\alpha = 0.9$) gives a slight reduction of peak stresses. On the other hand, the fourth plot, for $\alpha = 0.5$ shows a very significant reduction of stress, so it is clear that very soft (silt) boundaries can have a useful mitigating effect on the peak earthquake response stresses. Entirely equivalent conclusions can be drawn from the four plots of Fig. 5.12, which depict the arch direction stresses on the downstream face. It is apparent that the dynamic stresses on this face are somewhat smaller than those on the upstream face, but the relationship between the four plots is equivalent to that shown in Fig. 5.11. Note that the contour interval in Fig. 5.12d

is only 25 psi because the stresses in this case tend to be so low.

Very similar conclusions can be drawn from the four plots of Fig. 5.13, which show cantilever direction stresses on the upstream face. The shapes of the contours obtained from ADAP show greater differences from the EACD contour shapes for $\alpha = 1.0$, but the potential for cracking of the dam is very similar in the two analyses. The reduction of cantilever stress with diminishing reflection coefficients seems to be less pronounced than the arch stress reduction of Fig. 5.11, but again this is not a major factor in the analysis.

The first two plots in Fig. 5.14, on the other hand, show a remarkable difference in the stresses computed by ADAP from the EACD ($\alpha = 1.0$) results. For some reason the water compressibility appears to cause an increase in the cantilever stresses on the downstream face, but it is surprising that the effect is so much more pronounced on the downstream face as compared with the upstream. The conclusions to be drawn from these results will be presented and discussed in Chapter 6, but it is worth noting at this point that the differences in assumed reflection coefficients seem to have a greater effect on the dam stresses than the difference between compressible and incompressible reservoir water. On the other hand, it is only by assuming compressible reservoir water that the boundary flexibility effects can be considered.

Chapter 6

CONCLUSIONS AND RECOMMENDATIONS

6.1 Conclusions

This intensive study of dynamic interaction of the reservoir with Monticello Dam has led to a number of conclusions -- about the effectiveness of the experimental procedure, about the validity of the analytical methods for simulating the harmonic test behavior, about the influence of compressibility of the reservoir water on its interaction effects, and about the analytical prediction of arch dam response to earthquakes. Comments and conclusions on each of these topics are grouped under appropriate headings in the following sections of this report.

6.1.1 Experimental Procedure

(a) The rotating mass shakers provide a convenient means of measuring vibration frequencies, mode shapes, and damping of an arch dam -- including effects of the dynamic interaction with the reservoir and the foundation material. However, the results show that one or more vibration modes may be overlooked if they are not sufficiently excited by the shakers located at predetermined positions on the dam.

(b) Mode shapes and frequencies determined in this study agreed well with those measured in 1966, demonstrating the general reliability of the procedure; however, the same mode was overlooked in both test programs because the shakers were positioned in essentially the same locations.

(c) Harmonic forces produced by the two 5 kip shakers were sufficient to generate significant hydrodynamic pressures in the reservoir; these were sensed effectively by the pressure transducers, not only at the dam face, but at distances from the face as great as 250 ft.

6.1.2 Validation of the Analytical Model

(a) The most reliable estimate of the modulus of elasticity of the dam and foundation is given by matching the calculated and experimental frequencies of the lowest three or four modes. In the present study, matching of the lowest three frequencies gave excellent agreement up to the sixth mode, except for the mode that was not identified experimentally.

(b) Damping ratios obtained from experimental data by the half-power method are in fair agreement with those determined by matching analytical and experimental harmonic displacement amplitudes for each mode; values typically are in the range of 1.5 to 3.0 percent for this very low amplitude deformation.

(c) Harmonic pressures induced at the dam face are very small, hence the comparison of analytical and experimental results is subject to considerable error in both types of data. Nevertheless, the good order of magnitude agreement for pressures at the dam face suggests that the ADAP-II analytical model will be reasonably effective in accounting for reservoir interaction effects in predicting the earthquake response of the dam.

(d) On the other hand, the pressures predicted by the ADAP

program (either considering or neglecting liquid compressibility) along the reservoir axis at various distances from the dam face were at least two orders of magnitude smaller than the measured values. Thus it is clear that the ADAP program reservoir model has some serious deficiencies; further research is needed to determine if there are similar deficiencies in the EACD-3D program.

6.1.3 Influence of Liquid Compressibility

(a) Measured hydrodynamic pressure-frequency response curves obtained in this study show little evidence of reservoir resonance effects. However, the fundamental reservoir frequency indicated both by EACD and by ADAP including liquid compressibility is about 60 percent higher than the fundamental frequency of the dam-foundation system without reservoir; hence for this dam-reservoir system the coupling effect of the reservoir with the dam response is not expected to be great.

(b) Measured pressure-frequency response curves for modes 4 and 6 show shifts of peak response frequency with changing position in the reservoir which may be due to compressibility effects, but no hypothesis has been developed to explain the shifts.

(c) Including compressibility in the ADAP reservoir model had only minor effects on the harmonic excitation pressures calculated at the dam face, and did not improve the comparison with measured results.

(d) When the pressure measured at the dam face was normalized by dividing by the crest acceleration measured at the

same frequency, the resulting ratio showed a significant variation with frequency -- thus demonstrating a measurable effect of reservoir compressibility. However, the compressibility mechanism leading to the observed frequency response effect is not yet understood.

6.1.4 Earthquake Response Behavior

It is important to recognize that the earthquake response results presented in this study are very limited in scope, and therefore should not be used to draw general conclusions about the earthquake behavior of arch dams. Only a single dam-reservoir system has been considered, with only a single earthquake excitation; and it is well recognized that both the ratio of dam and reservoir frequencies as well as the frequency content of the earthquake motions can have controlling influences on the earthquake response of an arch dam. In spite of these limitations, however, the results of the analyses demonstrate several interesting facts that apply to this specific dam-earthquake combination, and thus represent one point in the range of behavior that may be observed in the earthquake response of arch dams. The points of interest that have been noted are as follows:

(a) For practical purposes, the stress envelope results obtained by the ADAP analysis (incompressible water) are equivalent to those given for the rigid boundary case by the EACD-3D program. Thus it may be concluded that the compressibility effect (which is considered by EACD-3D) is not important in the earthquake response of Monticello Dam. This observation is not surprising in this case because the three lowest modes of the dam have frequencies below the lowest

mode frequency of the reservoir, hence compressibility does not influence the interaction mechanism very much.

(b) On the other hand, when the compressible reservoir was considered together with a very soft boundary (reflection coefficient $\alpha = 0.5$), the absorption of the reservoir pressure waves into the boundary led to a very significant reduction of the envelope stress results. Thus it is clear that a soft reservoir boundary can have a very beneficial effect on the earthquake safety of an arch dam, but it is only possible to take advantage of this effect by using a compressible reservoir analysis program such as EACD-3D. Consequently the extra computational cost of a frequency domain analysis (such as EACD-3D) may be easily justified if a dam is located in a region of high seismicity and if the reservoir boundary may be assumed to be flexible.

(c) The principal question that remains if an EACD-3D analysis is considered appropriate in a given situation is the value to be assumed for the boundary reflection coefficient, α. The results obtained here show that a wide range of results may be obtained by using different values of α, and there is essentially no information as to the value that would apply to any given arch dam reservoir. It is believed that the range of values considered in this study ($1.0 \geq \alpha \geq 0.5$) would include any practical case, but no guidance is available as to the choice of values within that range.

(d) The results of this study suggest that the relatively simple ADAP-II type of analysis is appropriate for use in

preliminary design, because it is likely to give conservative results (i.e. to overestimate the seismic stresses), especially if the reservoir can be assumed to have a relatively soft boundary. If the dam demonstrates an adequate margin of safety in these preliminary analyses, there is no need to perform an additional analysis considering reservoir compressibility. On the other hand, if the margin of safety indicated by the ADAP-II type of analysis is not considered adequate, additional analyses using EACD-3D may be justified, considering both upper and lower bound estimates of the reservoir boundary reflection coefficient. Also, if the design has been based on an earthquake having a relatively short return period, additional analysis of the EACD-3D type may be desirable in assessing the expected performance of the dam during a maximum credible earthquake; in this event higher damping would apply and some moderate cracking might be acceptable. This additional analysis would provide a measure of the margin of safety of the dam design in terms of the increased seismic excitation that could be accommodated.

6.2 Recommendations

Although considerable progress has been made during this investigation toward understanding of reservoir interaction effects in the earthquake response of arch dams, it is evident that further study on this subject still is needed. Two specific areas recommended for further research are discussed below; undoubtedly several other topics also could be identified.

6.2.1 Extension of the EACD-3D Program

In its present version, the program EACD-3D is intended only to evaluate response due to earthquake excitation; the earthquake motions are considered as rigid body accelerations of the base beneath the foundation rock model. An important improvement of the program would be to modify it so that it can evaluate response to forces acting at specified points on the body of the dam. With this change, the program could be used to evaluate the response to the harmonic loading applied by the rotating mass shakers at the dam crest; then the hydrodynamic pressures developed at the dam face and within the reservoir could be calculated and compared with the pressures measured during this field test program. It is of primary importance to determine whether EACD-3D gives a reliable estimate of the pressure wave propagation up the reservoir, in contrast with the failure of the ADAP-II program to do this. If so, further study could be devoted to the ADAP program to understand why it does not perform correctly and then to make appropriate changes in it.

6.2.2 Parametric Study of Earthquake Response

As noted above, the earthquake response analyses of Monticello Dam done with ADAP-II and with EACD-3D have provided very useful information about the effects of reservoir interaction on the earthquake behavior of arch dams. However, it is recognized that conclusions cannot be drawn from this single case, and it is essential that the analyses be repeated for cases involving wide changes in the basic

parameters of the problem. To fully understand the problem, it is recommended that a broad program of analyses be carried out; some appropriate parameter variations would be as follows:

(a) Earthquake Characteristics - repeat the analyses of Monticello Dam and reservoir done for the Morgan Hill earthquake, using the standard Cal Tech artificial earthquakes, Types A, B and C using the two versions of each type. Note that at least the same three reservoir boundary reflection coefficients should be considered in each case. In addition, it would be useful to do analyses with one or two other real earthquakes, to include examples of the random variability that has been eliminated from the artificial ground motions.

(b) Dam Scale - repeat the Morgan Hill earthquake analysis using scale models of Monticello Dam and reservoir; initial studies should be done for half scale and double scale models.

(c) Dam Design - repeat the Morgan Hill analysis of Monticello Dam considering arch dams with a wide range of geometry and size. Examples of interest would be McKay's Point Dam, the proposed Auburn Dam with double curvature geometry, Morrow Point Dam and possibly Xiang Hong Dian and Quan Shui Dams that were tested in China.

With this range of variations, it is expected that general conclusions could be drawn with regard to the importance of reservoir and boundary compressibility on the earthquake response.

REFERENCES

1. R. W. Clough, K-T Chang, et al, "Dynamic Response Behavior of Xiang Hong Dian Dam," University of California Earthquake Engineering Research Center Report No. UCB/EERC-84/02, Berkeley, California, April 1984.

2. R. W. Clough, K-T Chang, et al, "Dynamic Response Behavior of Quan Shui Dam," University of California Earthquake Engineering Research Center Report No. UCB/EERC-84/20, Berkeley, California, November 1984.

3. R. W. Clough, K-T Chang et al, "Dynamic Interaction Effects in Arch Dams," University of California Earthquake Engineering Research Center Report No. UCB/EERC-85/11, Berkeley, California, October 1985.

4. U. S. Department of the Interior, Bureau of Reclamation, Design of Arch Dams, Denver, Colorado, 1977 (pp 422 and 423).

5. G. C. Rouse and J. G. Bouwkamp, "Vibration Studies of Monticello Dam," U. S. Department of the Interior, Bureau of Reclamation Research Report No. 9, 1967.

6. L. H. Roehm, "Comparison of Computed and Measured Dynamic Response of Monticello Dam," Engineering and Research Center, U. S. Bureau of Reclamation, Report No. REC-ERC-71-45, December 1971.

7. R. W. Clough, J. M. Raphael, S. Mojtahedi, "ADAP - A Computer Program for Static and Dynamic Analysis of Arch Dams," University of California Earthquake Engineering Research Center Report No. UCB/EERC-73/14, Berkeley, California, June 1973.

8. J. S-H Kuo, "Fluid Structure Interaction: Added Mass Computations for Incompressible Fluid," University of California Earthquake Engineering Research Center Report No. UCB/EERC-82/19, Berkeley, California, August 1982.

9. D. E. Hudson, "Synchronized Vibration Generators for Dynamic Testing of Full Scale Structures," Earthquake Engineering Research Laboratory Report, California Institute of Technology, Pasadena, California, 1962.

10. K-L Fok, J. F. Hall, and A. K. Chopra, "EACD-3D: A Computer Program for Three-Dimensional Earthquake Analysis of Concrete Dams," University of California Earthquake Engineering Research Center Report No. UCB/EERC-86/09, Berkeley, California, July 1986.

11. A. F. Shakal, M. J. Huang, et al., "Processed Data from the Strong Motion Records of the Morgan Hill Earthquake of 24 April 1984 -- Part I. Ground Response Records," California Department of Conservation, Division of Mines and Geology Report No. OSMS 85-04, May 1986.

Table 2.1 Measured and Calculated Natural Frequencies (Hz)
(Reservoir at 433 ft Elevation)
Ec = 5,100,000 psi

	(a)	(b)	(c)	(d)
Foundation Reservoir	NO NO	YES NO	YES YES	Measured (1966)
1	4.38	4.18	3.45	3.12
2	4.80	4.54	3.93	3.55
3	6.05	5.80	5.17	4.63
4	7.34	7.00	6.46	6.00
5	8.58	8.48	7.60	7.60
6	9.83	9.20	8.02	
7	10.53	10.08	9.44	

Table 2.2 Measured and Calculated Frequencies for
Two Reservoir Levels (Hz)
Ec = 4,141,000 psi

Mode No	Water Level 433 ft	Water Level 420 ft	Measured (1966) 433 ft
1	3.11	3.23	3.12
2	3.54	3.67	3.55
3	4.66	4.83	4.63
4	5.82	6.00	6.00
5	6.85	6.91	7.60
6	7.23	7.40	
7	8.51	8.58	

Table 4.1 Measured and Adjusted Calculated Frequencies (Hz)
(Reservoir Elevation = 436.2 ft)

Mode No	Measured (June 1986)	Calculated ($E_c=4.141\times10^6$)	Ec for Perfect Match($\times10^6$ psi)	Calculated ($E_c=4.262\times10^6$)	Measured (Ambient)
1	3.12	3.078	4.256	3.122	3.09
2	3.55	3.507	4.242	3.558	3.56
3	4.70	4.619	4.288	4.686	4.62
4	6.00	5.772	4.475	5.856	5.84
5	missed	6.834	--	6.933	--
6	7.60	7.172	4.650	7.276	--
7	8.49	8.476	4.155	8.598	--

Table 4.2 Forced Vibration Analysis of Damping Ratio

Mode No	Matching Station	Matched Max. Displacement (x 10^4 in.)	Damping Ratio (%)	
			SDOF Fit	Ampl. Match
1	f	8.54	3.00	2.71
2	h	14.05	1.83	2.55
3	e	3.28	1.80	3.16
4	f	7.20	1.38	1.14
5	-	(missed)	--	--
6	f	5.21	2.40	0.77

Table 4.3 Forced Vibration Hydrodynamic Pressures at Dam Face (x 1000 psi)

Pressure Station	f	h	j	k	Elev (ft)	Mode No
Incompressible	-6.288	-11.12	-7.459	-2.631		
Compressible	-6.726	-11.68	-7.908	-2.898	400	
Measured	-3.000	-4.56				
Incompressible	-6.735	-10.57	-8.063	-3.541		
Compressible	-7.726	-11.80	-9.068	-4.171	350	
Measured		-6.17	-3.500			1
Incompressible	-6.741	-9.928	-7.605	-4.218		
Compressible	-8.152	-11.630	-9.017	-5.160	300	
Measured	-5.410	-7.380	-5.760	-3.610		
Incompressible	-5.991	-7.777	-6.554	-5.253		
Compressible	-7.694	-9.776	-8.236	-6.477	250	
Measured				-3.330		
Incompressible	17.12	3.742	-17.53	-14.19		
Compressible	17.76	3.937	-18.02	-14.78	400	
Incompressible	15.52	4.620	-13.78	-13.77		
Compressible	16.80	5.026	-14.71	-14.99	350	
Measured				-10.00		2
Incompressible	12.90	3.389	-11.67	-13.25		
Compressible	14.47	3.915	-12.76	-14.84	300	
Measured	12.70		-11.90	-17.00		
Incompressible	9.249	2.368	-8.086	-13.54		
Compressible	10.89	2.959	-9.127	-15.43	250	
Incompressible	-3.987	2.628	-2.344	-5.553		
Compressible	-4.389	2.439	-2.629	-5.947	400	
Incompressible	-3.578	1.452	-1.139	-4.626		
Compressible	-4.435	0.942	-1.777	-5.435	350	
Measured		2.110	-4.090	-7.270		3
Incompressible	-2.761	0.949	-1.295	-4.016		
Compressible	-3.891	0.155	-2.183	-5.076	300	
Measured	-1.900	4.160	-1.970	-2.980		
Incompressible	-1.927	0.262	-1.031	-3.310		
Compressible	-3.193	-0.733	-2.062	-4.514	250	
Measured		-6.390	-1.860			

Table 4.3 Forced Vibration Hydrodynamic Pressures at Dam Face (Cont'd)

Pressure Station	f	h	j	k	Elev (ft)	Mode No
Incompressible	3.264	5.093	-7.526	8.439		
Compressible	3.087	5.225	-7.782	8.998	400	
Measured		3.270				
Incompressible	2.129	5.085	-6.370	5.379		
Compressible	1.648	5.213	-6.711	6.337	350	
Measured		2.520	-2.740	2.190		
Incompressible	1.908	3.444	-3.632	4.057		4
Compressible	1.268	3.447	-3.925	5.073	300	
Measured	2.520	1.740	-3.780	2.790		
Incompressible	1.124	2.042	-1.589	1.215		
Compressible	0.4811	1.929	-1.847	1.890	250	
Measured			-2.370			
Incompressible	-8.412	10.20	-4.826	0.779		
Compressible	-8.098	11.40	-4.423	1.219	400	
Measured		3.02				
Incompressible	-8.582	1.856	-4.430	-1.557		
Compressible	-7.539	4.089	-3.394	-0.734	350	
Measured		3.600		-11.770		
Incompressible	-7.922	-1.937	-5.133	-2.156		6
Compressible	-6.157	0.957	-3.569	-1.241	300	
Measured	-1.715	3.760				
Incompressible	-6.216	-4.034	-4.563	-4.441		
Compressible	-3.919	-0.609	-2.622	-4.034	250	
Measured		-1.810				

Table 4.4 Calculated and Measured Hydrodynamic Pressures Along Reservoir Center-line at Various Elevations (x 1000 psi)

	DISTANCE FROM DAM FACE						
	0′	98′	246′	380′	900′	ELEV	MODE
Incompressible	-11.120	-7.929E-3	-6.914E-3	-1.568E-3	3.300E-4		
Compressible	-11.680	-1.378E-2	-1.119E-2	-3.648E-3	5.060E-4	400	
Measured	4.560	1.510	7.030E-1				
Incompressible	-10.570	-3.453E-2	-1.293E-2	-3.932E-3	9.158E-4		
Compressible	-11.800	-4.939E-2	-2.285E-2	-8.713E-3	1.324E-3	350	
Measured	6.170	2.940	1.056				1
Incompressible	-9.928	-6.050E-2	-1.919E-2	-5.800E-3	1.350E-3		
Compressible	-11.630	-8.573E-2	-3.422E-2	-1.286E-2	1.952E-3	300	
Measured	7.380						
Incompressible	-7.777	-8.692E-2	-2.454E-2	-7.070E-3	1.626E-3		
Compressible	-9.776	-1.246E-1	-4.375E-2	-1.580E-2	2.359E-3	250	
Measured							
Incompressible	3.742	7.936E-3	2.331E-3	6.731E-4	-1.453E-4		
Compressible	3.937	1.070E-2	4.297E-3	1.779E-3	-1.919E-4	400	
Measured			2.310E-1				
Incompressible	4.620	1.885E-2	4.844E-3	1.673E-3	-3.908E-4		
Compressible	5.026	2.573E-2	9.363E-3	4.223E-3	-5.013E-4	350	
Measured			2.990E-1				2
Incompressible	3.389	2.942E-2	6.730E-3	2.556E-3	-6.179E-4		
Compressible	3.915	4.086E-2	1.351E-2	6.327E-3	-7.827E-4	300	
Measured			2.500				
Incompressible	2.368	3.689E-2	8.875E-3	3.118E-3	-1.458E-4		
Compressible	2.959	5.269E-2	1.748E-2	7.776E-3	-9.439E-4	250	
Measured							

Table 4.4 Calculated and Measured Hydrodynamic Pressures Along Reservoir Center-line at Various Elevations (Cont'd)

	0'	98'	246'	380'	900'	ELEV	MODE
Incompressible	2.628	-1.729E-3	9.226E-5	-1.638E-4	5.228E-5		
Compressible	2.439	-4.721E-3	-2.483E-3	-1.673E-3	-1.151E-4	400	
Measured		6.540E-1	5.610E-1				
Incompressible	1.452	-3.407E-4	-8.015E-4	-2.625E-4	6.293E-5		
Compressible	0.942	-7.927E-3	-6.779E-3	-3.727E-3	-3.218E-4	350	
Measured	2.110	1.750E-1	1.080				3
Incompressible	0.949	-1.371E-3	-1.190E-3	-3.817E-4	8.883E-5		
Compressible	0.155	-1.447E-2	-1.017E-2	-5.496E-3	-4.841E-4	300	
Measured	4.160		9.880E-1				
Incompressible	0.262	-3.170E-3	-1.389E-3	-4.645E-4	1.058E-4		
Compressible	-0.733	2.302E-2	-1.263E-2	-6.785E-3	-6.146E-4	250	
Measured	6.390						
Incompressible	5.093	3.205E-3	1.139E-3	1.451E-4	-7.196E-6		
Compressible	5.225	5.184E-3	8.852E-3	1.442E-2	2.633E-2	400	
Measured	3.270	3.200E-1	3.200E-1				
Incompressible	5.085	9.487E-3	1.614E-3	5.393E-4	-1.127E-4		
Compressible	5.213	1.292E-2	1.915E-2	3.337E-2	6.039E-2	350	
Measured	2.520	4.140E-1	4.340E-1				4
Incompressible	3.444	1.400E-2	2.125E-3	8.696E-4	-2.061E-4		
Compressible	3.447	1.538E-2	2.783E-2	4.949E-2	8.935E-2	300	
Measured	1.740		1.410				
Incompressible	2.042	1.593E-2	3.133E-3	1.055E-3	-2.484E-4		
Compressible	1.929	1.113E-2	3.519E-2	6.129E-2	1.111E-1	250	
Measured			1.720E-1				

Table 4.4 Calculated and Measured Hydrodynamic Pressures Along Reservoir Center-line at Various Elevations (Cont'd)

	0'	98'	246'	380'	900'	ELEV	MODE
Incompressible	10.200	-1.420E-2	-8.772E-2	-1.116E-3	3.227E-4		
Comopressible	11.400	2.241E-3	3.822E-2	4.229E-2	-4.563E-2	400	
Measured	3.020	5.410E-1	2.430E-1				
Incompressible	1.856	-1.421E-2	-6.882E-3	-2.062E-3	4.860E-4		
Compressible	4.089	2.502E-2	8.355E-2	9.780E-2	-1.052E-1	350	
Measured	3.600	1.007	4.160E-1				6
Incompressible	-1.937	-2.396E-2	-1.068E-2	-3.015E-3	7.009E-4		
Compressible	0.957	3.676E-2	1.258E-1	1.448E-1	-1.558E-1	300	
Measured	3.760	7.060E-1	5.120E-1				
Incompressible	-4.034	-4.015E-2	-1.305E-2	-3.704E-3	8.531E-4		
Compressible	-0.609	7.004E-2	1.555E-1	1.798E-1	-1.936E-1	250	
Measured	1.810						

Table 5.1 Calculated Frequencies of Dam-Foundation System Without Reservoir (Ec = 4.141 x 10^6 psi)

Mode No	EACD-3D (Hz)	ADAP-II (Hz)
1	3.850	3.766
2	4.244	4.091
3	5.467	5.226
4	6.686	6.307
5	8.166	7.641
6	8.574	8.290
7	9.807	9.083

Note:

EACD-3D .. Thickshell elements only, 9 mesh levels
ADAP-II .. Thickshell and 3D-Shell elements, 8 mesh levels

Table 5.2 EACD-3D Calculated Frequencies of Infinite Reservoir

Mode No.	Frequency (Hz)
1	6.02
2	11.42
3	14.19
4	18.27
5	19.31
6	21.79
7	24.04
8	26.10
9	27.06
10	29.78
11	31.83
12	32.18

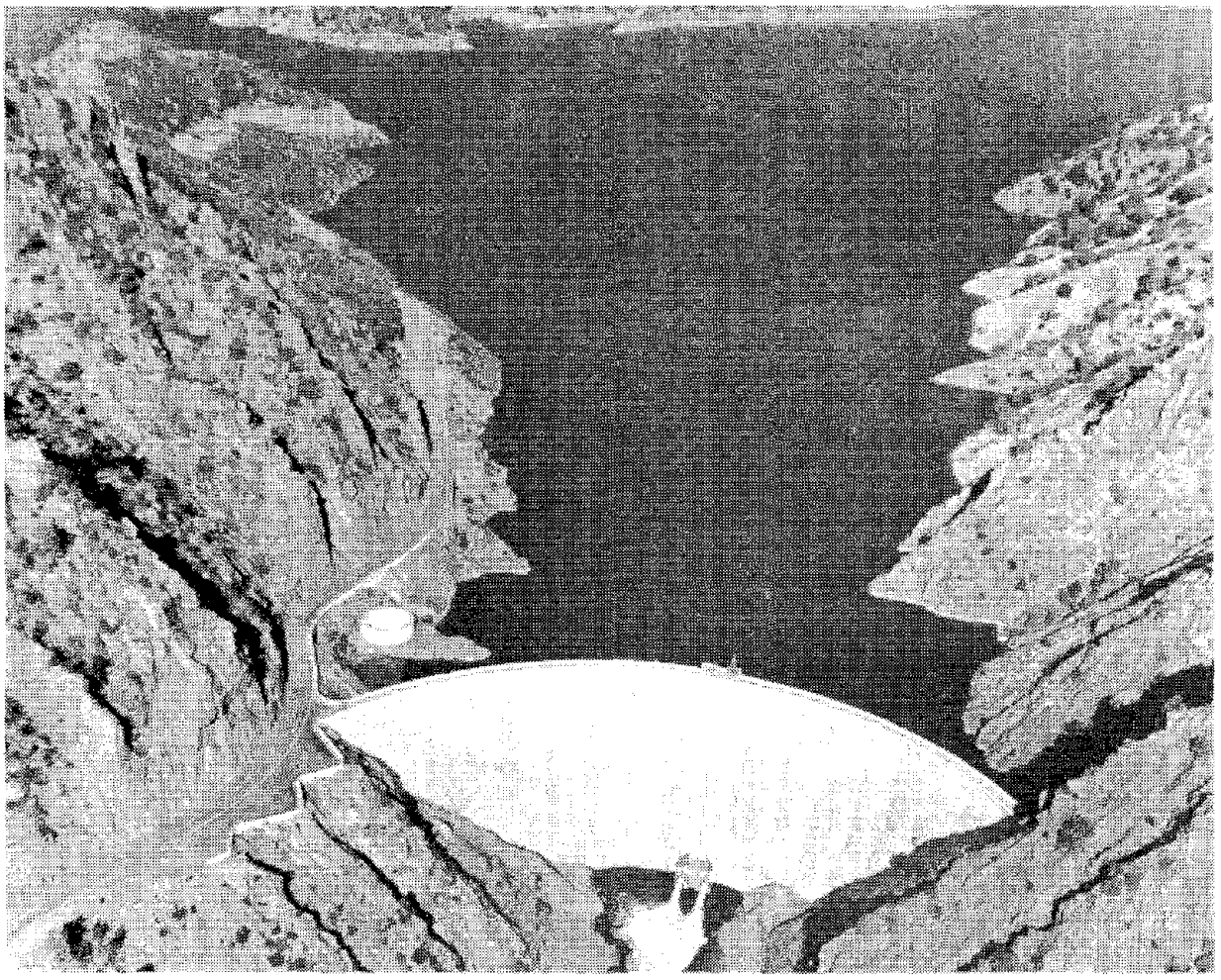

Fig. 1.1 Aerial View of U.S.B.R. Monticello Dam, California (from Reference 4)

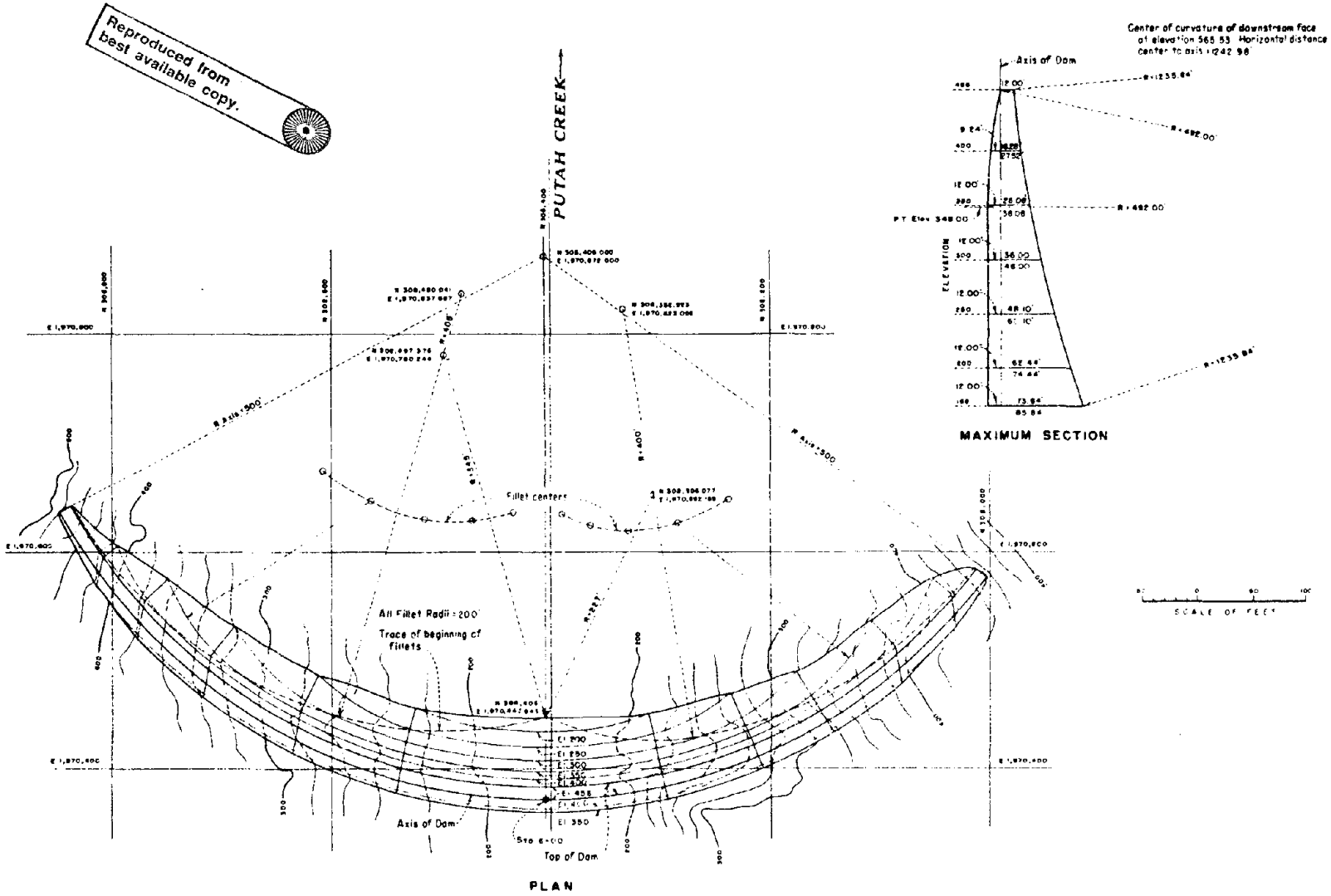

Fig. 2.1 Monticello Dam, Plan and Section Views (from Reference 4)

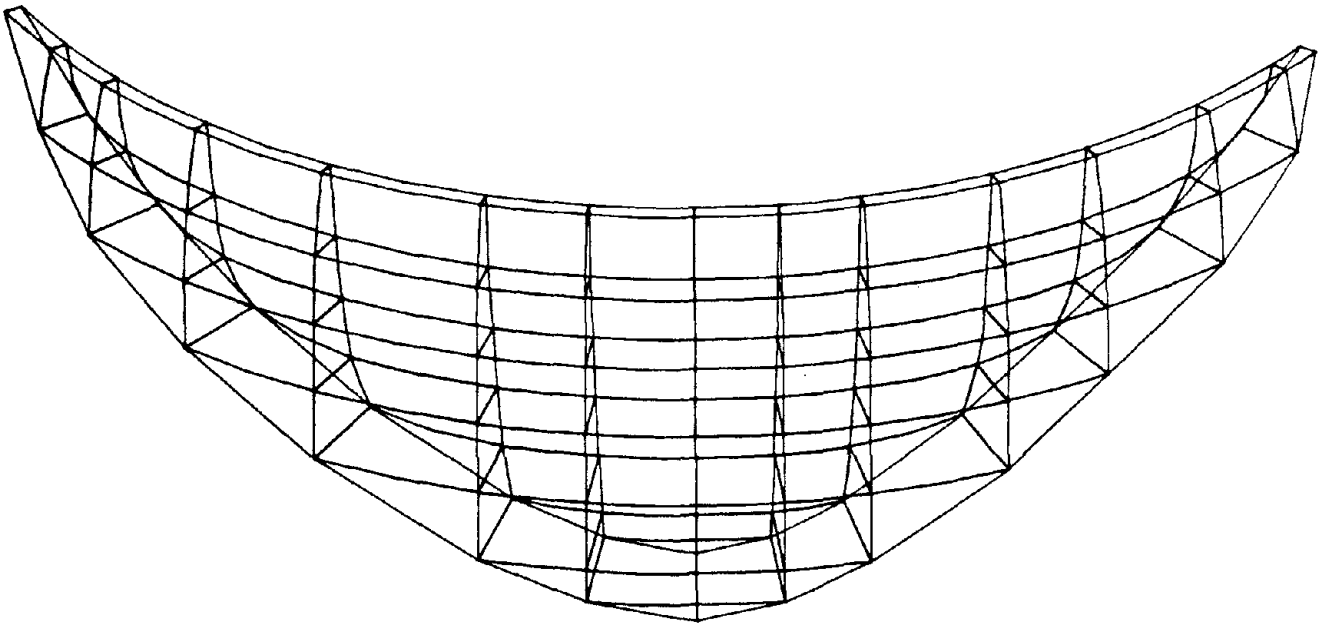

Fig. 2.2 Finite Element Model Monticello Dam

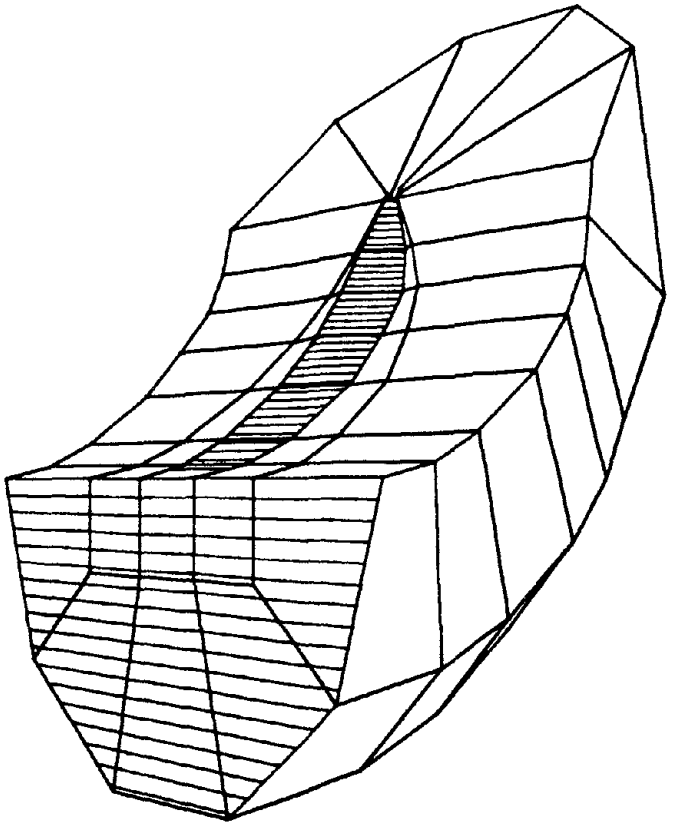

Fig. 2.3 Perspective View of Foundation Model, Right Half

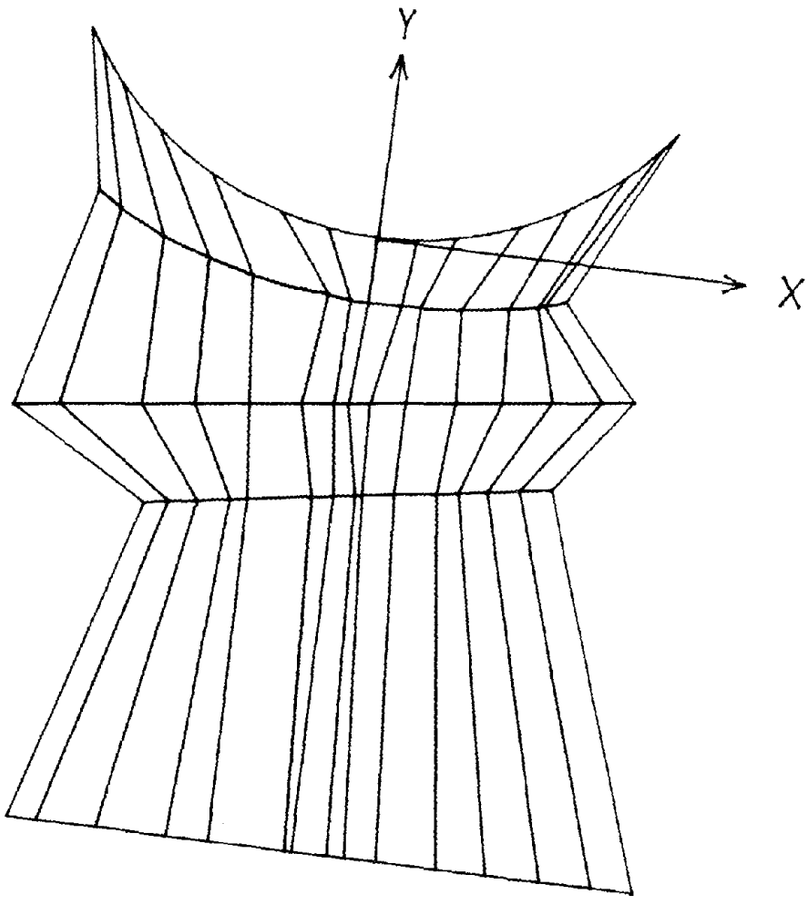

(a) Plan View

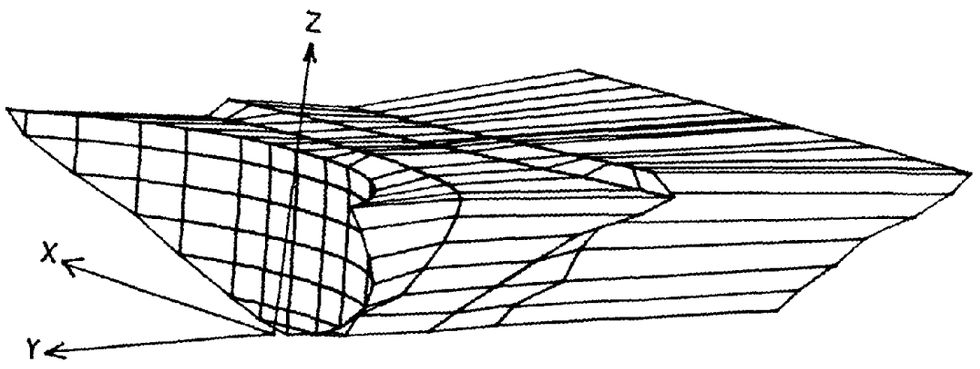

(b) Isometric View

Fig. 2.4 Finite Element Reservoir Model

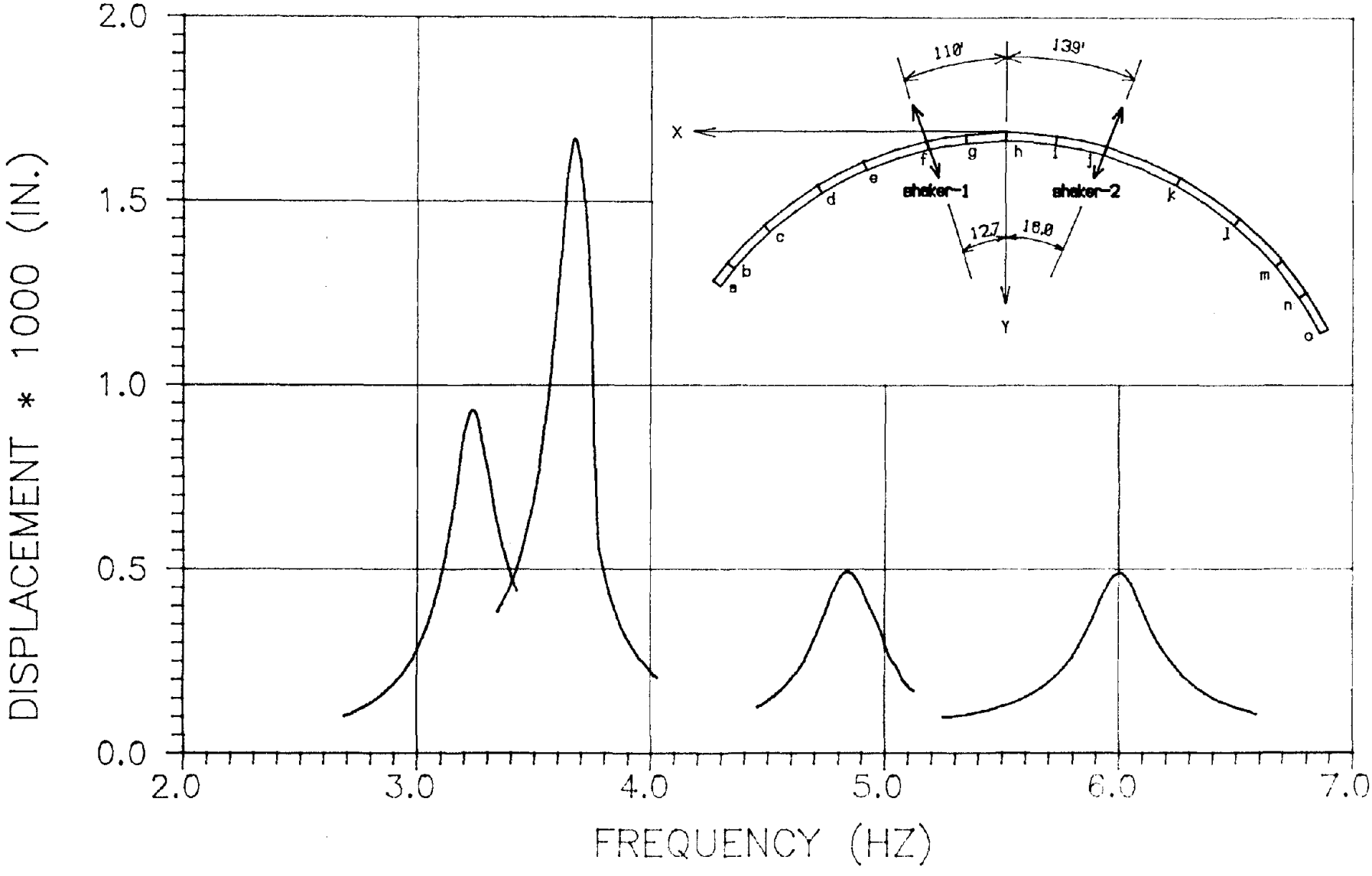

Fig. 2.5 Calculated Crest Displacement Response and Shaker Locations

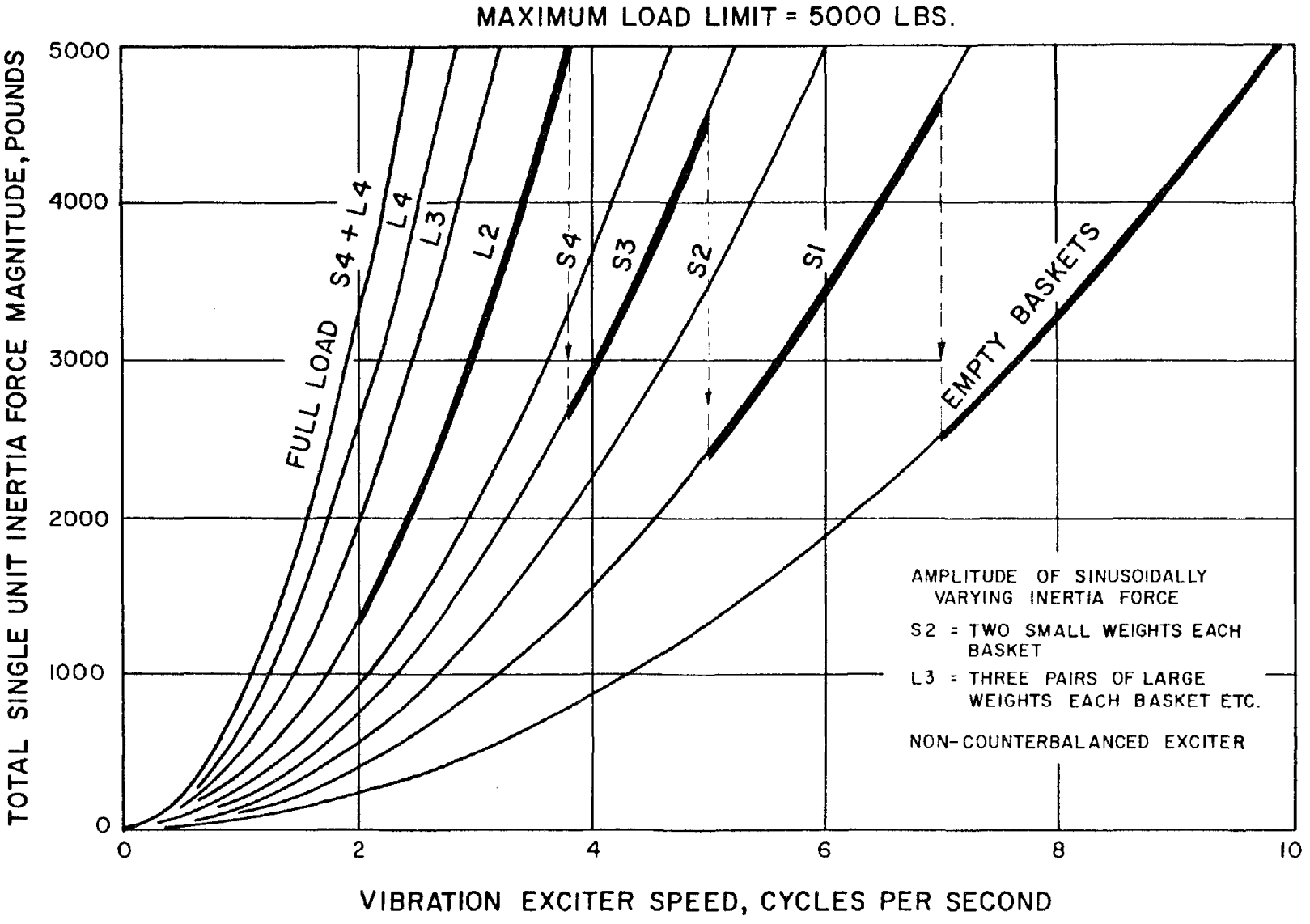

Fig. 2.6 Harmonic Force Output vs. Speed of U.C. Shaking Machine
(Adapted from Reference 9)

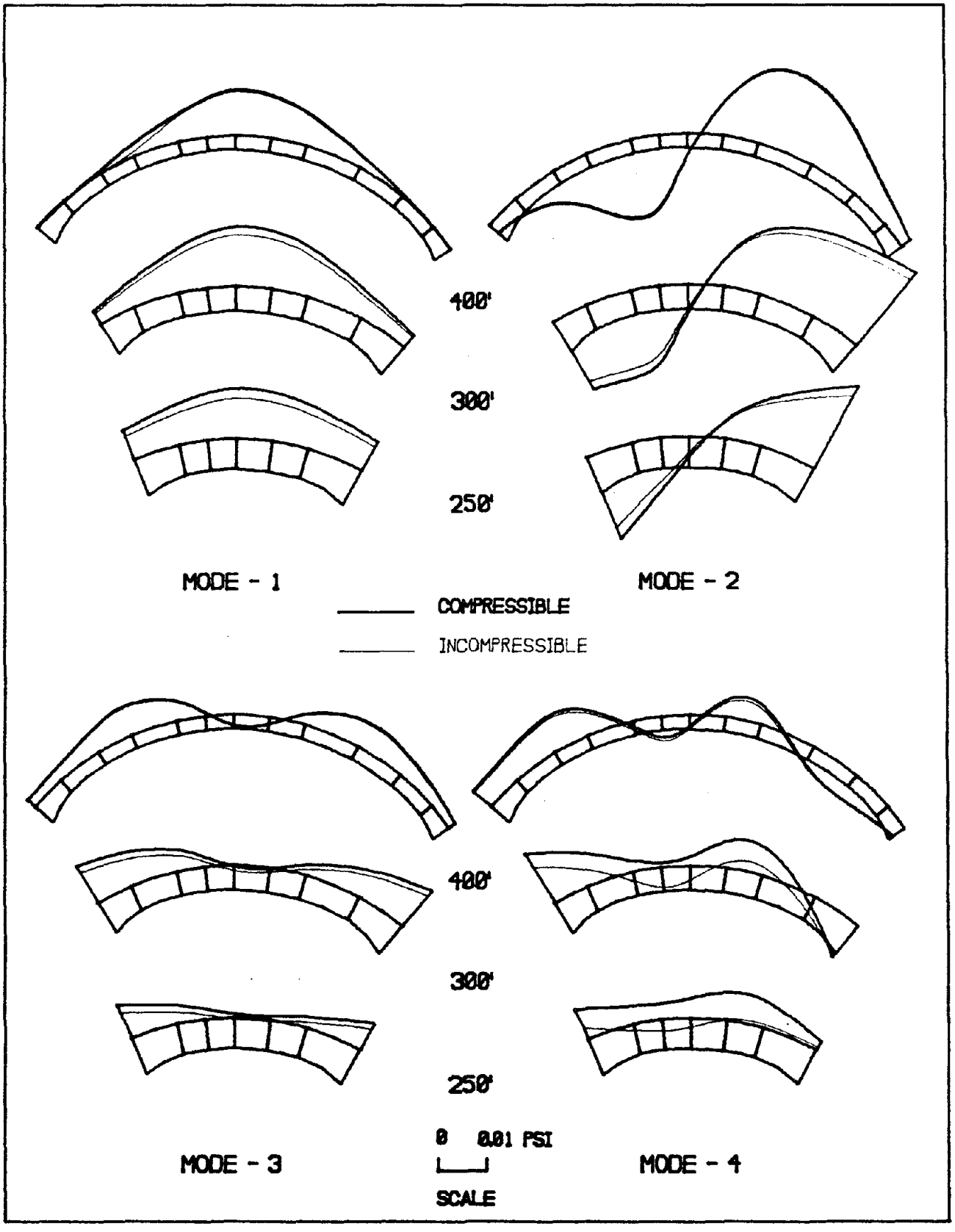

Fig. 2.7 Forced Vibration Pressures Calculated at Dam Face

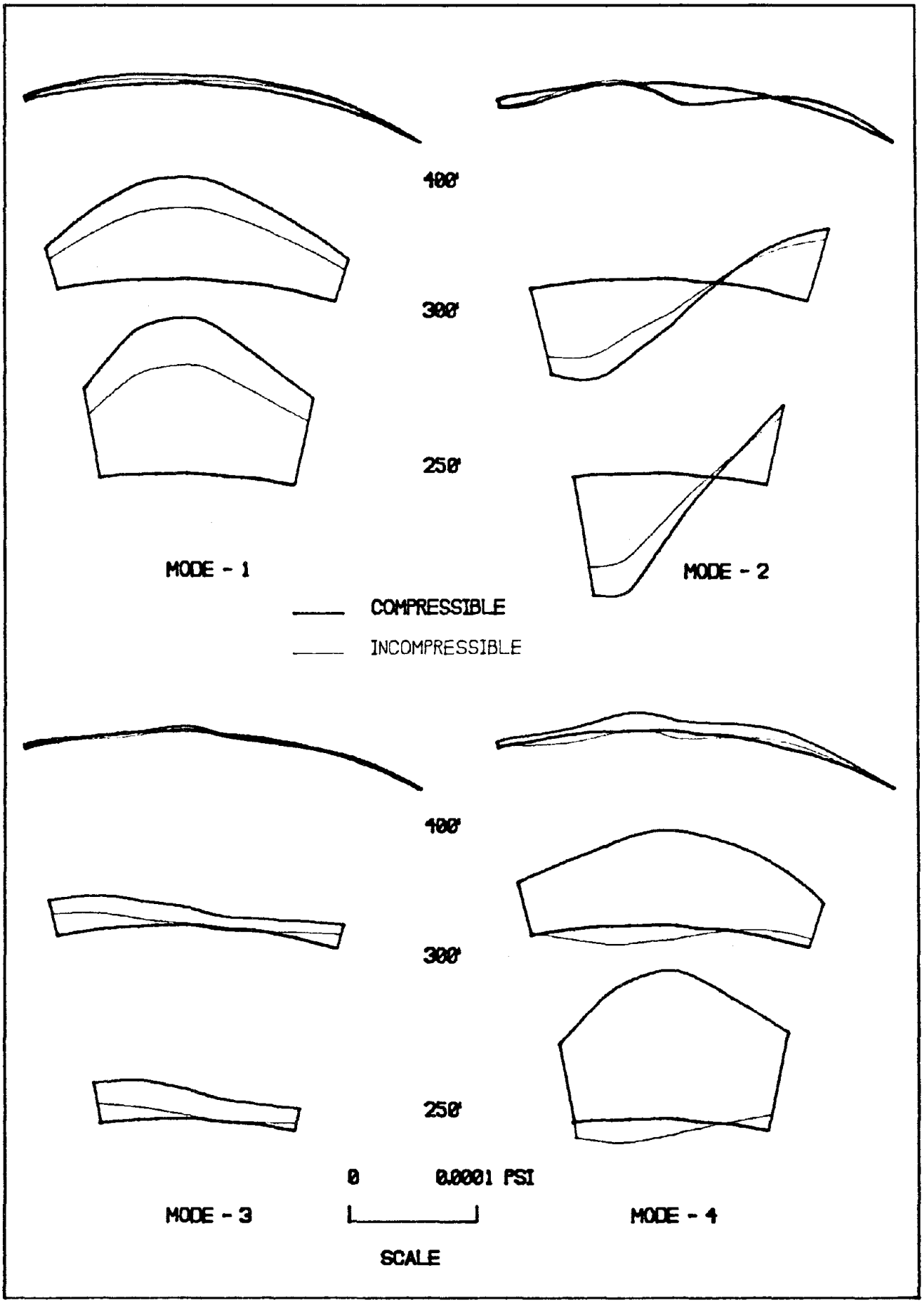

Fig. 2.8 Forced Vibration Pressures Calculated 98 ft From Dam Face

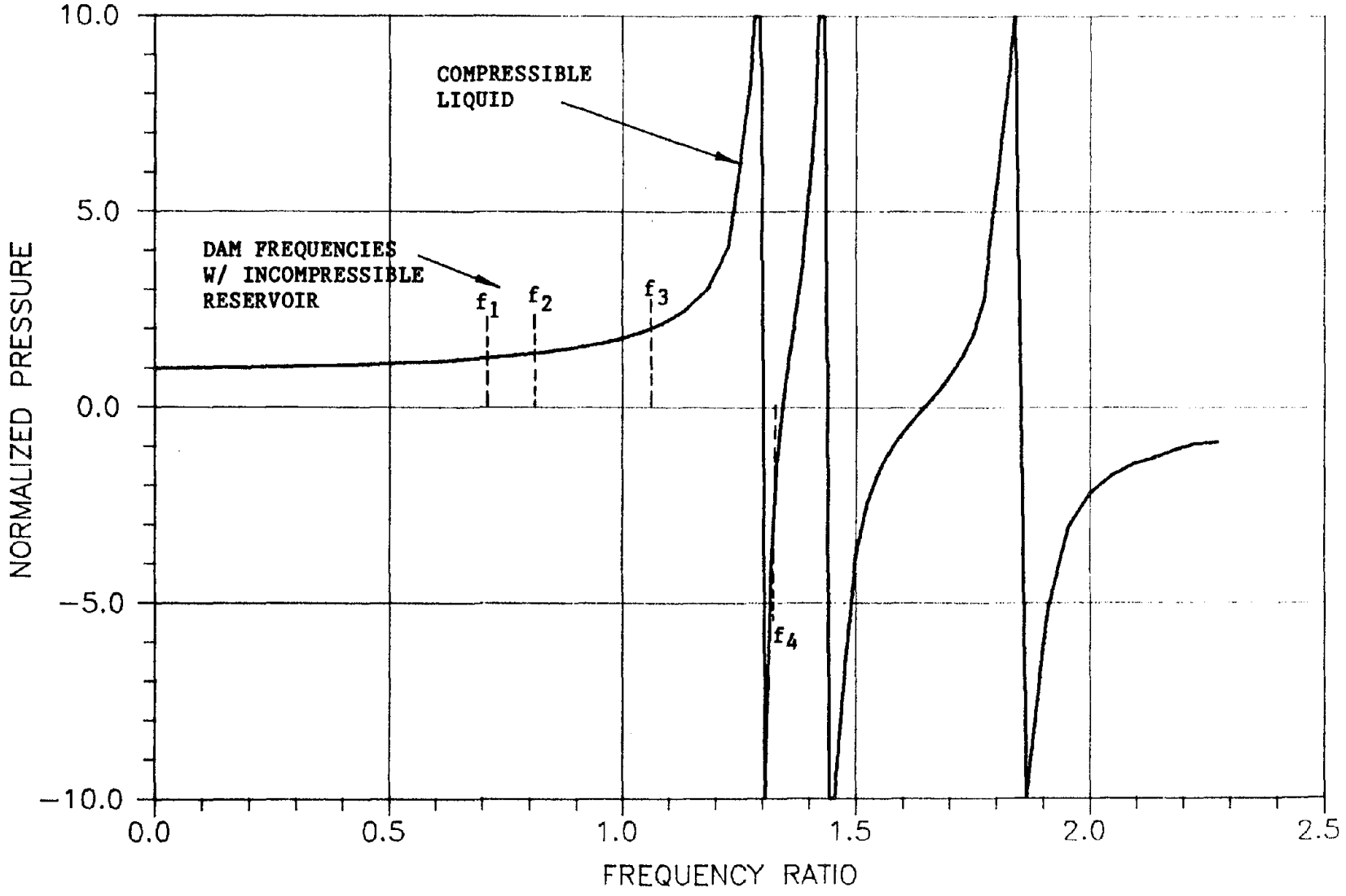

Fig. 2.9 Normalized Pressure at Base of Face; Rigid Dam Upstream Excitation

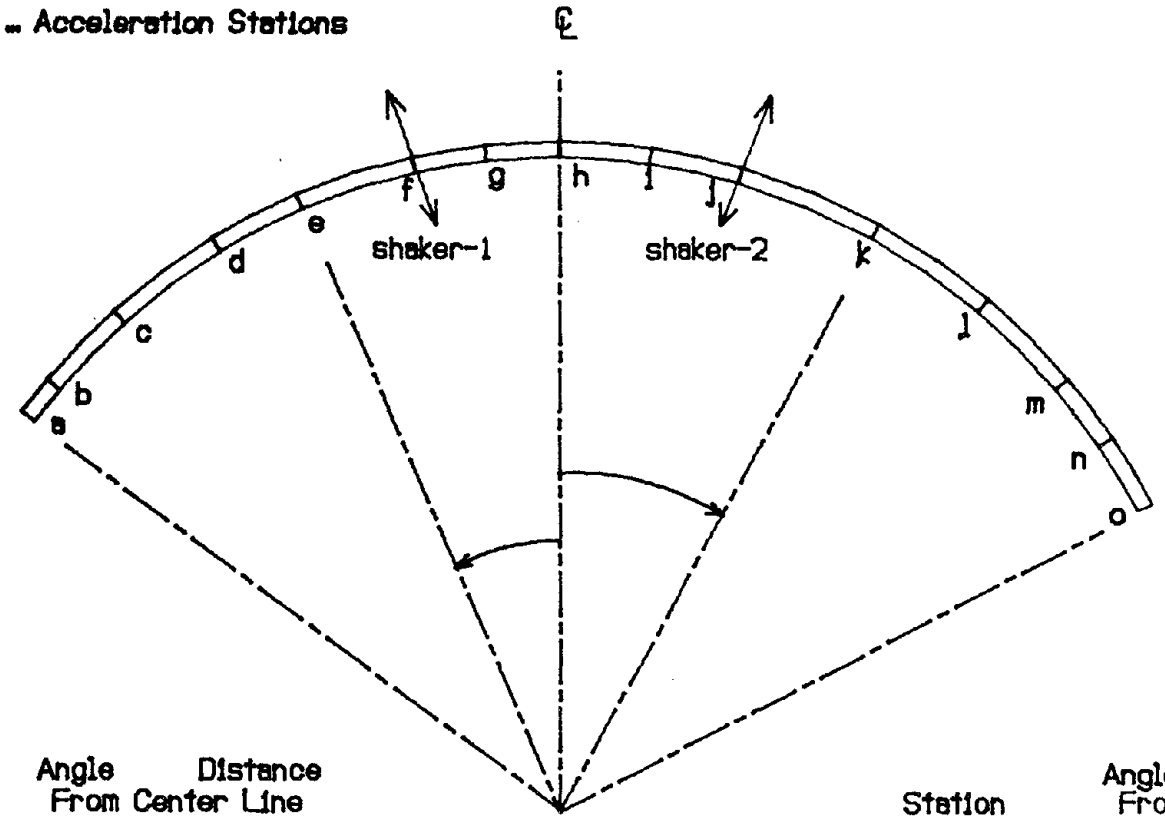

Station	Angle From Center Line	Distance
a	53.5	466.87
b	50.0	436.33
c	41.8	364.77
d	31.3	273.14
e	23.2	202.46
f	12.7	110.83
g	6.35	55.41

Station	Angle From Center Line	Distance
h	0.0	0.00
i	8.0	69.81
j	16.0	139.63
k	28.7	250.45
l	40.0	349.06
m	49.6	432.84
n	55.9	487.82
o	62.5	545.42

Fig. 3.1 Shaking Machine Locations and Accelerometer Stations on Dam Crest

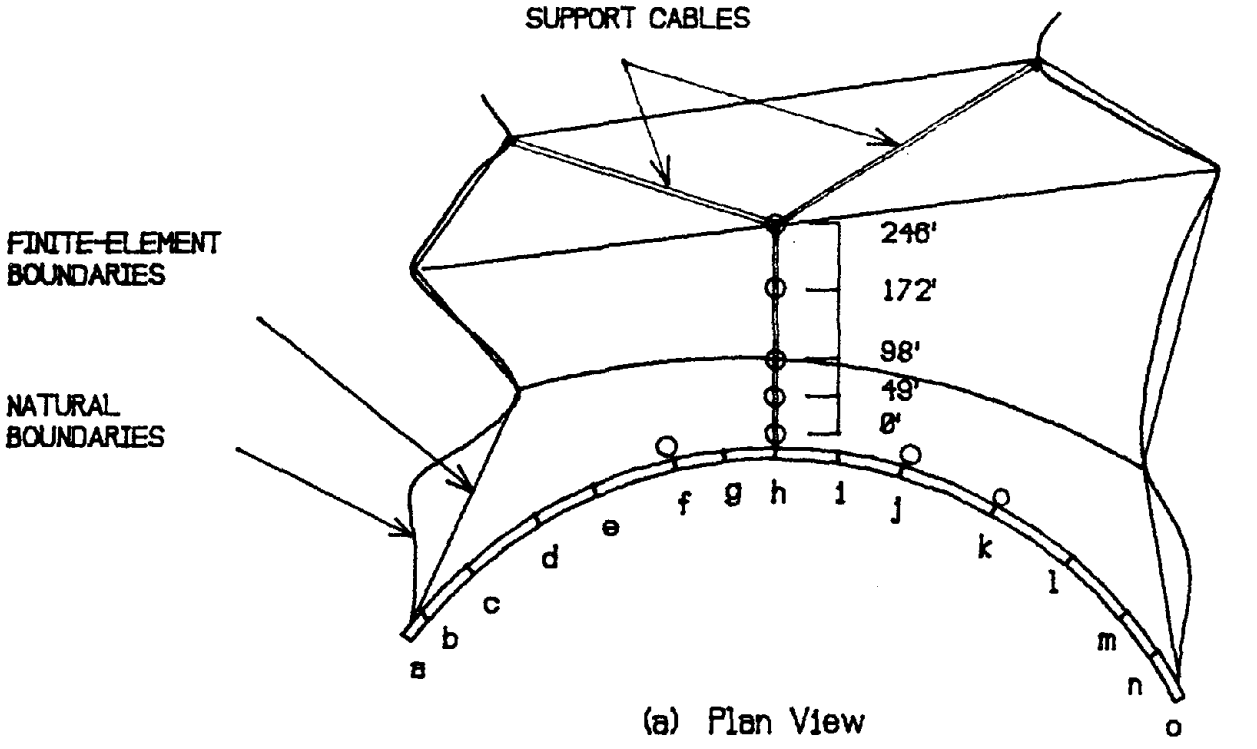

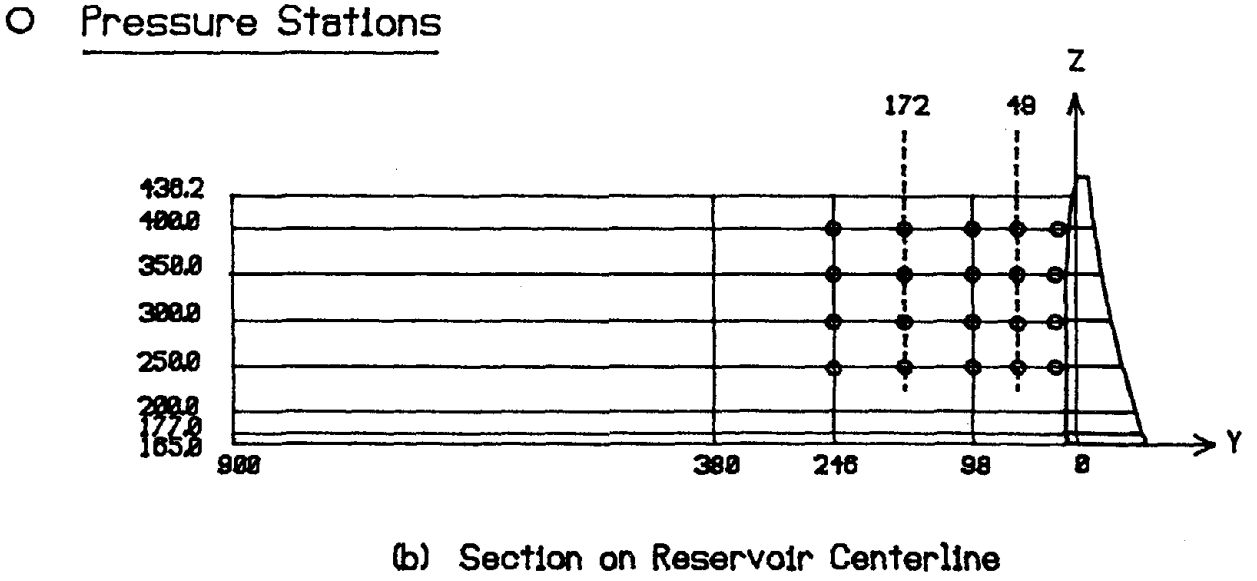

Fig. 3.2 Locations of Hydrodynamic Pressure Gage Stations

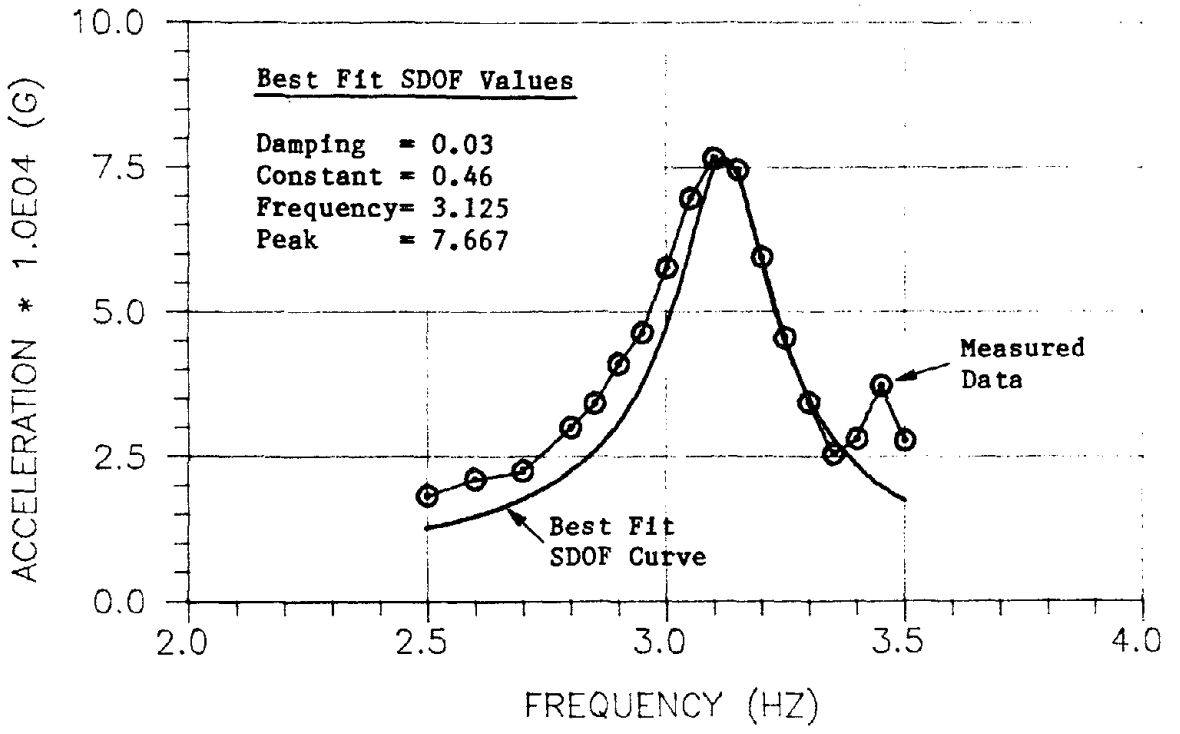

Fig. 3.3 Measured Data and Smoothed Crest Acceleration Response Curve, f_1 = 3.125 Hz

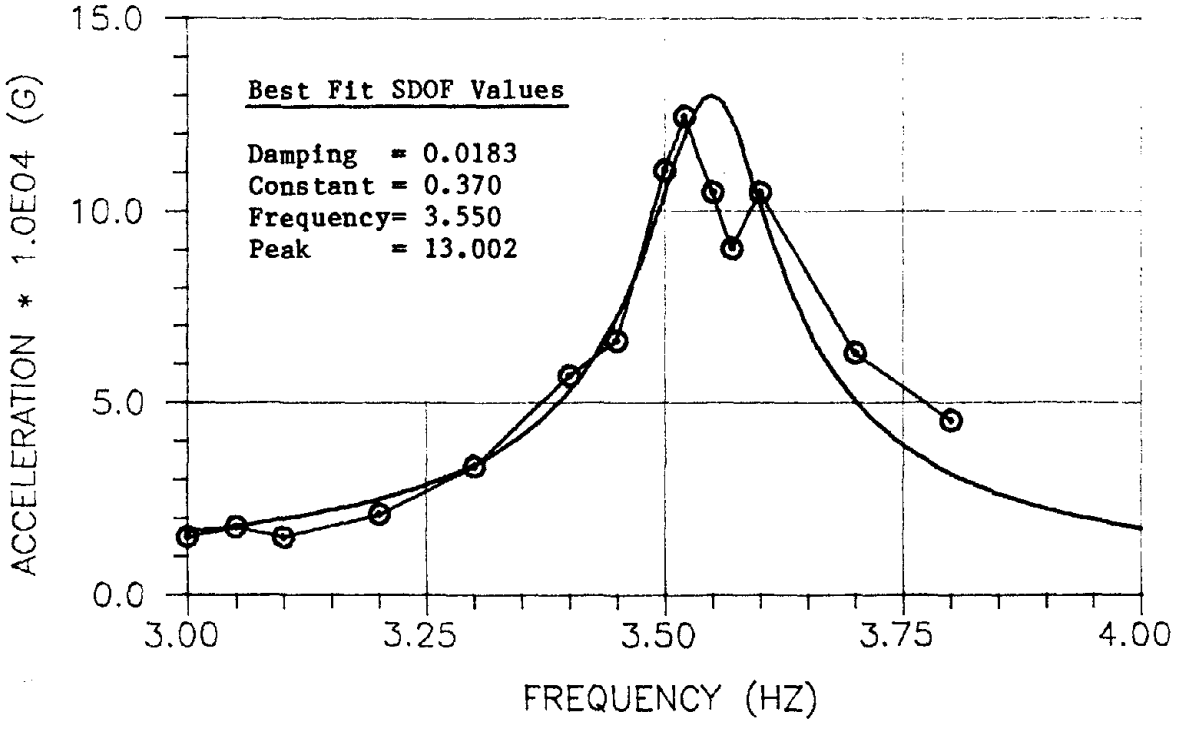

Fig. 3.4 Measured Data and Smoothed Crest Acceleration Response Curve, f_2 = 3.55 Hz

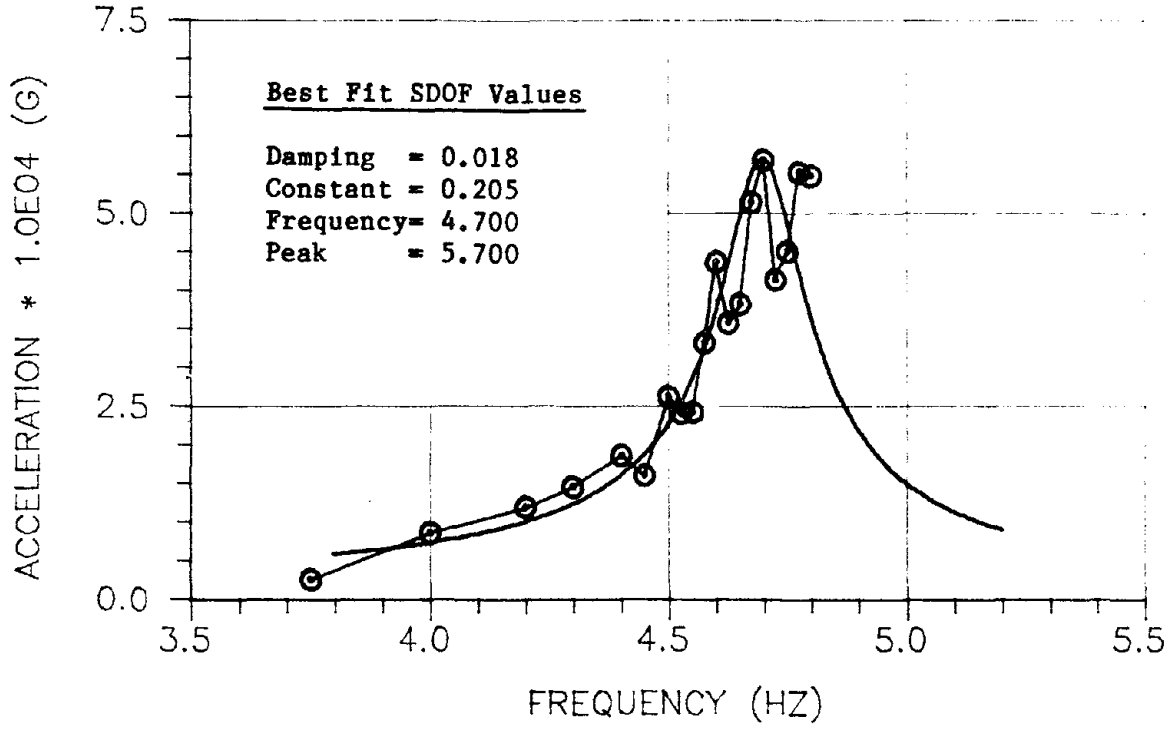

Fig. 3.5 Measured Data and Smoothed Crest Acceleration Response Curve, f_3 = 4.70 Hz

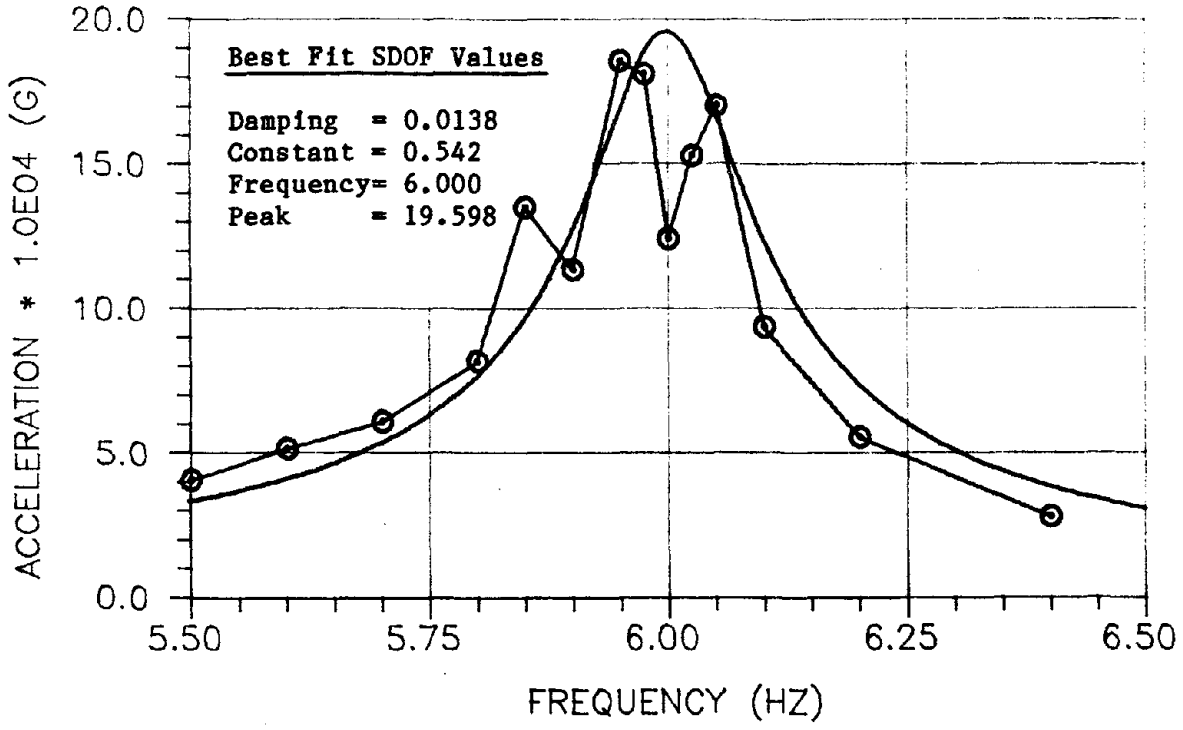

Fig. 3.6 Measured Data and Smoothed Crest Acceleration Response Curve, f_4 = 6.00 Hz

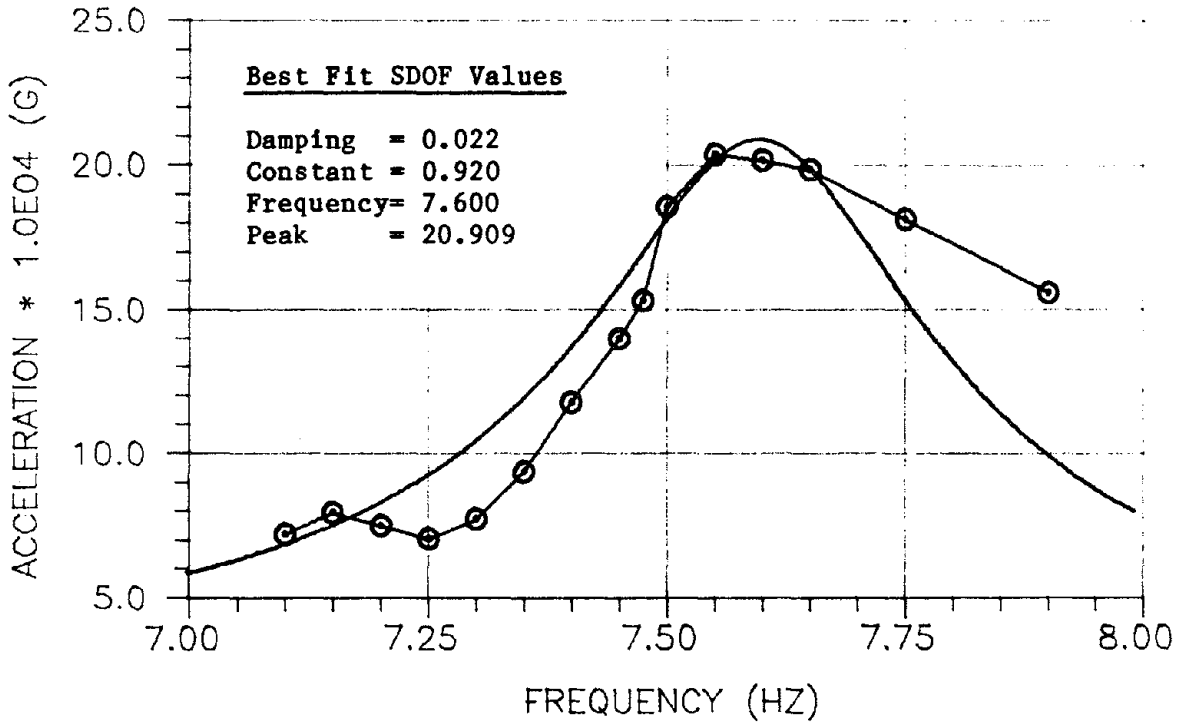

Fig. 3.7 Measured Data and Smoothed Crest Acceleration Response Curve, f_6 = 7.60 Hz

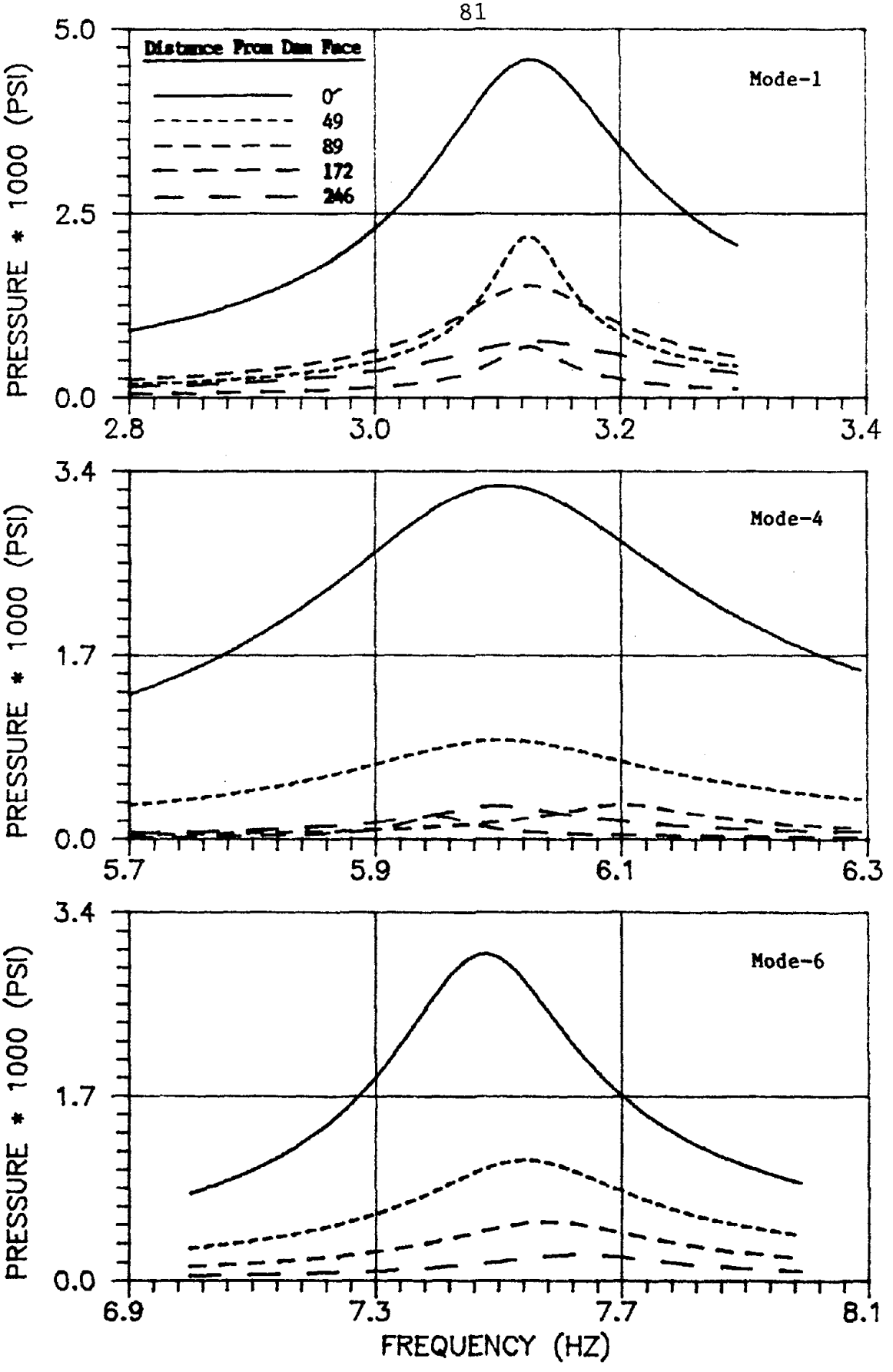

Fig. 3.8 Smoothed Measured Pressure Response Curves Mid-section at 400 ft Elevation

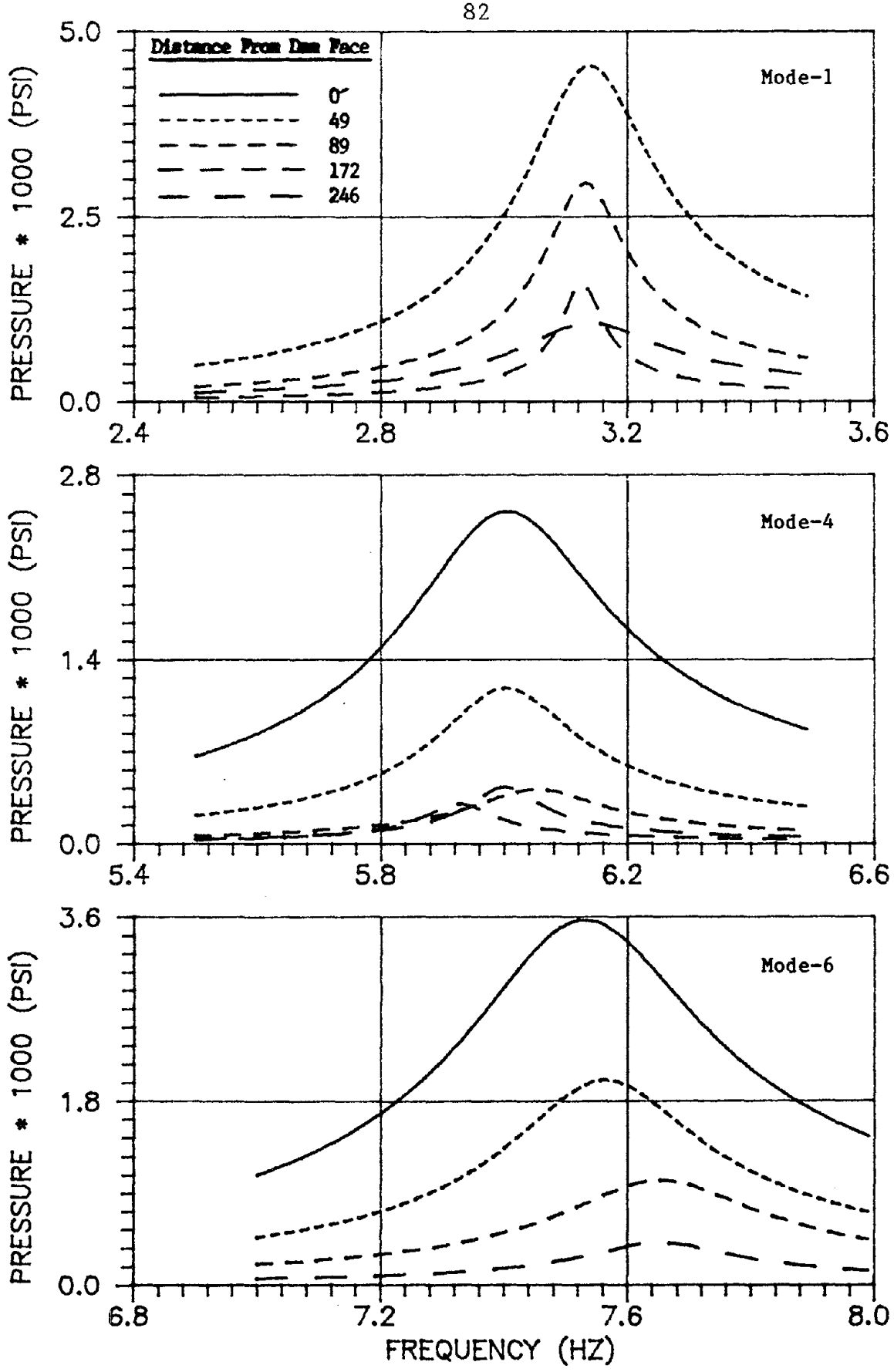

Fig. 3.9 Smoothed Measured Pressure Response Curves
Mid-section at 350 ft Elevation

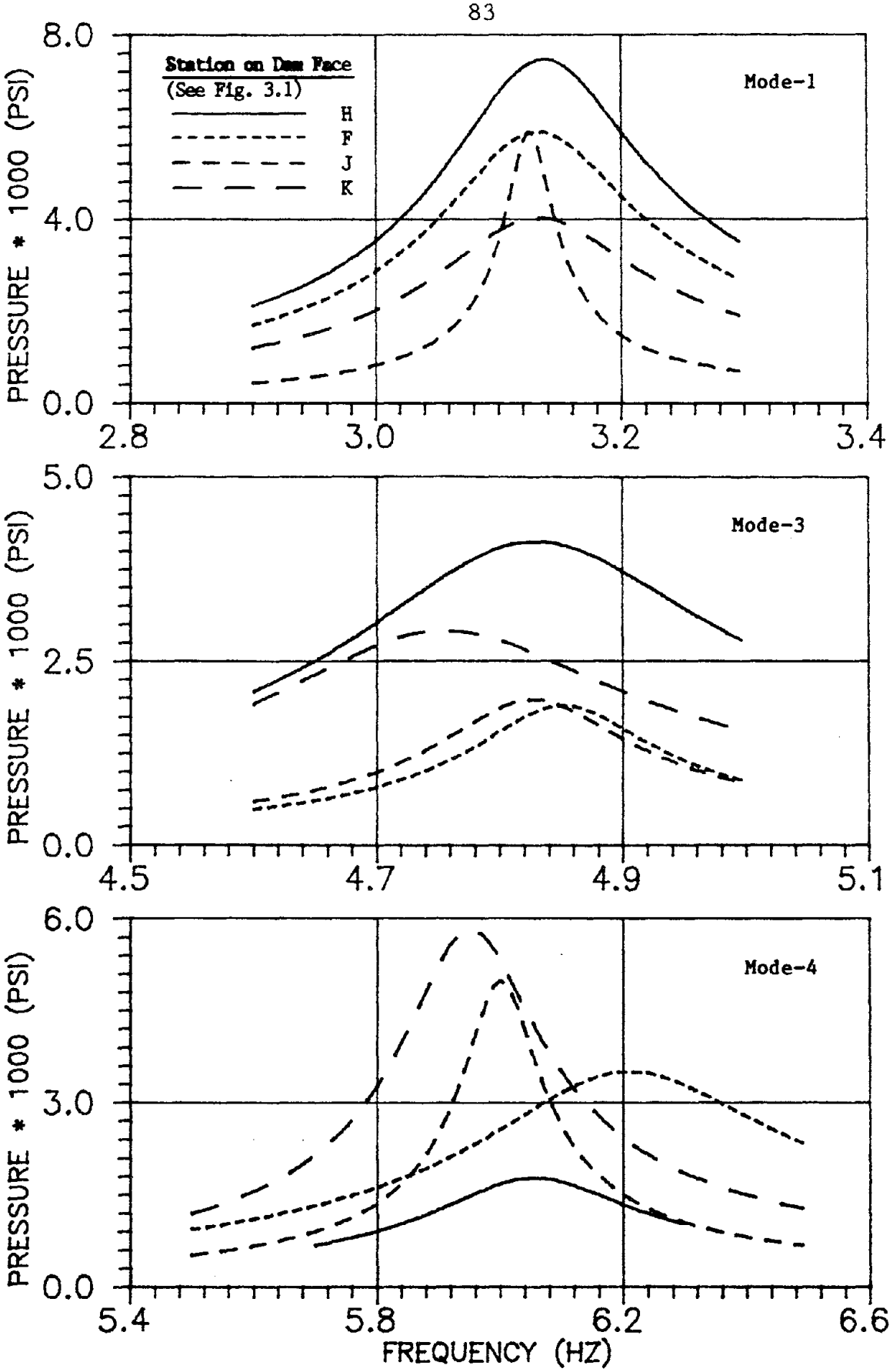

Fig. 3.10 Smoothed Measured Pressure Response Curves
Dam Face at 300 ft Elevation

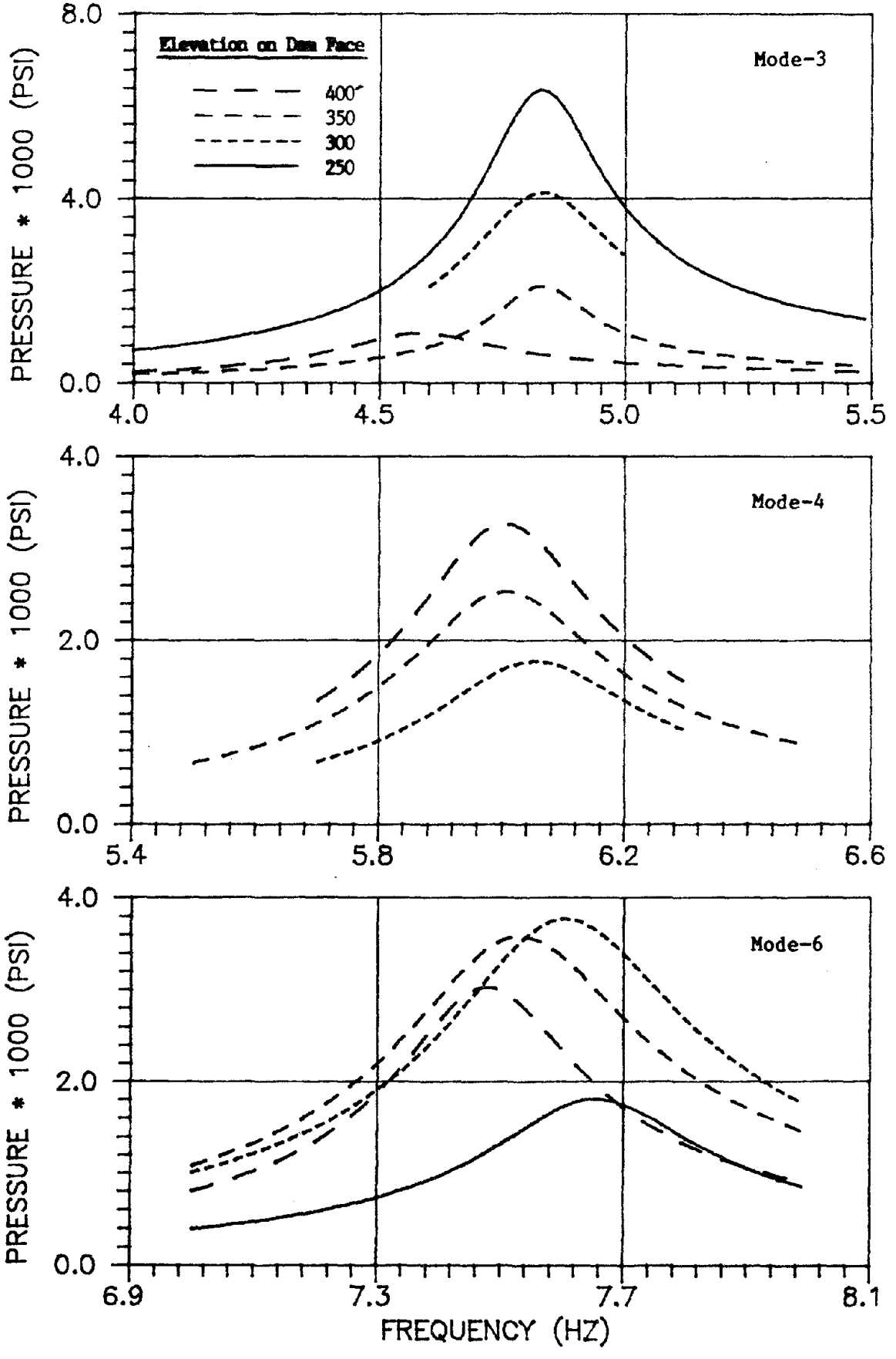

Fig. 3.11 Smoothed Measured Pressure Response Curves
Mid-section of Dam Face

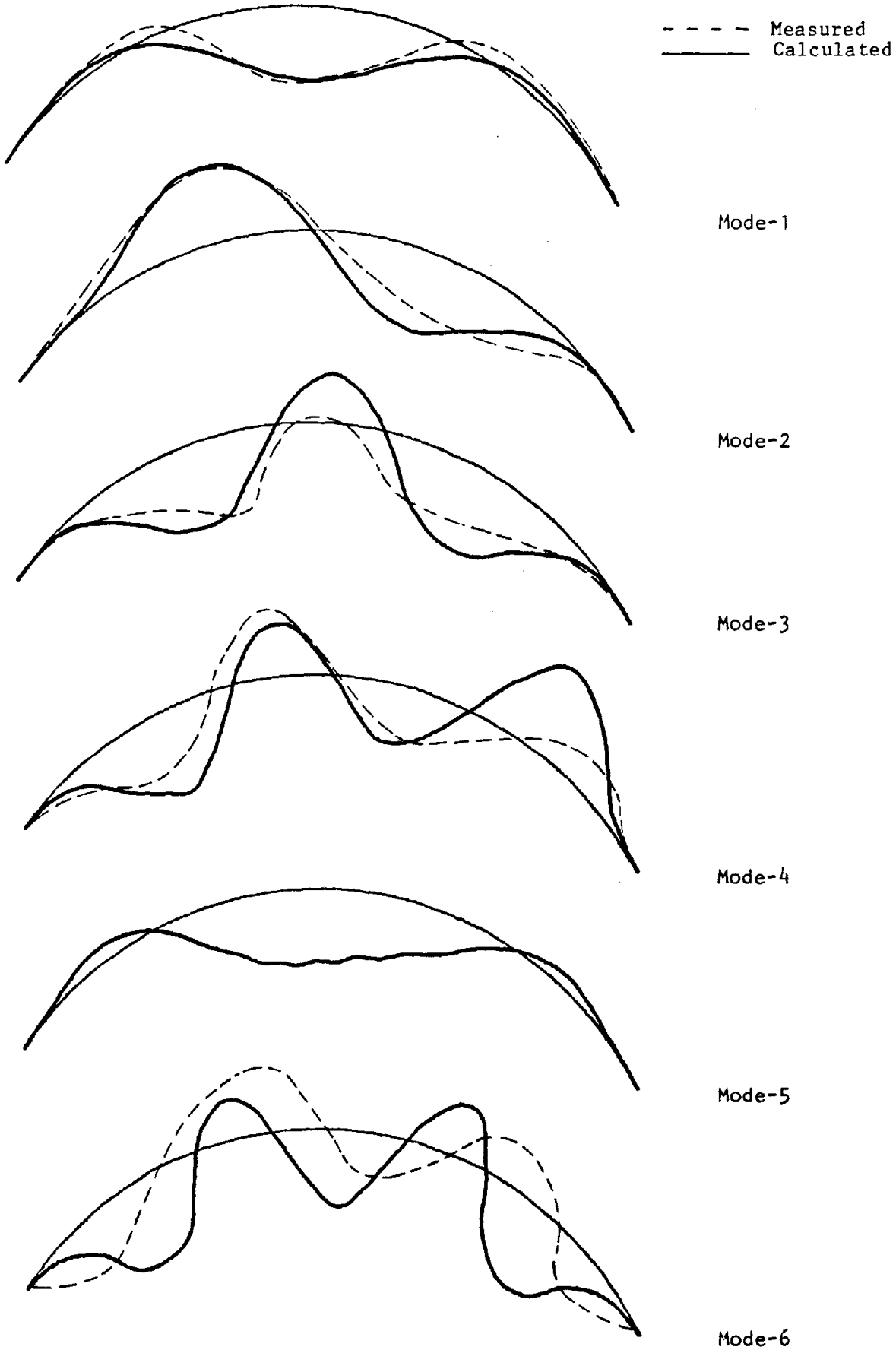

Fig. 4.1 Comparison of Measured and Calculated Vibration Mode Crest Displacements

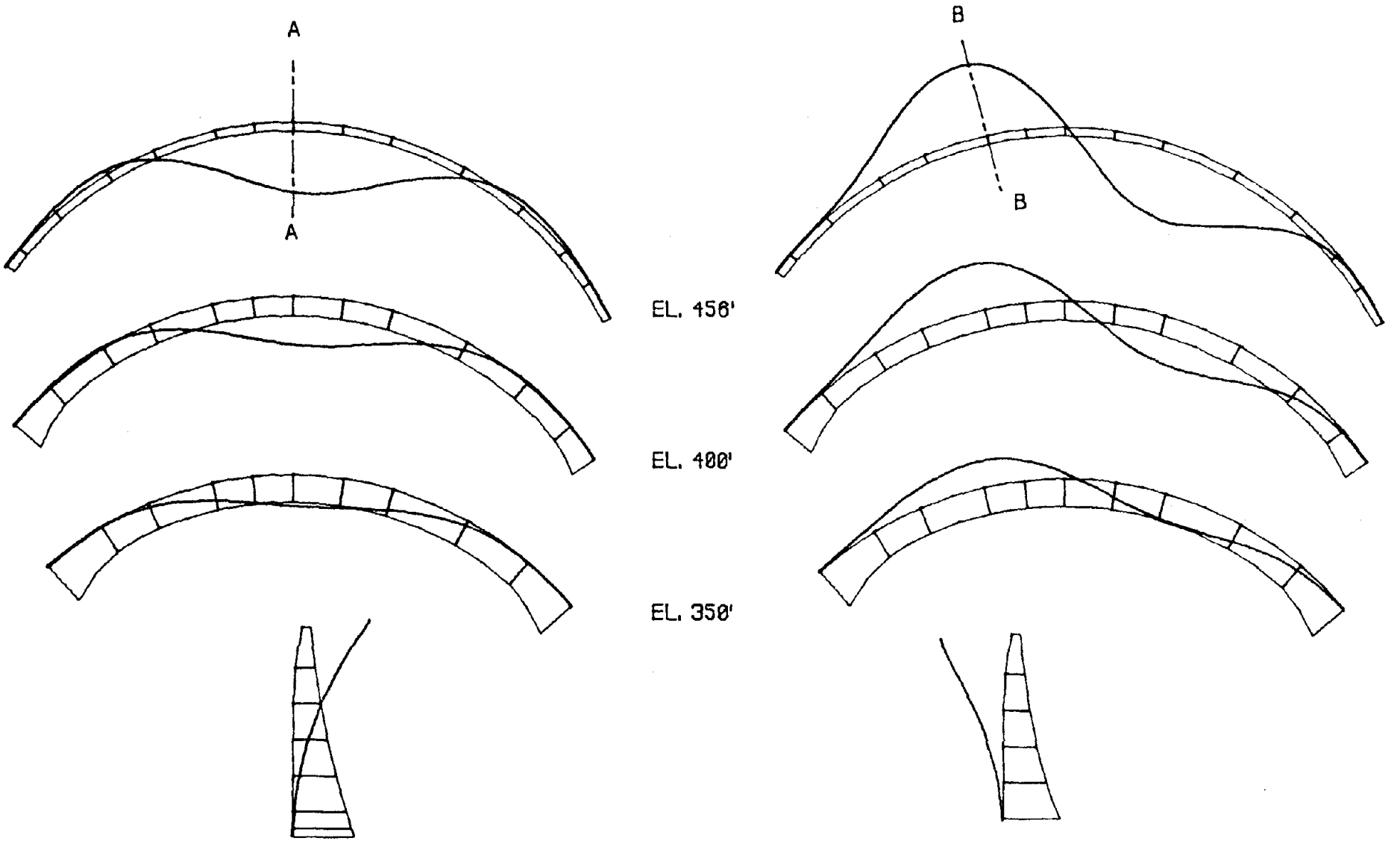

SECTION A-A

(a) Mode 1 : f_1 = 3.12 Hz

SECTION B-B

(b) Mode 2 : f_2 = 3.56 Hz

Fig. 4.2 Calculated Vibration Mode Shapes

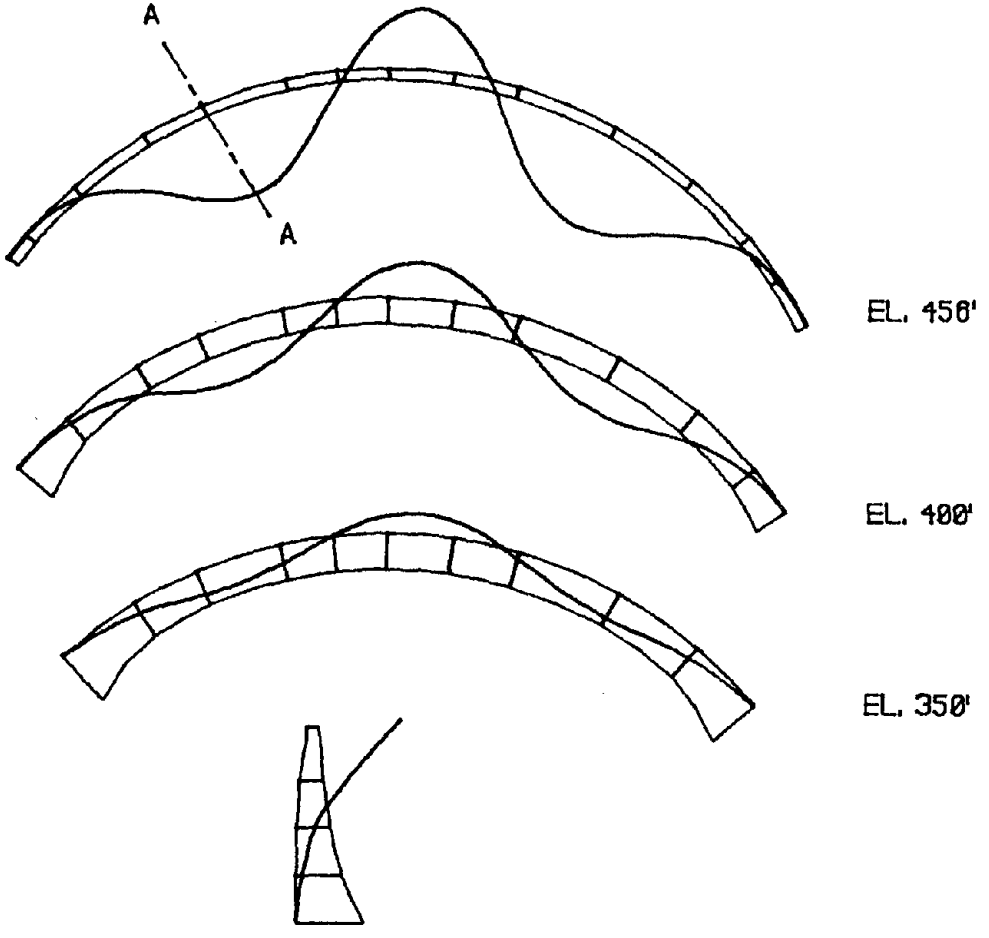

SECTION A-A

(c) Mode 3 : f_3 = 4.67 Hz

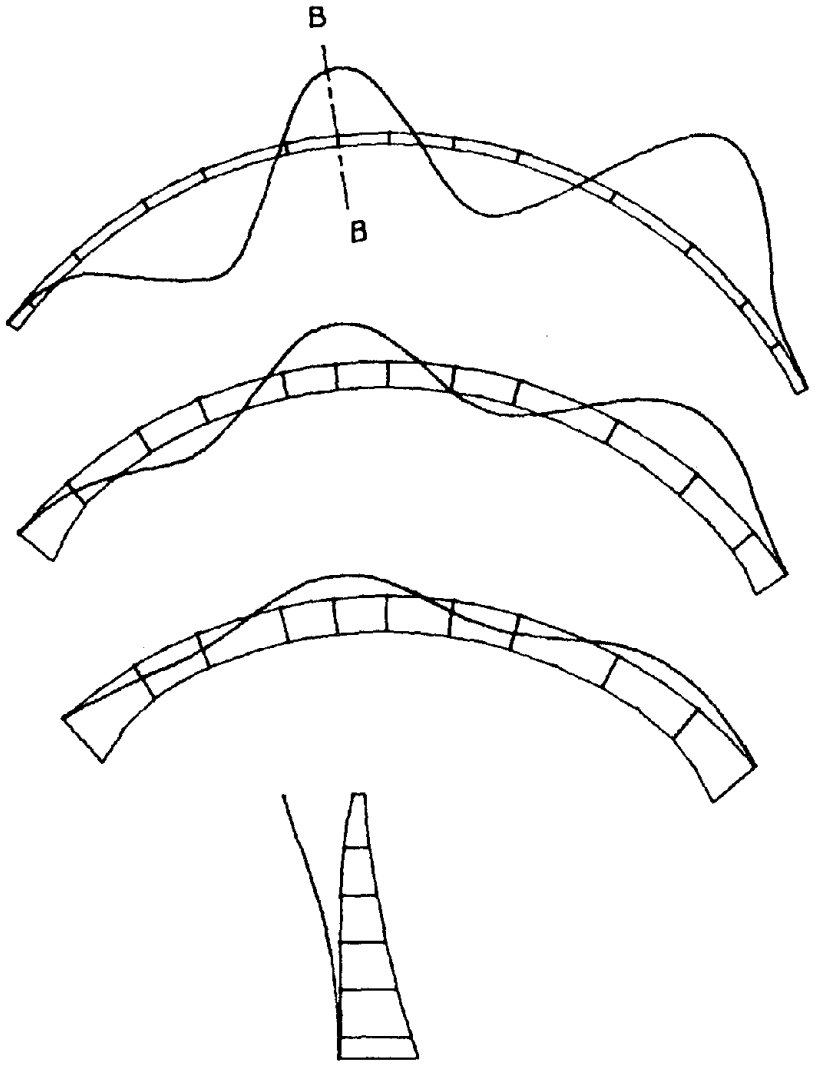

SECTION B-B

(d) Mode 4 : f_4 = 5.86 Hz

Fig. 4.2 Calculated Mode Shapes (Cont'd)

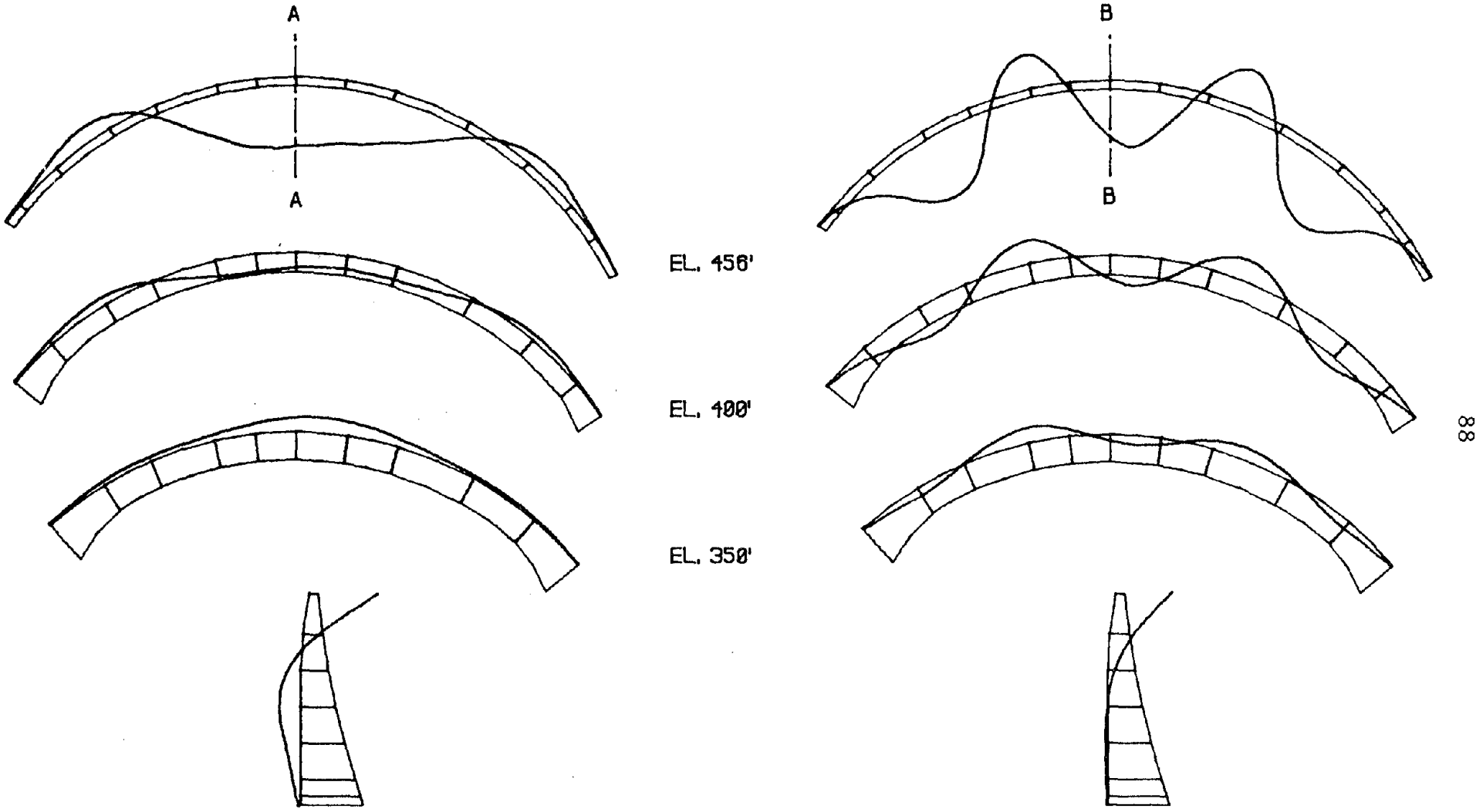

SECTION A-A

(e) Mode 5 : f_5 = 6.93 Hz

SECTION B-B

(f) Mode 6 : f_6 = 7.28 Hz

Fig. 4.2 Calculated Mode Shapes (Cont'd)

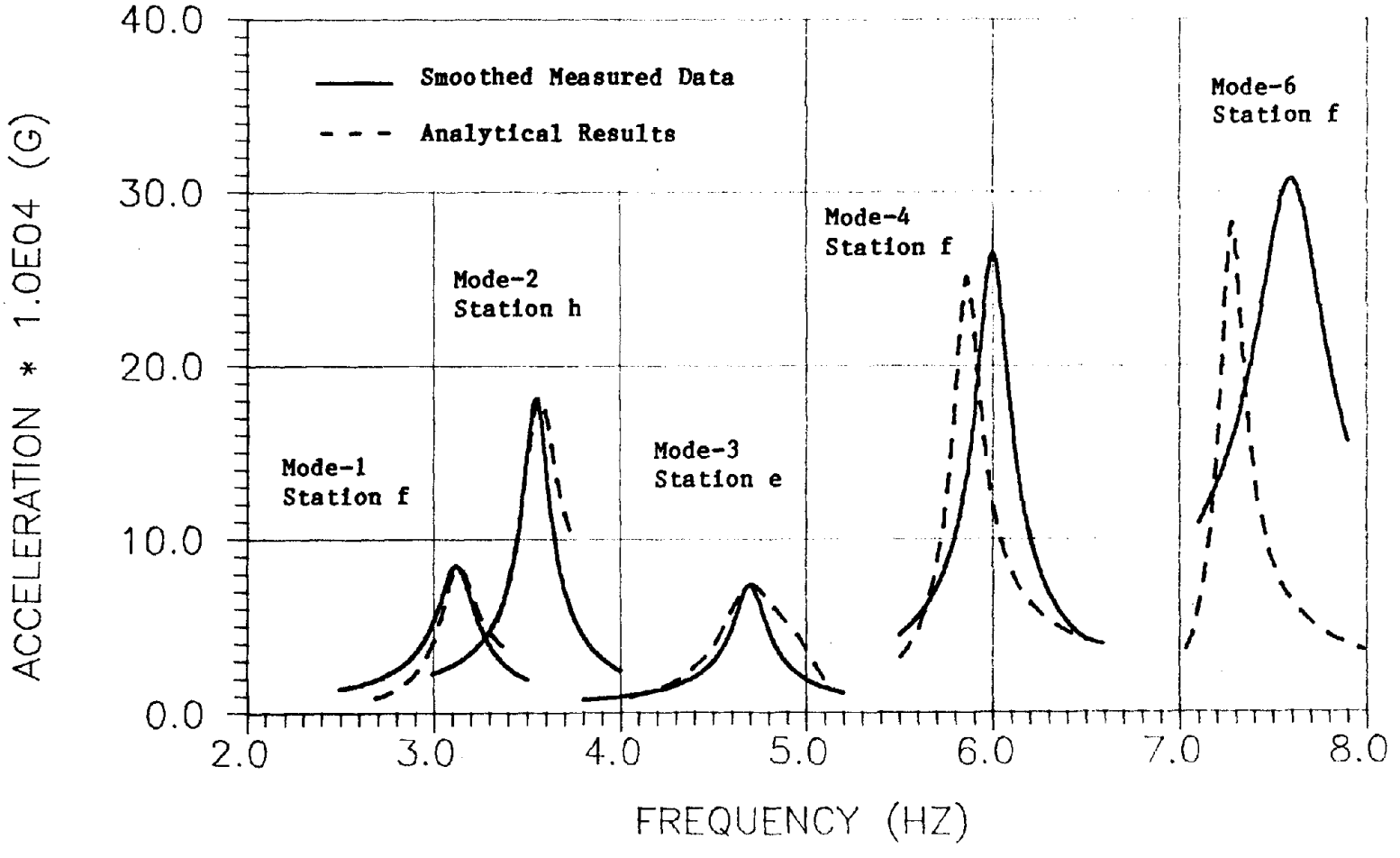

Fig. 4.3 Analytical and Experimental Crest Acceleration Response Curves

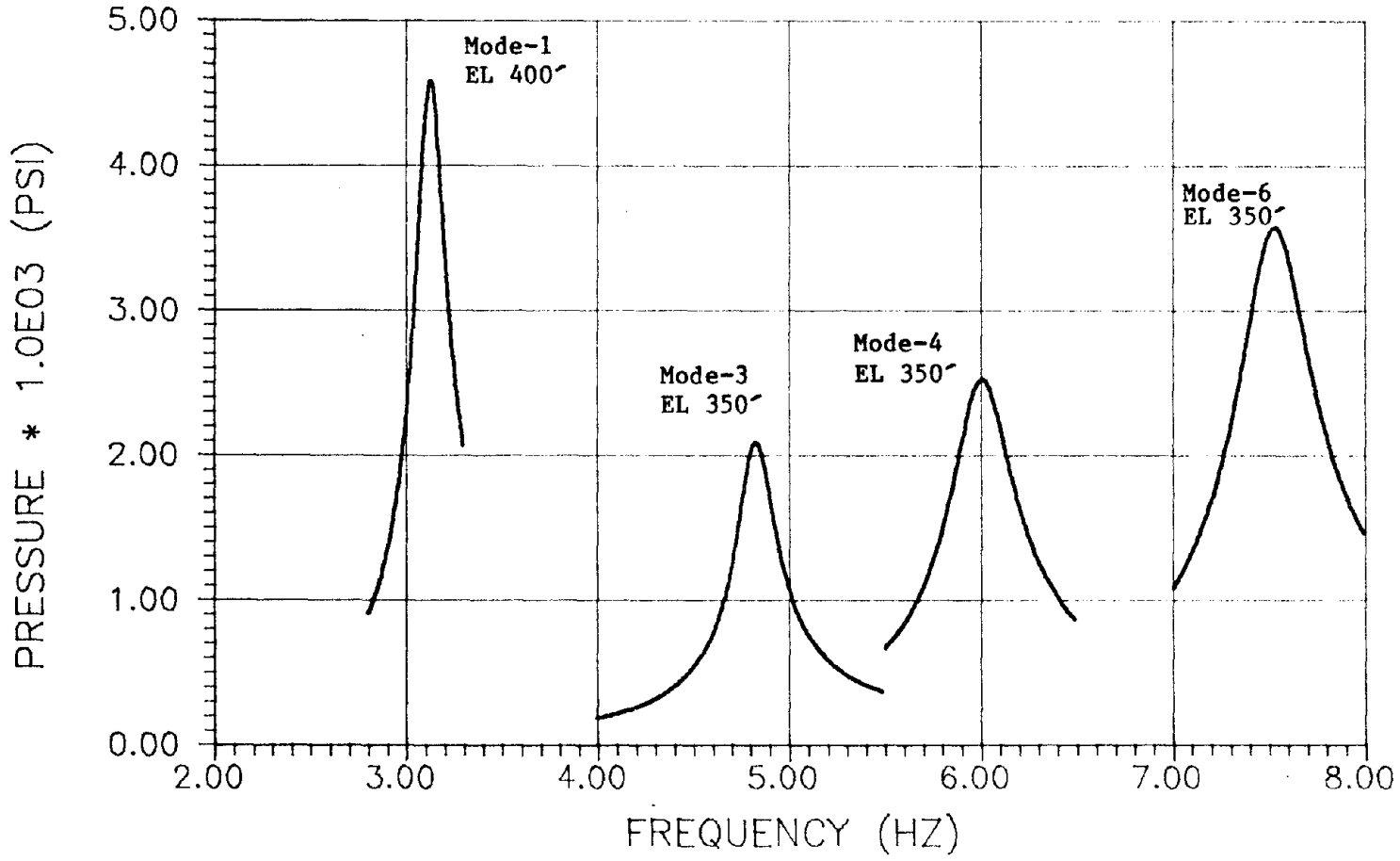

Fig. 4.4 Experimental Pressure Response Curves, Centerline of Dam Face

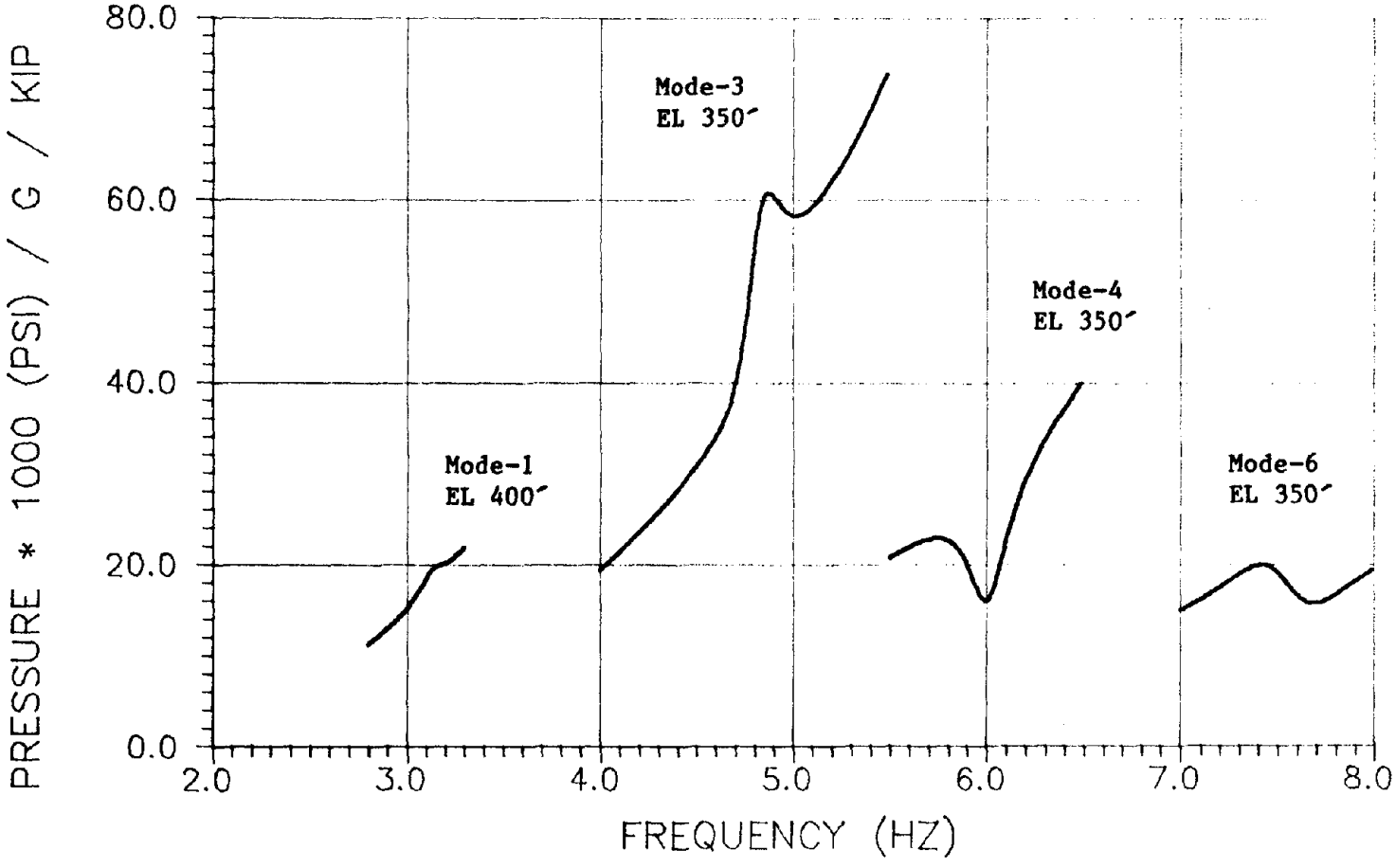

Fig. 4.5 Measured Face Centerline Pressures Divided by Measured Crest Accelerations

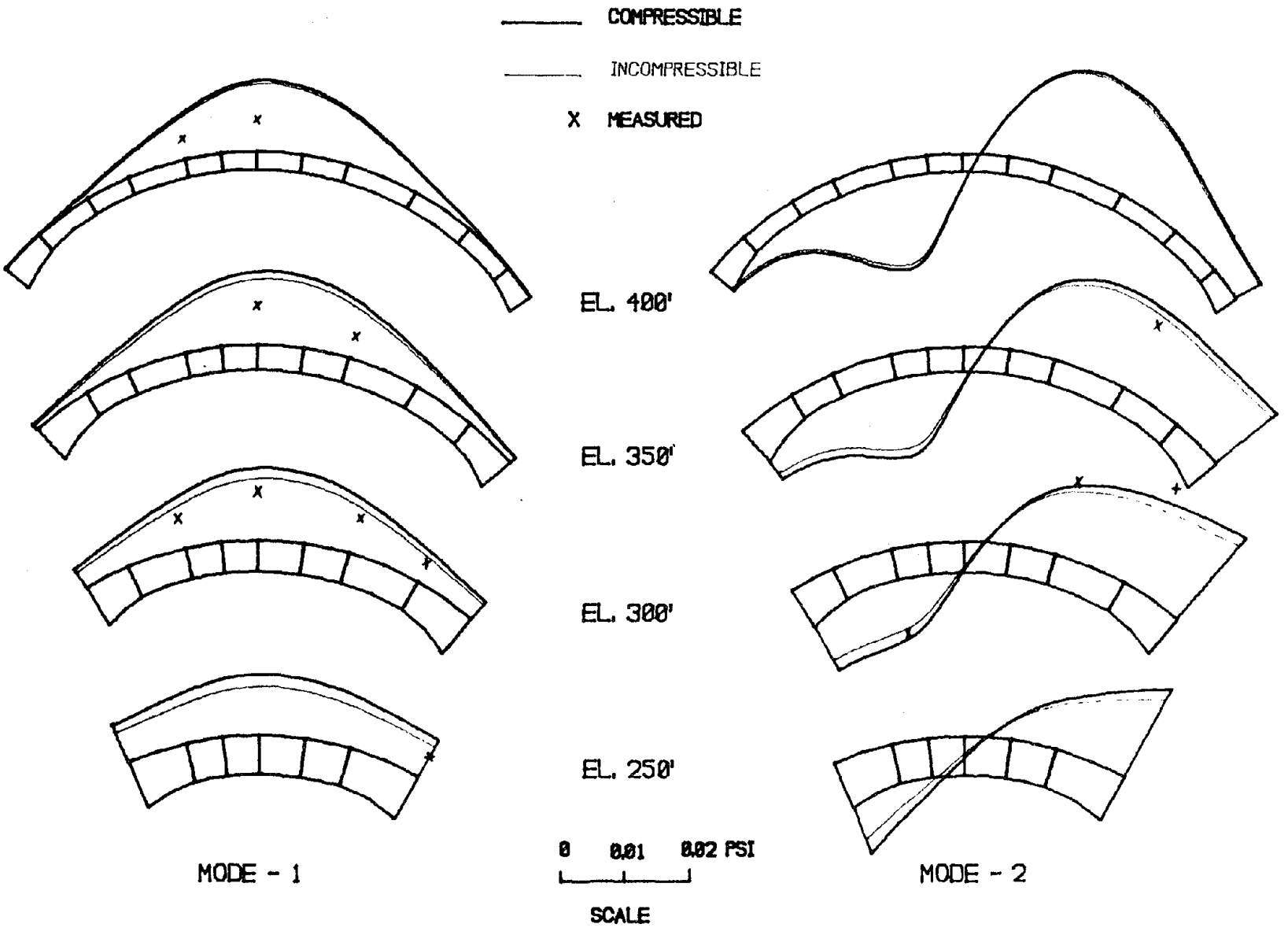

Fig. 4.6 Forced Vibration Hydrodynamic Pressures at Dam Face

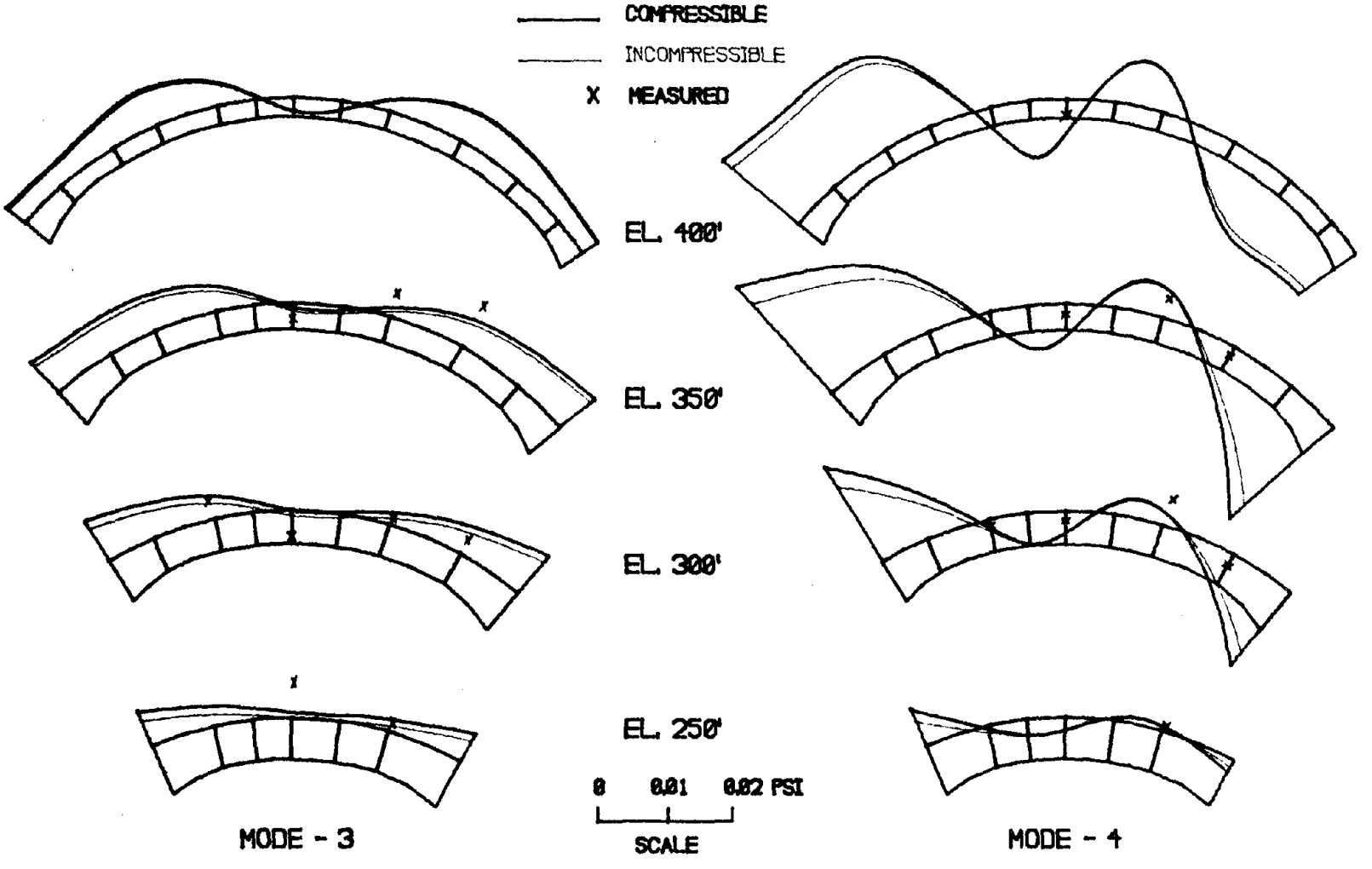

Fig. 4.6 Forced Vibration Hydrodynamic Pressures at Dam Face (Cont'd)

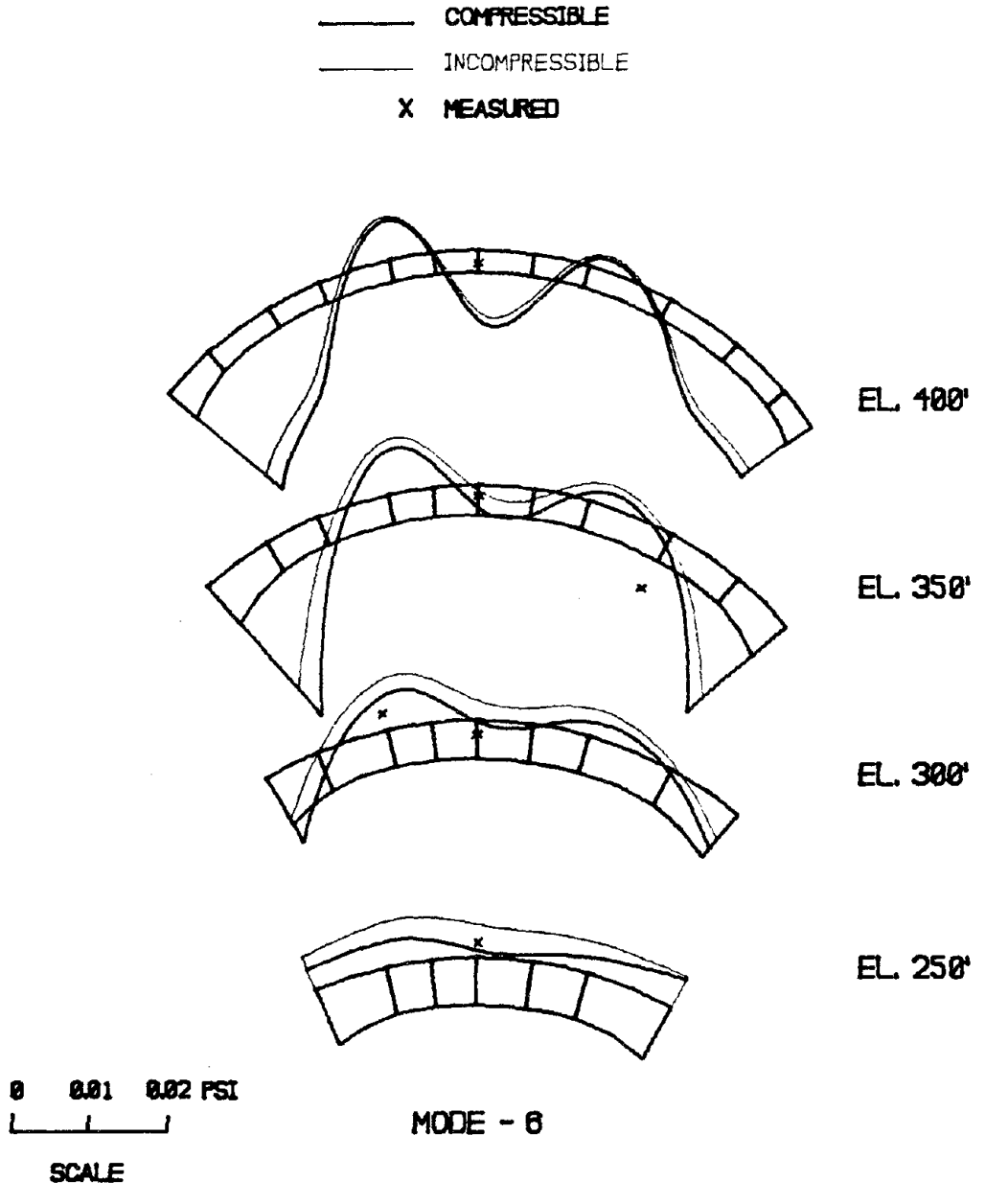

Fig. 4.6 Forced Vibration Hydrodynamic Pressures at Dam Face (Cont'd)

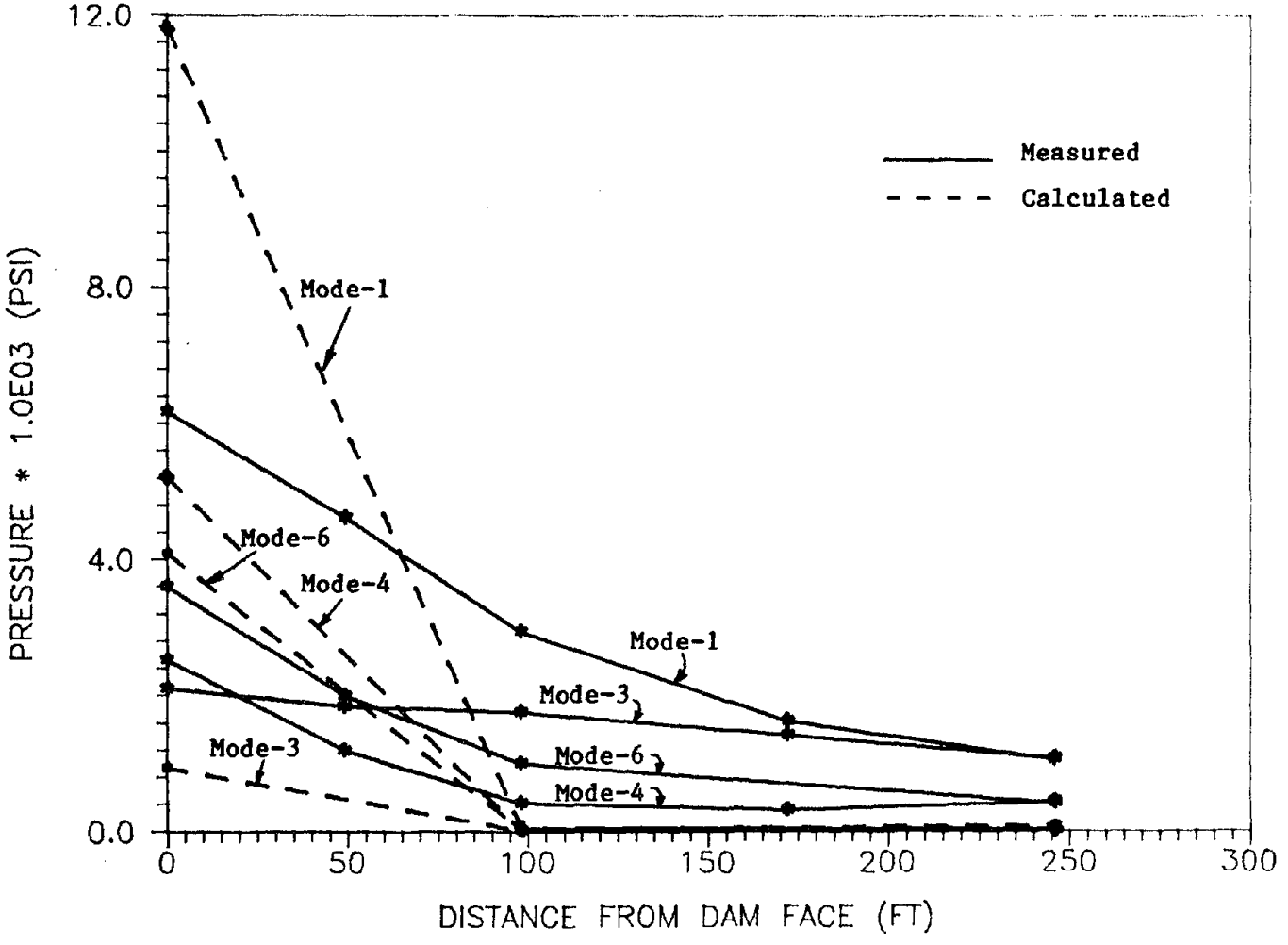

Fig. 4.7 Calculated and Measured Forced Vibration Pressures Reservoir Mid-section at 350 ft Elevation

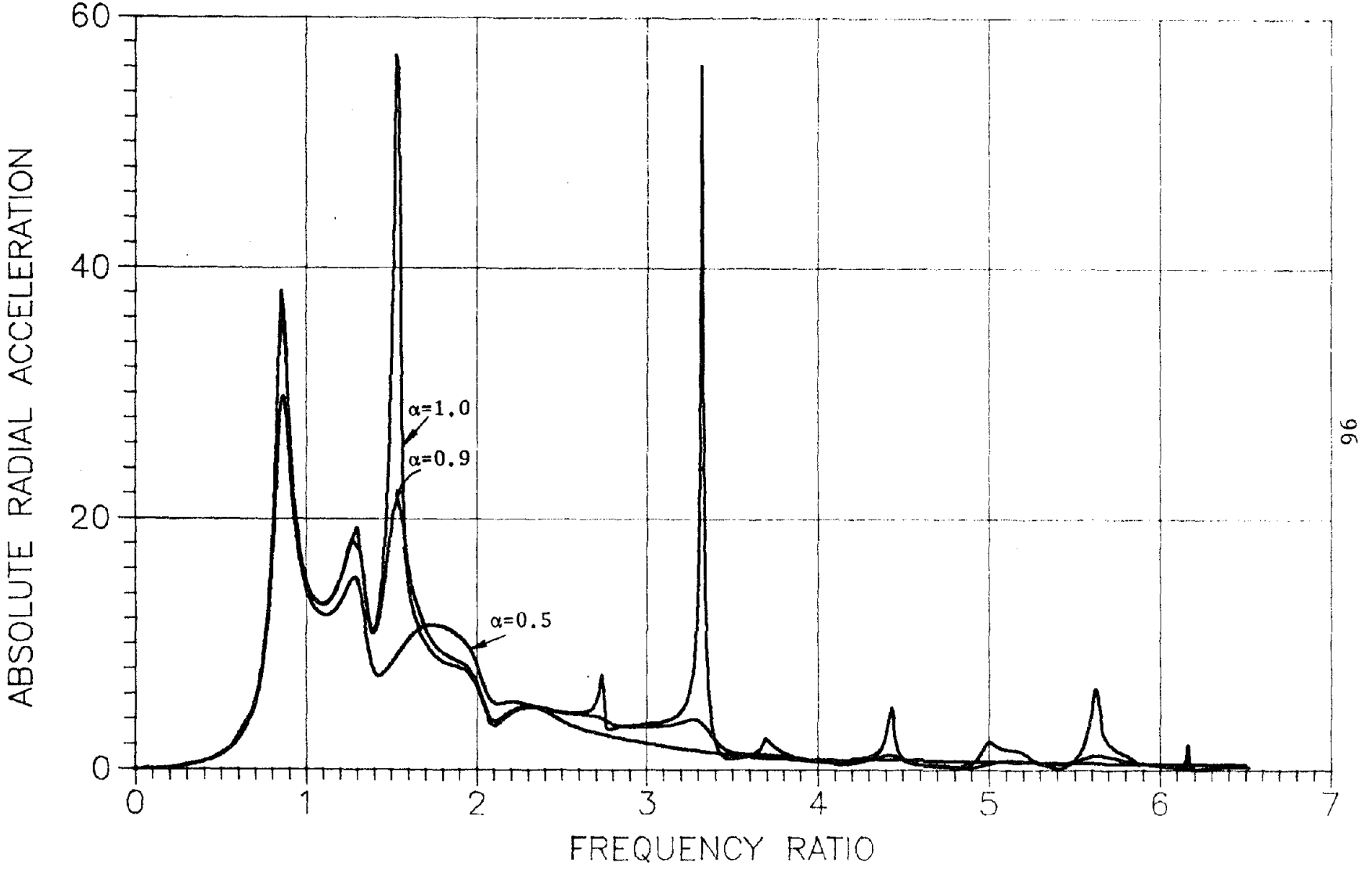

Fig. 5.1 Transfer Function for Radial Midcrest Acceleration due to Upstream Seismic Input

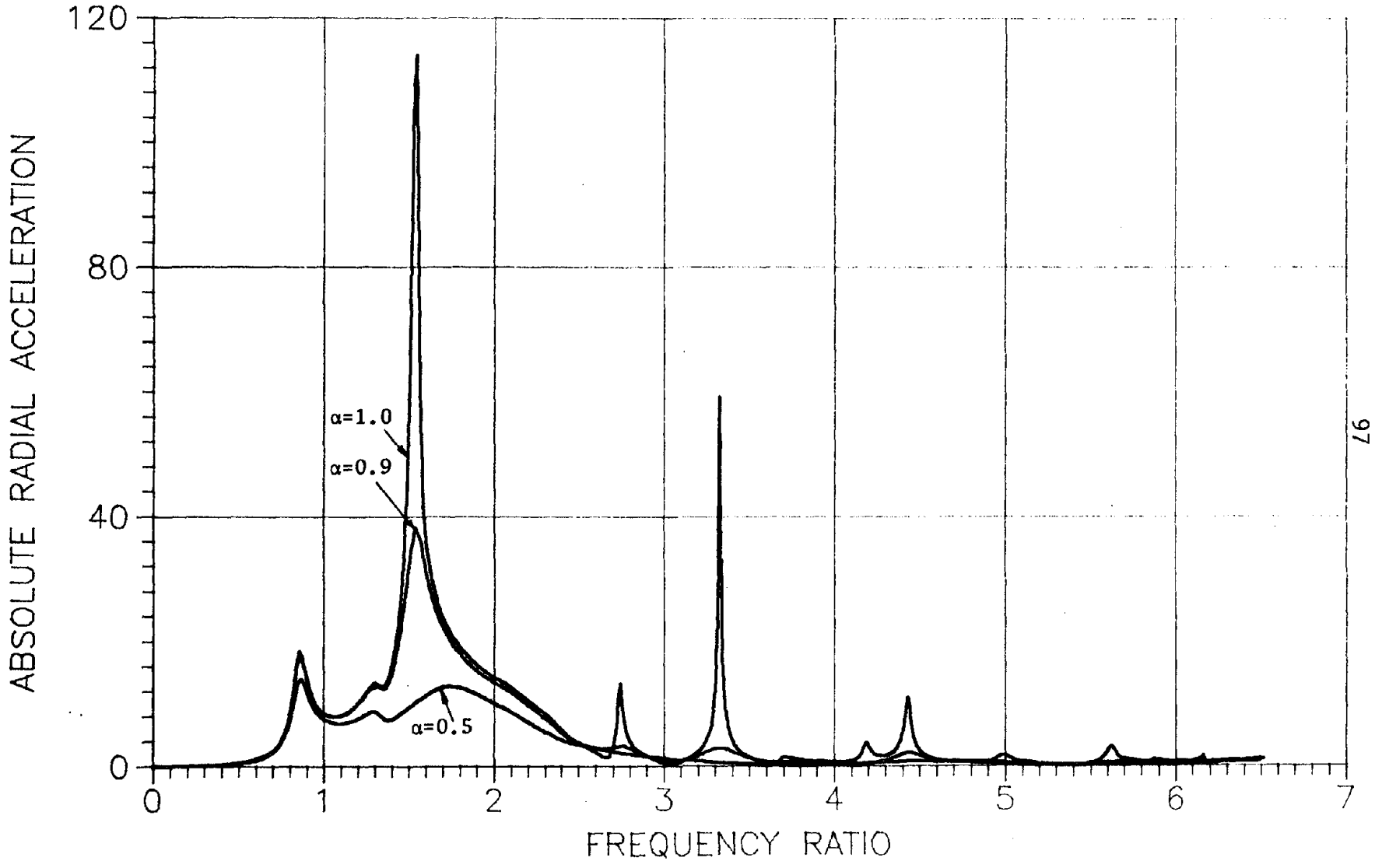

Fig. 5.2 Transfer Function for Radial Crest Acceleration due to Vertical Seismic Input

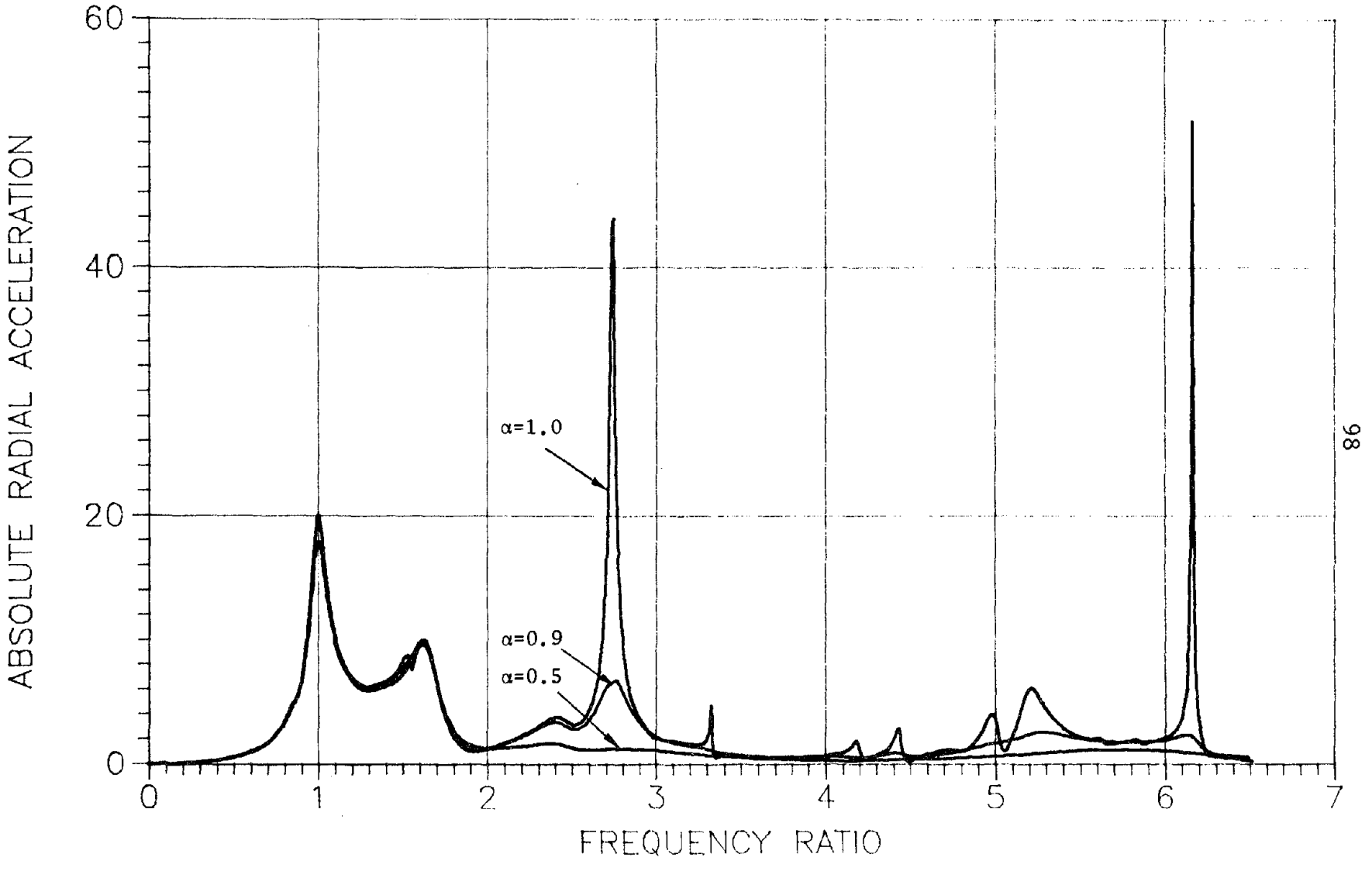

Fig. 5.3 Transfer Function for Radial Crest Acceleration due to Cross-Canyon Seismic Input

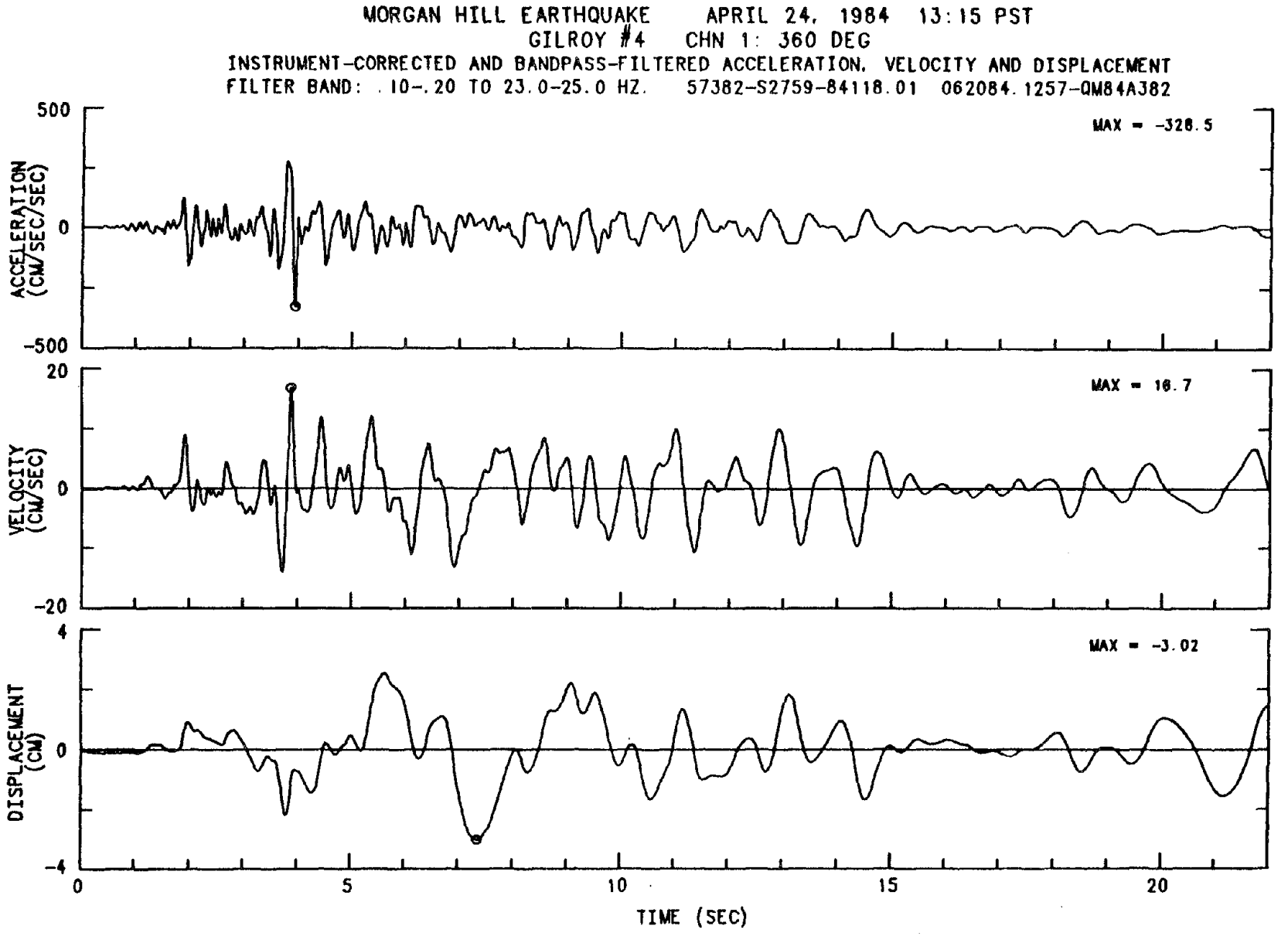

Fig. 5.4 Time History of Upstream Earthquake Motion (From Ref. 11)

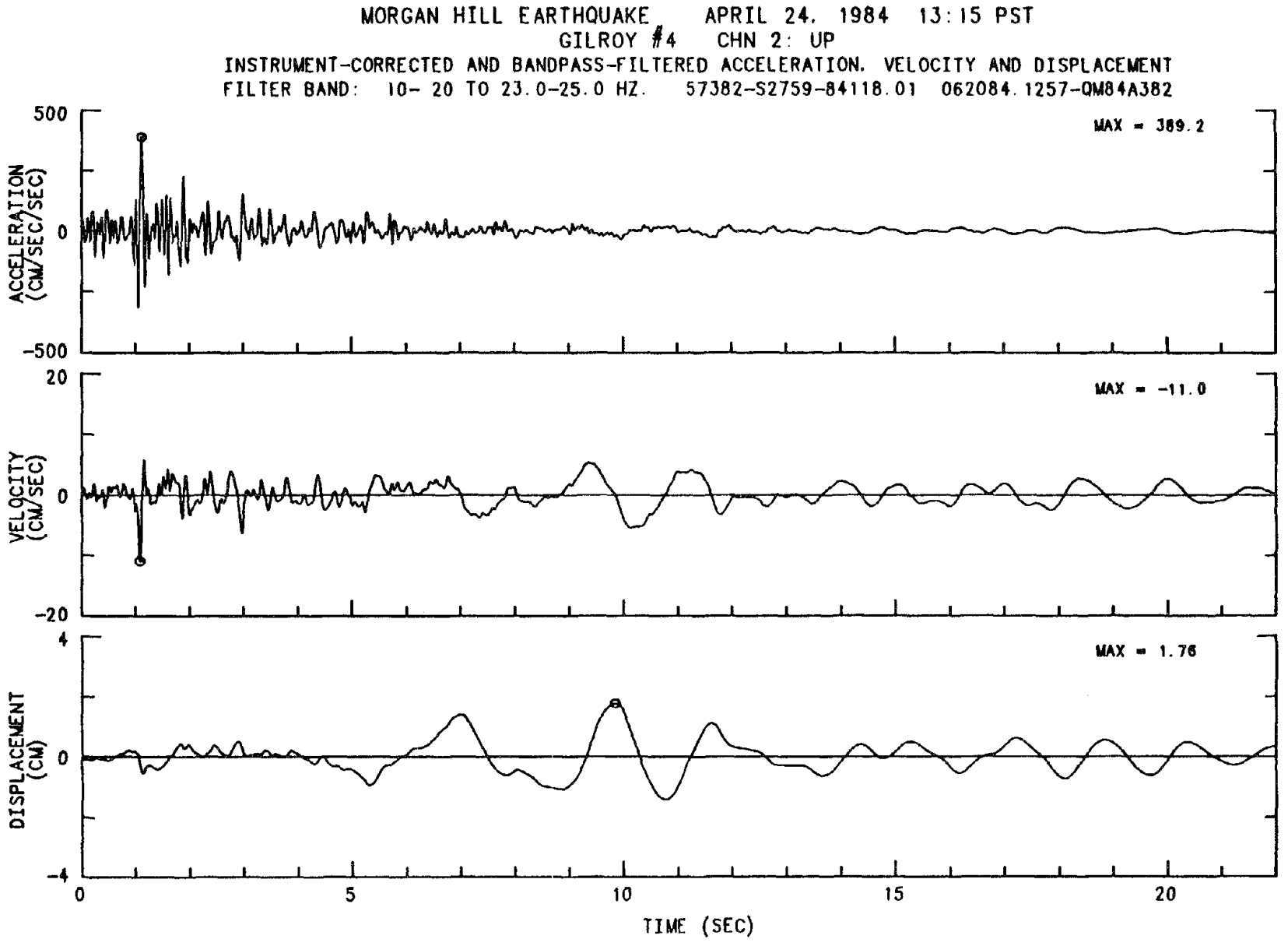

Fig. 5.5 Time History of Vertical Earthquake Motion (From Ref. 11)

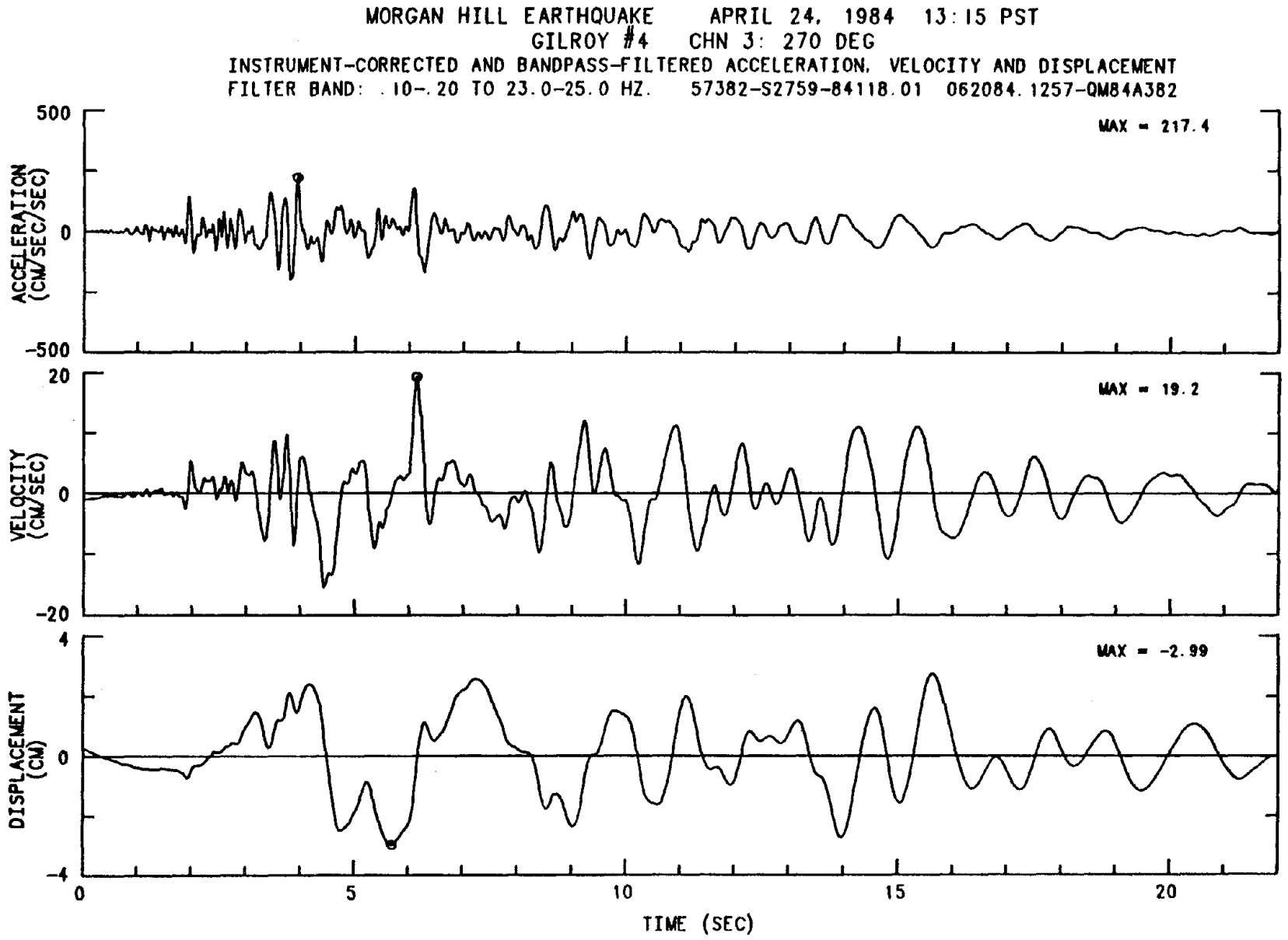

Fig. 5.6 Time History of Cross-Canyon Earthquake Motion (From Ref. 11)

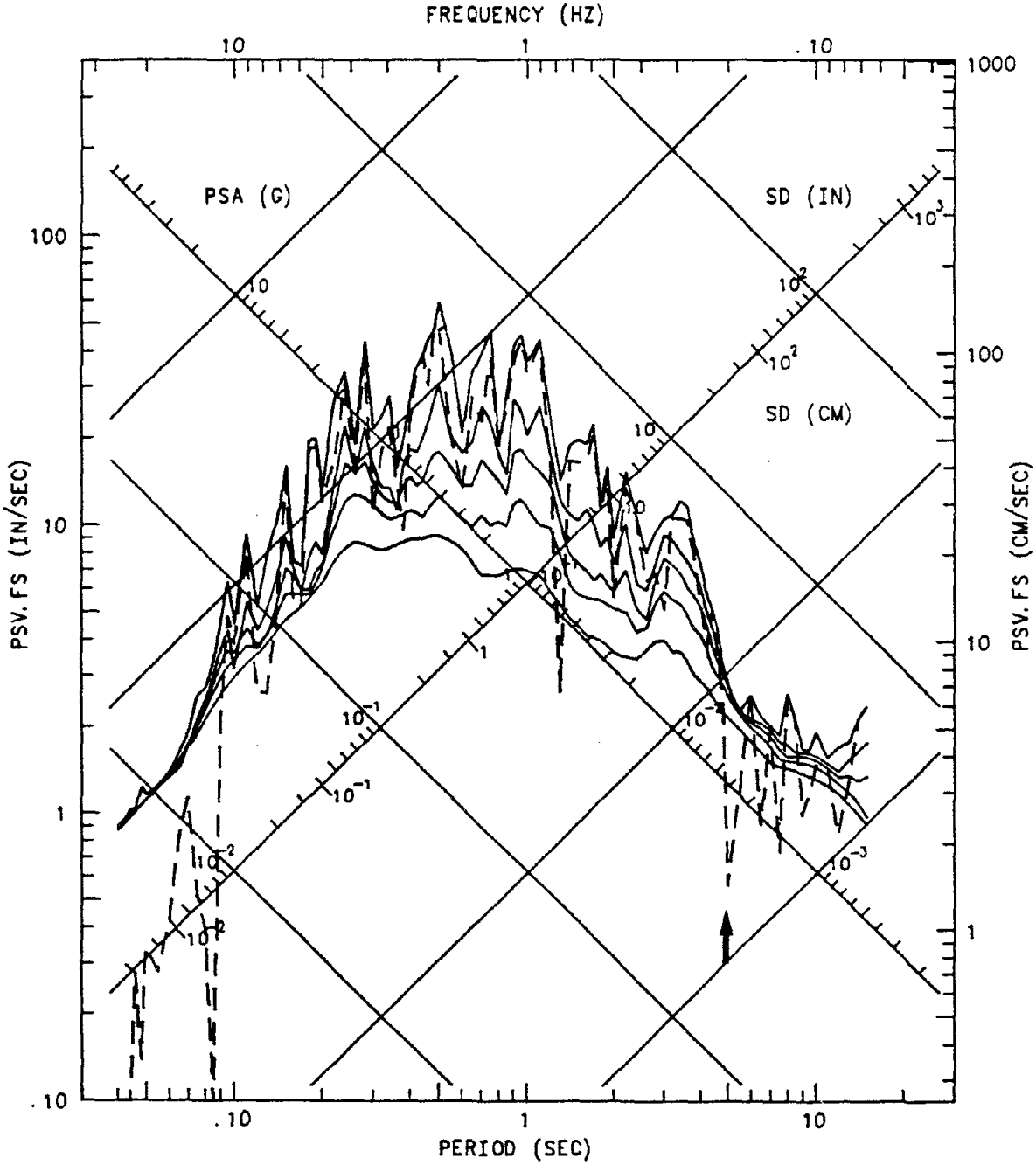

Fig. 5.7 Response Spectra of Upstream Earthquake Motion (From Ref. 11)

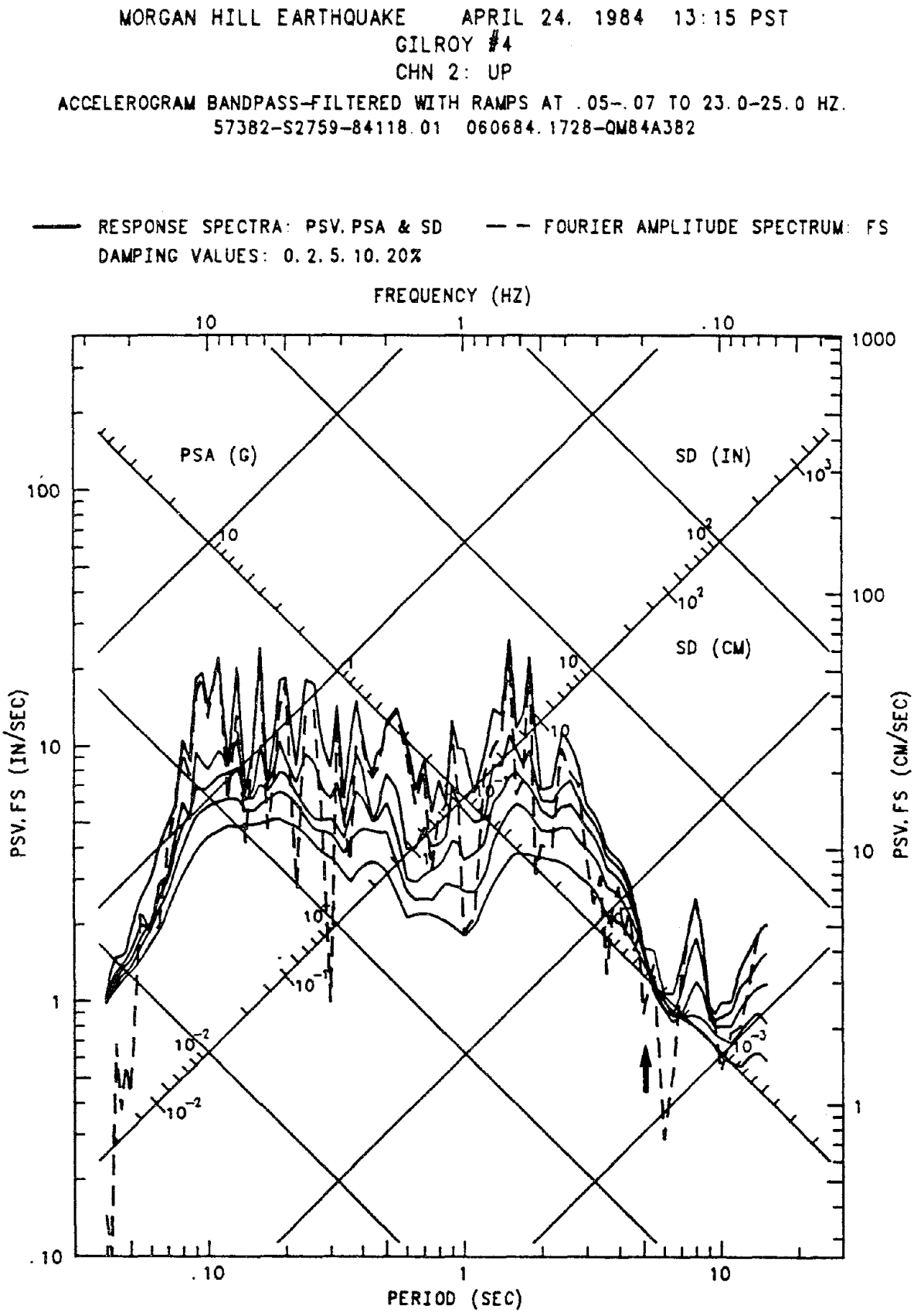

Fig. 5.8 Response Spectra of Vertical Earthquake Motion (From Ref. 11)

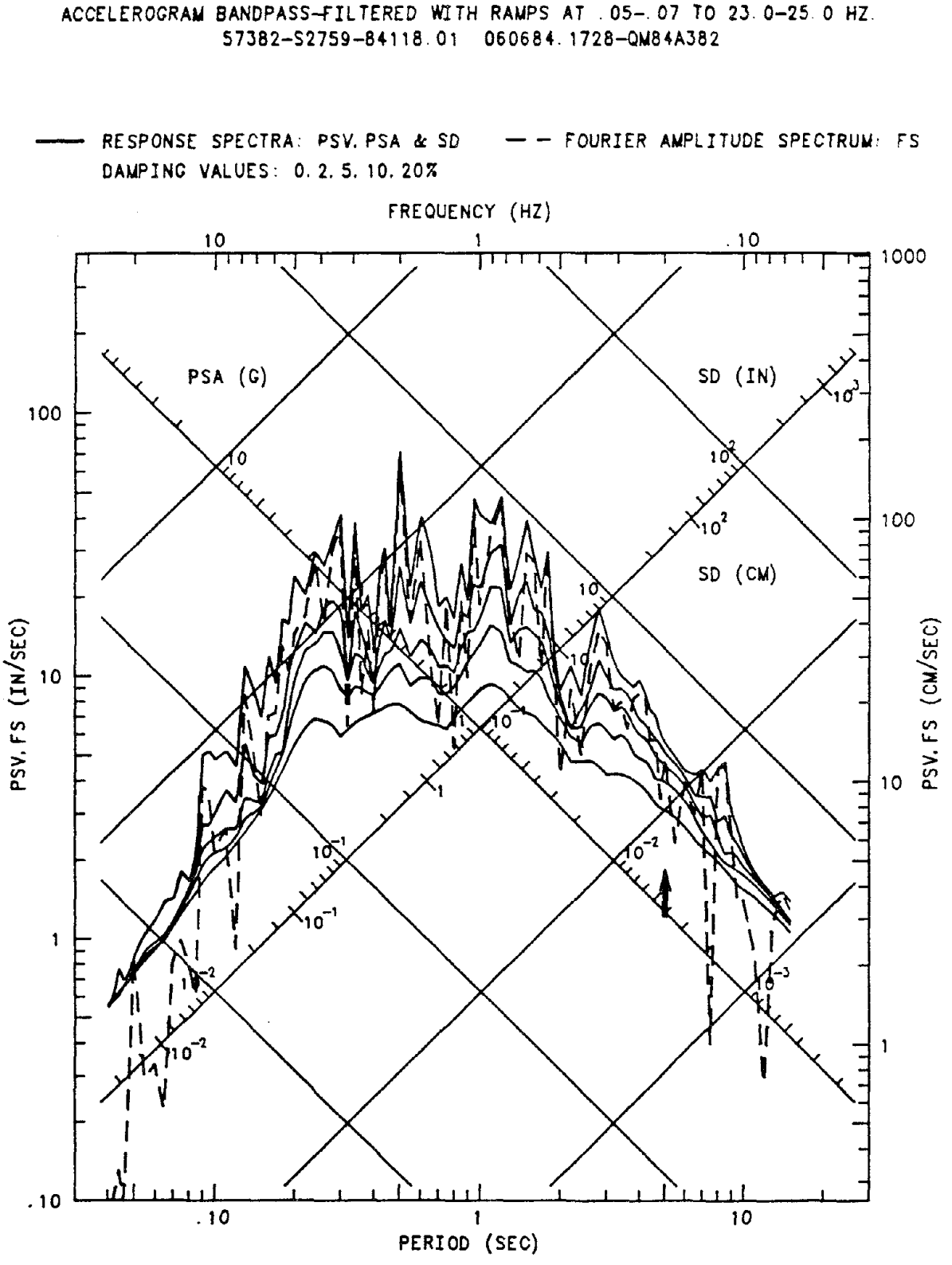

Fig. 5.9 Response Spectra of Cross-Canyon Earthquake Motion (From Ref. 11)

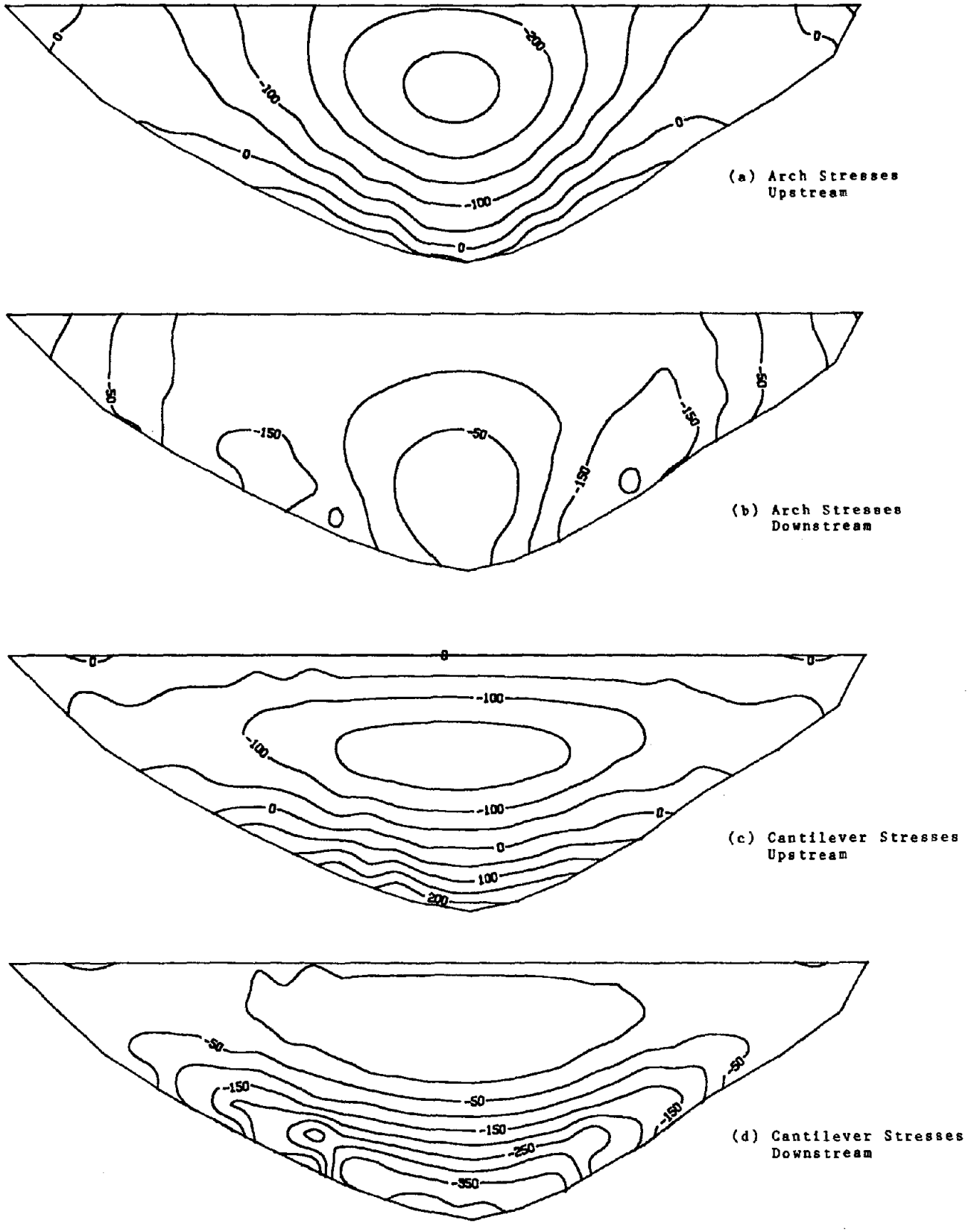

Fig. 5.10 Static Stresses due to Gravity and Reservoir Load (420 ft Elev.)

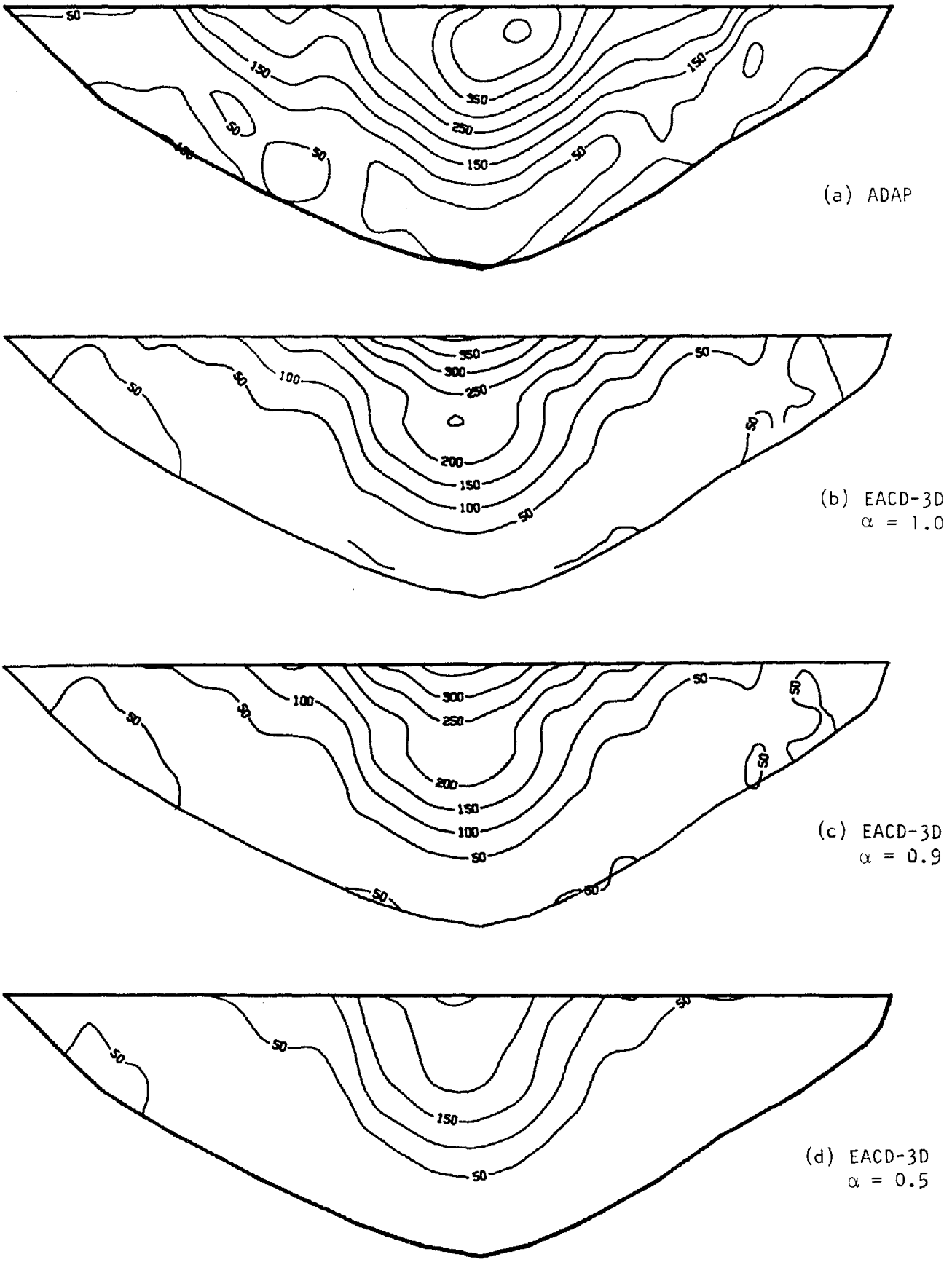

Fig. 5.11 Envelope Earthquake Arch Stresses on Upstream Face

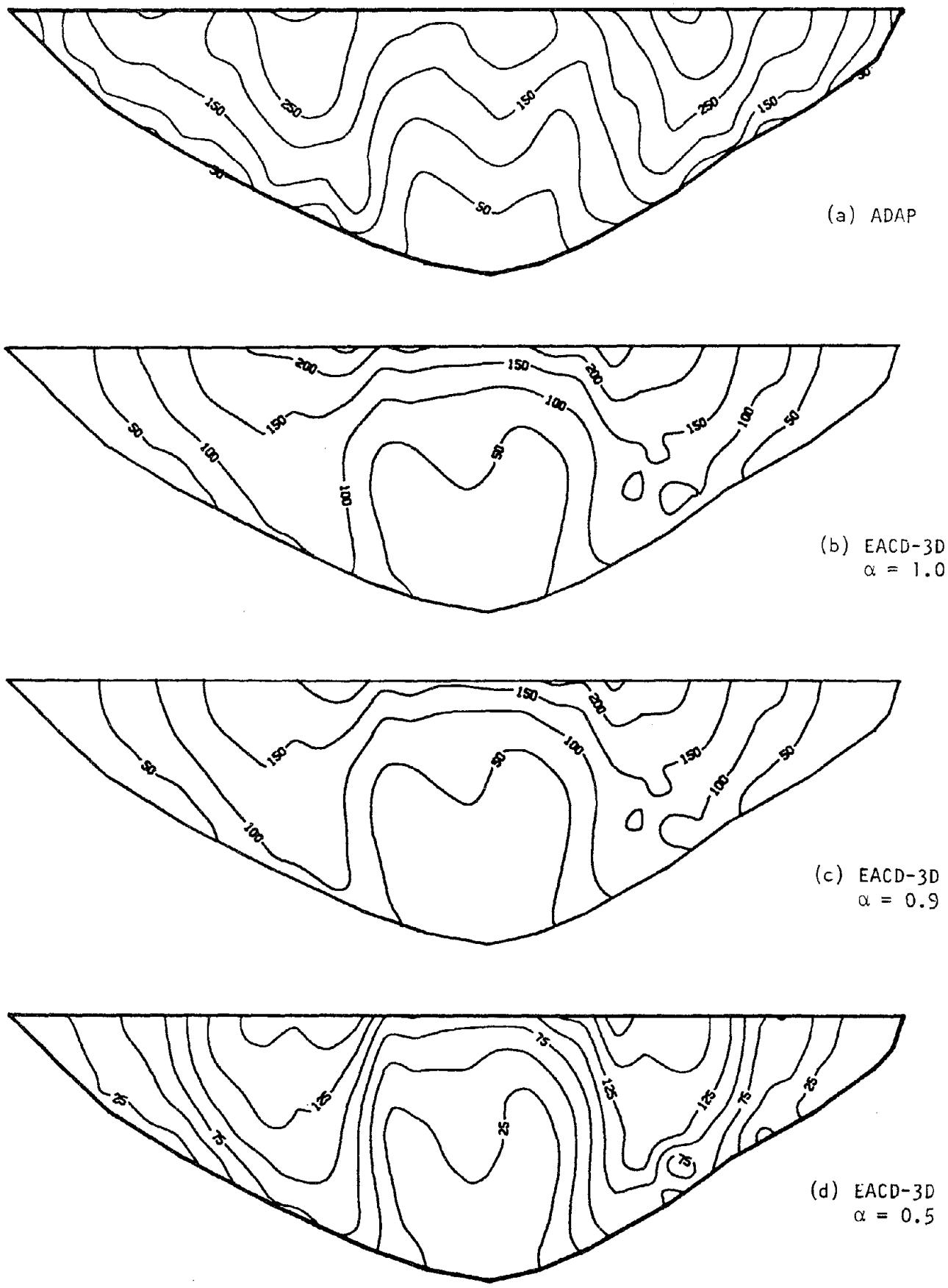

Fig. 5.12 Envelope Earthquake Arch Stresses on Downstream Face

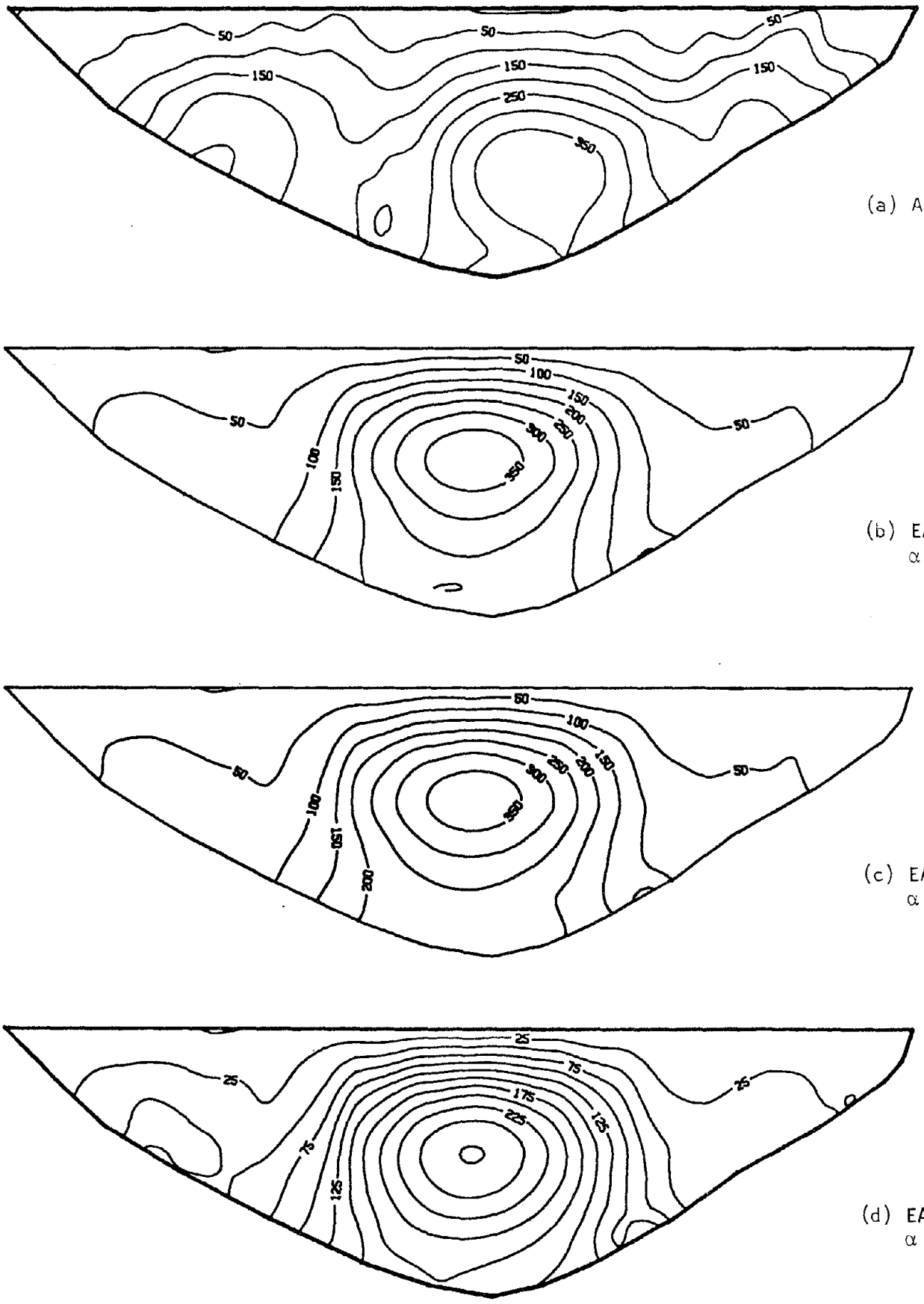

Fig. 5.13 Envelope Earthquake Cantilever Stresses on Upstream Face

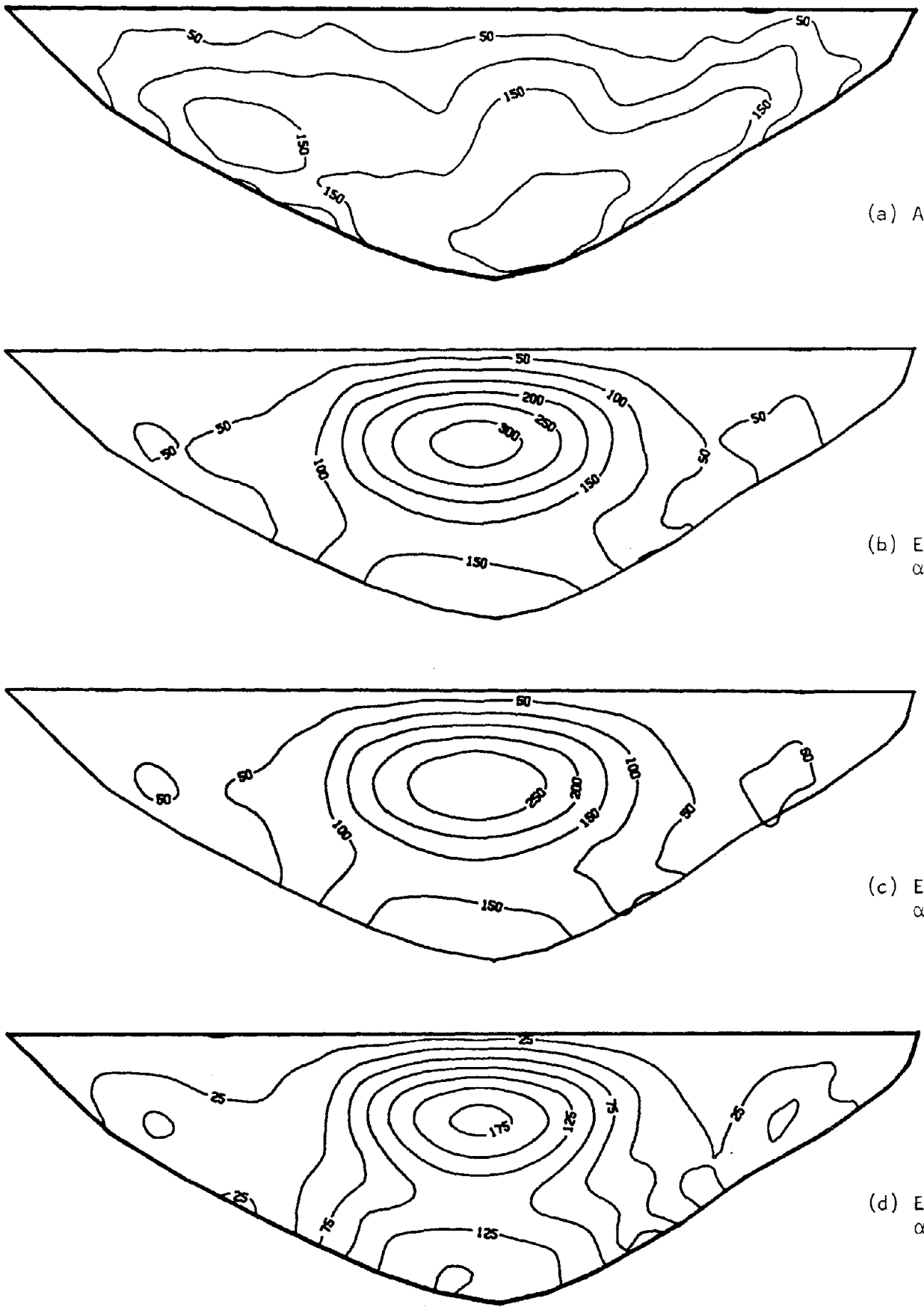

Fig. 5.14 Envelope Earthquake Cantilever Stresses on Downstream Face

EARTHQUAKE ENGINEERING RESEARCH CENTER REPORT SERIES

EERC reports are available from the National Information Service for Earthquake Engineering(NISEE) and from the National Technical Information Service(NTIS). Numbers in parentheses are Accession Numbers assigned by the National Technical Information Service: these are followed by a price code. Contact NTIS, 5285 Port Royal Road, Springfield Virginia, 22161 for more information. Reports without Accession Numbers were not available from NTIS at the time of printing. For a current complete list of EERC reports (from EERC 67-1) and availablity information, please contact University of California, EERC, NISEE, 1301 South 46th Street, Richmond, California 94804.

UCB/EERC-80/01 "Earthquake Response of Concrete Gravity Dams Including Hydrodynamic and Foundation Interaction Effects," by Chopra, A.K., Chakrabarti, P. and Gupta, S., January 1980, (AD-A087297)A10.

UCB/EERC-80/02 "Rocking Response of Rigid Blocks to Earthquakes," by Yim, C.S., Chopra, A.K. and Penzien, J., January 1980, (PB80 166 002)A04.

UCB/EERC-80/03 "Optimum Inelastic Design of Seismic-Resistant Reinforced Concrete Frame Structures," by Zagajeski, S.W. and Bertero, V.V., January 1980, (PB80 164 635)A06.

UCB/EERC-80/04 "Effects of Amount and Arrangement of Wall-Panel Reinforcement on Hysteretic Behavior of Reinforced Concrete Walls," by Iliya, R. and Bertero, V.V., February 1980, (PB81 122 525)A09.

UCB/EERC-80/05 "Shaking Table Research on Concrete Dam Models," by Niwa, A. and Clough, R.W., September 1980, (PB81 122 368)A06.

UCB/EERC-80/06 "The Design of Steel Energy-Absorbing Restrainers and their Incorporation into Nuclear Power Plants for Enhanced Safety (Vol 1a): Piping with Energy Absorbing Restrainers: Parameter Study on Small Systems," by Powell, G.H., Oughourlian, C. and Simons, J., June 1980.

UCB/EERC-80/07 "Inelastic Torsional Response of Structures Subjected to Earthquake Ground Motions," by Yamazaki, Y., April 1980, (PB81 122 327)A08.

UCB/EERC-80/08 "Study of X-Braced Steel Frame Structures under Earthquake Simulation," by Ghanaat, Y., April 1980, (PB81 122 335)A11.

UCB/EERC-80/09 "Hybrid Modelling of Soil-Structure Interaction," by Gupta, S., Lin, T.W. and Penzien, J., May 1980, (PB81 122 319)A07.

UCB/EERC-80/10 "General Applicability of a Nonlinear Model of a One Story Steel Frame," by Sveinsson, B.I. and McNiven, H.D., May 1980, (PB81 124 877)A06.

UCB/EERC-80/11 "A Green-Function Method for Wave Interaction with a Submerged Body," by Kioka, W., April 1980, (PB81 122 269)A07.

UCB/EERC-80/12 "Hydrodynamic Pressure and Added Mass for Axisymmetric Bodies," by Nilrat, F., May 1980, (PB81 122 343)A08.

UCB/EERC-80/13 "Treatment of Non-Linear Drag Forces Acting on Offshore Platforms," by Dao, B.V. and Penzien, J., May 1980, (PB81 153 413)A07.

UCB/EERC-80/14 "2D Plane/Axisymmetric Solid Element (Type 3-Elastic or Elastic-Perfectly Plastic)for the ANSR-II Program," by Mondkar, D.P. and Powell, G.H., July 1980, (PB81 122 350)A03.

UCB/EERC-80/15 "A Response Spectrum Method for Random Vibrations," by Der Kiureghian, A., June 1981, (PB81 122 301)A03.

UCB/EERC-80/16 "Cyclic Inelastic Buckling of Tubular Steel Braces," by Zayas, V.A., Popov, E.P. and Martin, S.A., June 1981, (PB81 124 885)A10.

UCB/EERC-80/17 "Dynamic Response of Simple Arch Dams Including Hydrodynamic Interaction," by Porter, C.S. and Chopra, A.K., July 1981, (PB81 124 000)A13.

UCB/EERC-80/18 "Experimental Testing of a Friction Damped Aseismic Base Isolation System with Fail-Safe Characteristics," by Kelly, J.M., Beucke, K.E. and Skinner, M.S., July 1980, (PB81 148 595)A04.

UCB/EERC-80/19 "The Design of Steel Energy-Absorbing Restrainers and their Incorporation into Nuclear Power Plants for Enhanced Safety (Vol.1B): Stochastic Seismic Analyses of Nuclear Power Plant Structures and Piping Systems Subjected to Multiple Supported Excitations," by Lee, M.C. and Penzien, J., June 1980, (PB82 201 872)A08.

UCB/EERC-80/20 "The Design of Steel Energy-Absorbing Restrainers and their Incorporation into Nuclear Power Plants for Enhanced Safety (Vol 1C): Numerical Method for Dynamic Substructure Analysis," by Dickens, J.M. and Wilson, E.L., June 1980.

UCB/EERC-80/21 "The Design of Steel Energy-Absorbing Restrainers and their Incorporation into Nuclear Power Plants for Enhanced Safety (Vol 2): Development and Testing of Restraints for Nuclear Piping Systems," by Kelly, J.M. and Skinner, M.S., June 1980.

UCB/EERC-80/22 "3D Solid Element (Type 4-Elastic or Elastic-Perfectly-Plastic) for the ANSR-II Program," by Mondkar, D.P. and Powell, G.H., July 1980, (PB81 123 242)A03.

UCB/EERC-80/23 "Gap-Friction Element (Type 5) for the Ansr-II Program," by Mondkar, D.P. and Powell, G.H., July 1980, (PB81 122 285)A03.

UCB/EERC-80/24 "U-Bar Restraint Element (Type 11) for the ANSR-II Program," by Oughourlian, C. and Powell, G.H., July 1980, (PB81 122 293)A03.

UCB/EERC-80/25 "Testing of a Natural Rubber Base Isolation System by an Explosively Simulated Earthquake," by Kelly, J.M., August 1980, (PB81 201 360)A04.

UCB/EERC-80/26 "Input Identification from Structural Vibrational Response," by Hu, Y., August 1980, (PB81 152 308)A05.

UCB/EERC-80/27 "Cyclic Inelastic Behavior of Steel Offshore Structures," by Zayas, V.A., Mahin, S.A. and Popov, E.P., August 1980, (PB81 196 180)A15.

UCB/EERC-80/28 "Shaking Table Testing of a Reinforced Concrete Frame with Biaxial Response," by Oliva, M.G., October 1980, (PB81 154 304)A10.

UCB/EERC-80/29 "Dynamic Properties of a Twelve-Story Prefabricated Panel Building," by Bouwkamp, J.G., Kollegger, J.P. and Stephen, R.M., October 1980, (PB82 138 777)A07.

UCB/EERC-80/30 "Dynamic Properties of an Eight-Story Prefabricated Panel Building," by Bouwkamp, J.G., Kollegger, J.P. and Stephen, R.M., October 1980, (PB81 200 313)A05.

UCB/EERC-80/31 "Predictive Dynamic Response of Panel Type Structures under Earthquakes," by Kollegger, J.P. and Bouwkamp, J.G., October 1980, (PB81 152 316)A04.

UCB/EERC-80/32 "The Design of Steel Energy-Absorbing Restrainers and their Incorporation into Nuclear Power Plants for Enhanced Safety (Vol 3): Testing of Commercial Steels in Low-Cycle Torsional Fatique," by Spanner, P., Parker, E.R., Jongewaard, E. and Dory, M., 1980.

UCB/EERC-80/33 "The Design of Steel Energy-Absorbing Restrainers and their Incorporation into Nuclear Power Plants for Enhanced Safety (Vol 4): Shaking Table Tests of Piping Systems with Energy-Absorbing Restrainers," by Stiemer, S.F. and Godden, W.G., September 1980, (PB82 201 880)A05.

UCB/EERC-80/34 "The Design of Steel Energy-Absorbing Restrainers and their Incorporation into Nuclear Power Plants for Enhanced Safety (Vol 5): Summary Report," by Spencer, P., 1980.

UCB/EERC-80/35 "Experimental Testing of an Energy-Absorbing Base Isolation System," by Kelly, J.M., Skinner, M.S. and Beucke, K.E., October 1980, (PB81 154 072)A04.

UCB/EERC-80/36 "Simulating and Analyzing Artificial Non-Stationary Earth Ground Motions," by Nau, R.F., Oliver, R.M. and Pister, K.S., October 1980, (PB81 153 397)A04.

UCB/EERC-80/37 "Earthquake Engineering at Berkeley - 1980," by , September 1980, (PB81 205 674)A09.

UCB/EERC-80/38 "Inelastic Seismic Analysis of Large Panel Buildings," by Schricker, V. and Powell, G.H., September 1980, (PB81 154 338)A13.

UCB/EERC-80/39 "Dynamic Response of Embankment, Concrete-Gavity and Arch Dams Including Hydrodynamic Interation," by Hall, J.F. and Chopra, A.K., October 1980, (PB81 152 324)A11.

UCB/EERC-80/40 "Inelastic Buckling of Steel Struts under Cyclic Load Reversal," by Black, R.G., Wenger, W.A. and Popov, E.P., October 1980, (PB81 154 312)A08.

UCB/EERC-80/41 "Influence of Site Characteristics on Buildings Damage during the October 3,1974 Lima Earthquake," by Repetto, P., Arango, I. and Seed, H.B., September 1980, (PB81 161 739)A05.

UCB/EERC-80/42 "Evaluation of a Shaking Table Test Program on Response Behavior of a Two Story Reinforced Concrete Frame," by Blondet, J.M., Clough, R.W. and Mahin, S.A., December 1980, (PB82 196 544)A11.

UCB/EERC-80/43 "Modelling of Soil-Structure Interaction by Finite and Infinite Elements," by Medina, F., December 1980, (PB81 229 270)A04.

UCB/EERC-81/01 "Control of Seismic Response of Piping Systems and Other Structures by Base Isolation," by Kelly, J.M., January 1981, (PB81 200 735)A05.

UCB/EERC-81/02 "OPTNSR- An Interactive Software System for Optimal Design of Statically and Dynamically Loaded Structures with Nonlinear Response," by Bhatti, M.A., Ciampi, V. and Pister, K.S., January 1981, (PB81 218 851)A09.

UCB/EERC-81/03 "Analysis of Local Variations in Free Field Seismic Ground Motions," by Chen, J.-C., Lysmer, J. and Seed, H.B., January 1981, (AD-A099508)A13.

UCB/EERC-81/04 "Inelastic Structural Modeling of Braced Offshore Platforms for Seismic Loading," by Zayas, V.A., Shing, P.-S.B., Mahin, S.A. and Popov, E.P., January 1981, (PB82 138 777)A07.

UCB/EERC-81/05 "Dynamic Response of Light Equipment in Structures," by Der Kiureghian, A., Sackman, J.L. and Nour-Omid, B., April 1981, (PB81 218 497)A04.

UCB/EERC-81/06 "Preliminary Experimental Investigation of a Broad Base Liquid Storage Tank," by Bouwkamp, J.G., Kollegger, J.P. and Stephen, R.M., May 1981, (PB82 140 385)A03.

UCB/EERC-81/07 "The Seismic Resistant Design of Reinforced Concrete Coupled Structural Walls," by Aktan, A.E. and Bertero, V.V., June 1981, (PB82 113 358)A11.

UCB/EERC-81/08 "Unassigned," by Unassigned, 1981.

UCB/EERC-81/09 "Experimental Behavior of a Spatial Piping System with Steel Energy Absorbers Subjected to a Simulated Differential Seismic Input," by Stiemer, S.F., Godden, W.G. and Kelly, J.M., July 1981, (PB82 201 898)A04.

UCB/EERC-81/10 "Evaluation of Seismic Design Provisions for Masonry in the United States," by Sveinsson, B.I., Mayes, R.L. and McNiven, H.D., August 1981, (PB82 166 075)A08.

UCB/EERC-81/11 "Two-Dimensional Hybrid Modelling of Soil-Structure Interaction," by Tzong, T.-J., Gupta, S. and Penzien, J., August 1981, (PB82 142 118)A04.

UCB/EERC-81/12 "Studies on Effects of Infills in Seismic Resistant R/C Construction," by Brokken, S. and Bertero, V.V., October 1981, (PB82 166 190)A09.

UCB/EERC-81/13 "Linear Models to Predict the Nonlinear Seismic Behavior of a One-Story Steel Frame," by Valdimarsson, H., Shah, A.H. and McNiven, H.D., September 1981, (PB82 138 793)A07.

UCB/EERC-81/14 "TLUSH: A Computer Program for the Three-Dimensional Dynamic Analysis of Earth Dams," by Kagawa, T., Mejia, L.H., Seed, H.B. and Lysmer, J., September 1981, (PB82 139 940)A06.

UCB/EERC-81/15 "Three Dimensional Dynamic Response Analysis of Earth Dams," by Mejia, L.H. and Seed, H.B., September 1981, (PB82 137 274)A12.

UCB/EERC-81/16 "Experimental Study of Lead and Elastomeric Dampers for Base Isolation Systems," by Kelly, J.M. and Hodder, S.B., October 1981, (PB82 166 182)A05.

UCB/EERC-81/17 "The Influence of Base Isolation on the Seismic Response of Light Secondary Equipment," by Kelly, J.M., April 1981, (PB82 255 266)A04.

UCB/EERC-81/18 "Studies on Evaluation of Shaking Table Response Analysis Procedures," by Blondet, J. M., November 1981, (PB82 197 278)A10.

UCB/EERC-81/19 "DELIGHT.STRUCT: A Computer-Aided Design Environment for Structural Engineering," by Balling, R.J., Pister, K.S. and Polak, E., December 1981, (PB82 218 496)A07.

UCB/EERC-81/20 "Optimal Design of Seismic-Resistant Planar Steel Frames," by Balling, R.J., Ciampi, V. and Pister, K.S., December 1981, (PB82 220 179)A07.

UCB/EERC-82/01 "Dynamic Behavior of Ground for Seismic Analysis of Lifeline Systems," by Sato, T. and Der Kiureghian, A., January 1982, (PB82 218 926)A05.

UCB/EERC-82/02 "Shaking Table Tests of a Tubular Steel Frame Model," by Ghanaat, Y. and Clough, R.W., January 1982, (PB82 220 161)A07.

UCB/EERC-82/03 "Behavior of a Piping System under Seismic Excitation: Experimental Investigations of a Spatial Piping System supported by Mechanical Shock Arrestors," by Schneider, S., Lee, H.-M. and Godden, W. G., May 1982, (PB83 172 544)A09.

UCB/EERC-82/04 "New Approaches for the Dynamic Analysis of Large Structural Systems," by Wilson, E.L., June 1982, (PB83 148 080)A05.

UCB/EERC-82/05 "Model Study of Effects of Damage on the Vibration Properties of Steel Offshore Platforms," by Shahrivar, F. and Bouwkamp, J.G., June 1982, (PB83 148 742)A10.

UCB/EERC-82/06 "States of the Art and Pratice in the Optimum Seismic Design and Analytical Response Prediction of R/C Frame Wall Structures," by Aktan, A.E. and Bertero, V.V., July 1982, (PB83 147 736)A05.

UCB/EERC-82/07 "Further Study of the Earthquake Response of a Broad Cylindrical Liquid-Storage Tank Model," by Manos, G.C. and Clough, R.W., July 1982, (PB83 147 744)A11.

UCB/EERC-82/08 "An Evaluation of the Design and Analytical Seismic Response of a Seven Story Reinforced Concrete Frame," by Charney, F.A. and Bertero, V.V., July 1982, (PB83 157 628)A09.

UCB/EERC-82/09 "Fluid-Structure Interactions: Added Mass Computations for Incompressible Fluid," by Kuo, J.S.-H., August 1982, (PB83 156 281)A07.

UCB/EERC-82/10 "Joint-Opening Nonlinear Mechanism: Interface Smeared Crack Model," by Kuo, J.S.-H., August 1982, (PB83 149 195)A05.

UCB/EERC-82/11 "Dynamic Response Analysis of Techi Dam," by Clough, R.W., Stephen, R.M. and Kuo, J.S.-H., August 1982, (PB83 147 496)A06.

UCB/EERC-82/12 "Prediction of the Seismic Response of R/C Frame-Coupled Wall Structures," by Aktan, A.E., Bertero, V.V. and Piazzo, M., August 1982, (PB83 149 203)A09.

UCB/EERC-82/13 "Preliminary Report on the Smart 1 Strong Motion Array in Taiwan," by Bolt, B.A., Loh, C.H., Penzien, J. and Tsai, Y.B., August 1982, (PB83 159 400)A10.

UCB/EERC-82/14 "Shaking-Table Studies of an Eccentrically X-Braced Steel Structure," by Yang, M.S., September 1982, (PB83 260 778)A12.

UCB/EERC-82/15 "The Performance of Stairways in Earthquakes," by Roha, C., Axley, J.W. and Bertero, V.V., September 1982, (PB83 157 693)A07.

UCB/EERC-82/16 "The Behavior of Submerged Multiple Bodies in Earthquakes," by Liao, W.-G., September 1982, (PB83 158 709)A07.

UCB/EERC-82/17 "Effects of Concrete Types and Loading Conditions on Local Bond-Slip Relationships," by Cowell, A.D., Popov, E.P. and Bertero, V.V., September 1982, (PB83 153 577)A04.

UCB/EERC-82/18 "Mechanical Behavior of Shear Wall Vertical Boundary Members: An Experimental Investigation," by Wagner, M.T. and Bertero, V.V., October 1982, (PB83 159 764)A05.

UCB/EERC-82/19 "Experimental Studies of Multi-support Seismic Loading on Piping Systems," by Kelly, J.M. and Cowell, A.D., November 1982.

UCB/EERC-82/20 "Generalized Plastic Hinge Concepts for 3D Beam-Column Elements," by Chen, P. F.-S. and Powell, G.H., November 1982, (PB83 247 981)A13.

UCB/EERC-82/21 "ANSR-II: General Computer Program for Nonlinear Structural Analysis," by Oughourlian, C.V. and Powell, G.H., November 1982, (PB83 251 330)A12.

UCB/EERC-82/22 "Solution Strategies for Statically Loaded Nonlinear Structures," by Simons, J.W. and Powell, G.H., November 1982, (PB83 197 970)A06.

UCB/EERC-82/23 "Analytical Model of Deformed Bar Anchorages under Generalized Excitations," by Ciampi, V., Eligehausen, R., Bertero, V.V. and Popov, E.P., November 1982, (PB83 169 532)A06.

UCB/EERC-82/24 "A Mathematical Model for the Response of Masonry Walls to Dynamic Excitations," by Sucuoglu, H., Mengi, Y. and McNiven, H.D., November 1982, (PB83 169 011)A07.

UCB/EERC-82/25 "Earthquake Response Considerations of Broad Liquid Storage Tanks," by Cambra, F.J., November 1982, (PB83 251 215)A09.

UCB/EERC-82/26 "Computational Models for Cyclic Plasticity, Rate Dependence and Creep," by Mosaddad, B. and Powell, G.H., November 1982, (PB83 245 829)A08.

UCB/EERC-82/27 "Inelastic Analysis of Piping and Tubular Structures," by Mahasuverachai, M. and Powell, G.H., November 1982, (PB83 249 987)A07.

UCB/EERC-83/01 "The Economic Feasibility of Seismic Rehabilitation of Buildings by Base Isolation," by Kelly, J.M., January 1983, (PB83 197 988)A05.

UCB/EERC-83/02 "Seismic Moment Connections for Moment-Resisting Steel Frames," by Popov, E.P., January 1983, (PB83 195 412)A04.

UCB/EERC-83/03 "Design of Links and Beam-to-Column Connections for Eccentrically Braced Steel Frames," by Popov, E.P. and Malley, J.O., January 1983, (PB83 194 811)A04.

UCB/EERC-83/04 "Numerical Techniques for the Evaluation of Soil-Structure Interaction Effects in the Time Domain," by Bayo, E. and Wilson, E.L., February 1983, (PB83 245 605)A09.

UCB/EERC-83/05 "A Transducer for Measuring the Internal Forces in the Columns of a Frame-Wall Reinforced Concrete Structure," by Sause, R. and Bertero, V.V., May 1983, (PB84 119 494)A06.

UCB/EERC-83/06 "Dynamic Interactions Between Floating Ice and Offshore Structures," by Croteau, P., May 1983, (PB84 119 486)A16.

UCB/EERC-83/07 "Dynamic Analysis of Multiply Tuned and Arbitrarily Supported Secondary Systems," by Igusa, T. and Der Kiureghian, A., July 1983, (PB84 118 272)A11.

UCB/EERC-83/08 "A Laboratory Study of Submerged Multi-body Systems in Earthquakes," by Ansari, G.R., June 1983, (PB83 261 842)A17.

UCB/EERC-83/09 "Effects of Transient Foundation Uplift on Earthquake Response of Structures," by Yim, C.-S. and Chopra, A.K., June 1983, (PB83 261 396)A07.

UCB/EERC-83/10 "Optimal Design of Friction-Braced Frames under Seismic Loading," by Austin, M.A. and Pister, K.S., June 1983, (PB84 119 288)A06.

UCB/EERC-83/11 "Shaking Table Study of Single-Story Masonry Houses: Dynamic Performance under Three Component Seismic Input and Recommendations," by Manos, G.C., Clough, R.W. and Mayes, R.L., July 1983, (UCB/EERC-83/11)A08.

UCB/EERC-83/12 "Experimental Error Propagation in Pseudodynamic Testing," by Shiing, P.B. and Mahin, S.A., June 1983, (PB84 119 270)A09.

UCB/EERC-83/13 "Experimental and Analytical Predictions of the Mechanical Characteristics of a 1/5-scale Model of a 7-story R/C Frame-Wall Building Structure," by Aktan, A.E., Bertero, V.V., Chowdhury, A.A. and Nagashima, T., June 1983, (PB84 119 213)A07.

UCB/EERC-83/14 "Shaking Table Tests of Large-Panel Precast Concrete Building System Assemblages," by Oliva, M.G. and Clough, R.W., June 1983, (PB86 110 210/AS)A11.

UCB/EERC-83/15 "Seismic Behavior of Active Beam Links in Eccentrically Braced Frames," by Hjelmstad, K.D. and Popov, E.P., July 1983, (PB84 119 676)A09.

UCB/EERC-83/16 "System Identification of Structures with Joint Rotation," by Dimsdale, J.S., July 1983, (PB84 192 210)A06.

UCB/EERC-83/17 "Construction of Inelastic Response Spectra for Single-Degree-of-Freedom Systems," by Mahin, S. and Lin, J., June 1983, (PB84 208 834)A05.

UCB/EERC-83/18 "Interactive Computer Analysis Methods for Predicting the Inelastic Cyclic Behaviour of Structural Sections," by Kaba, S. and Mahin, S., July 1983, (PB84 192 012)A06.

UCB/EERC-83/19 "Effects of Bond Deterioration on Hysteretic Behavior of Reinforced Concrete Joints," by Filippou, F.C., Popov, E.P. and Bertero, V.V., August 1983, (PB84 192 020)A10.

UCB/EERC-83/20 "Analytical and Experimental Correlation of Large-Panel Precast Building System Performance," by Oliva, M.G., Clough, R.W., Velkov, M. and Gavrilovic, P., November 1983.

UCB/EERC-83/21 "Mechanical Characteristics of Materials Used in a 1/5 Scale Model of a 7-Story Reinforced Concrete Test Structure," by Bertero, V.V., Aktan, A.E., Harris, H.G. and Chowdhury, A.A., October 1983, (PB84 193 697)A05.

UCB/EERC-83/22 "Hybrid Modelling of Soil-Structure Interaction in Layered Media," by Tzong, T.-J. and Penzien, J., October 1983, (PB84 192 178)A08.

UCB/EERC-83/23 "Local Bond Stress-Slip Relationships of Deformed Bars under Generalized Excitations," by Eligehausen, R., Popov, E.P. and Bertero, V.V., October 1983, (PB84 192 848)A09.

UCB/EERC-83/24 "Design Considerations for Shear Links in Eccentrically Braced Frames," by Malley, J.O. and Popov, E.P., November 1983, (PB84 192 186)A07.

UCB/EERC-84/01 "Pseudodynamic Test Method for Seismic Performance Evaluation: Theory and Implementation," by Shing, P.-S.B. and Mahin, S.A., January 1984, (PB84 190 644)A08.

UCB/EERC-84/02 "Dynamic Response Behavior of Kiang Hong Dian Dam," by Clough, R.W., Chang, K.-T., Chen, H.-Q. and Stephen, R.M., April 1984, (PB84 209 402)A08.

UCB/EERC-84/03 "Refined Modelling of Reinforced Concrete Columns for Seismic Analysis," by Kaba, S.A. and Mahin, S.A., April 1984, (PB84 234 384)A06.

UCB/EERC-84/04 "A New Floor Response Spectrum Method for Seismic Analysis of Multiply Supported Secondary Systems," by Asfura, A. and Der Kiureghian, A., June 1984, (PB84 239 417)A06.

UCB/EERC-84/05 "Earthquake Simulation Tests and Associated Studies of a 1/5th-scale Model of a 7-Story R/C Frame-Wall Test Structure," by Bertero, V.V., Aktan, A.E., Charney, F.A. and Sause, R., June 1984, (PB84 239 409)A09.

UCB/EERC-84/06 "R/C Structural Walls: Seismic Design for Shear," by Aktan, A.E. and Bertero, V.V., 1984.

UCB/EERC-84/07 "Behavior of Interior and Exterior Flat-Plate Connections subjected to Inelastic Load Reversals," by Zee, H.L. and Moehle, J.P., August 1984, (PB86 117 629/AS)A07.

UCB/EERC-84/08 "Experimental Study of the Seismic Behavior of a Two-Story Flat-Plate Structure," by Moehle, J.P. and Diebold, J.W., August 1984, (PB86 122 553/AS)A12.

UCB/EERC-84/09 "Phenomenological Modeling of Steel Braces under Cyclic Loading," by Ikeda, K., Mahin, S.A. and Dermitzakis, S.N., May 1984, (PB86 132 198/AS)A08.

UCB/EERC-84/10 "Earthquake Analysis and Response of Concrete Gravity Dams," by Fenves, G. and Chopra, A.K., August 1984, (PB85 193 902/AS)A11.

UCB/EERC-84/11 "EAGD-84: A Computer Program for Earthquake Analysis of Concrete Gravity Dams," by Fenves, G. and Chopra, A.K., August 1984, (PB85 193 613/AS)A05.

UCB/EERC-84/12 "A Refined Physical Theory Model for Predicting the Seismic Behavior of Braced Steel Frames," by Ikeda, K. and Mahin, S.A., July 1984, (PB85 191 450/AS)A09.

UCB/EERC-84/13 "Earthquake Engineering Research at Berkeley - 1984," by , August 1984, (PB85 197 341/AS)A10.

UCB/EERC-84/14 "Moduli and Damping Factors for Dynamic Analyses of Cohesionless Soils," by Seed, H.B., Wong, R.T., Idriss, I.M. and Tokimatsu, K., September 1984, (PB85 191 468/AS)A04.

UCB/EERC-84/15 "The Influence of SPT Procedures in Soil Liquefaction Resistance Evaluations," by Seed, H.B., Tokimatsu, K., Harder, L.F. and Chung, R.M., October 1984, (PB85 191 732/AS)A04.

UCB/EERC-84/16 "Simplified Procedures for the Evaluation of Settlements in Sands Due to Earthquake Shaking," by Tokimatsu, K. and Seed, H.B., October 1984, (PB85 197 887/AS)A03.

UCB/EERC-84/17 "Evaluation of Energy Absorption Characteristics of Bridges under Seismic Conditions," by Imbsen, R.A. and Penzien, J., November 1984.

UCB/EERC-84/18 "Structure-Foundation Interactions under Dynamic Loads," by Liu, W.D. and Penzien, J., November 1984, (PB87 124 889/AS)A11.

UCB/EERC-84/19 "Seismic Modelling of Deep Foundations," by Chen, C.-H. and Penzien, J., November 1984, (PB87 124 798/AS)A07.

UCB/EERC-84/20 "Dynamic Response Behavior of Quan Shui Dam," by Clough, R.W., Chang, K.-T., Chen, H.-Q., Stephen, R.M., Ghanaat, Y. and Qi, J.-H., November 1984, (PB86 115177/AS)A07.

UCB/EERC-85/01 "Simplified Methods of Analysis for Earthquake Resistant Design of Buildings," by Cruz, E.F. and Chopra, A.K., February 1985, (PB86 112299/AS)A12.

UCB/EERC-85/02 "Estimation of Seismic Wave Coherency and Rupture Velocity using the SMART 1 Strong-Motion Array Recordings," by Abrahamson, N.A., March 1985, (PB86 214 343)A07.

UCB/EERC-85/03 "Dynamic Properties of a Thirty Story Condominium Tower Building," by Stephen, R.M., Wilson, E.L. and Stander, N., April 1985, (PB86 118965/AS)A06.

UCB/EERC-85/04 "Development of Substructuring Techniques for On-Line Computer Controlled Seismic Performance Testing," by Dermitzakis, S. and Mahin, S., February 1985, (PB86 132941/AS)A08.

UCB/EERC-85/05 "A Simple Model for Reinforcing Bar Anchorages under Cyclic Excitations," by Filippou, F.C., March 1985, (PB86 112 919/AS)A05.

UCB/EERC-85/06 "Racking Behavior of Wood-framed Gypsum Panels under Dynamic Load," by Oliva, M.G., June 1985.

UCB/EERC-85/07 "Earthquake Analysis and Response of Concrete Arch Dams," by Fok, K.-L. and Chopra, A.K., June 1985, (PB86 139672/AS)A10.

UCB/EERC-85/08 "Effect of Inelastic Behavior on the Analysis and Design of Earthquake Resistant Structures," by Lin, J.P. and Mahin, S.A., June 1985, (PB86 135340/AS)A08.

UCB/EERC-85/09 "Earthquake Simulator Testing of a Base-Isolated Bridge Deck," by Kelly, J.M., Buckle, I.G. and Tsai, H.-C., January 1986, (PB87 124 152/AS)A06.

UCB/EERC-85/10 "Simplified Analysis for Earthquake Resistant Design of Concrete Gravity Dams," by Fenves, G. and Chopra, A.K., June 1986, (PB87 124 160/AS)A08.

UCB/EERC-85/11 "Dynamic Interaction Effects in Arch Dams," by Clough, R.W., Chang, K.-T., Chen, H.-Q. and Ghanaat, Y., October 1985, (PB86 135027/AS)A05.

UCB/EERC-85/12 "Dynamic Response of Long Valley Dam in the Mammoth Lake Earthquake Series of May 25-27, 1980," by Lai, S. and Seed, H.B., November 1985, (PB86 142304/AS)A05.

UCB/EERC-85/13 "A Methodology for Computer-Aided Design of Earthquake-Resistant Steel Structures," by Austin, M.A., Pister, K.S. and Mahin, S.A., December 1985, (PB86 159480/AS)A10 .

UCB/EERC-85/14 "Response of Tension-Leg Platforms to Vertical Seismic Excitations," by Liou, G.-S., Penzien, J. and Yeung, R.W., December 1985, (PB87 124 871/AS)A08.

UCB/EERC-85/15 "Cyclic Loading Tests of Masonry Single Piers: Volume 4 - Additional Tests with Height to Width Ratio of 1," by Sveinsson, B., McNiven, H.D. and Sucuoglu, H., December 1985.

UCB/EERC-85/16 "An Experimental Program for Studying the Dynamic Response of a Steel Frame with a Variety of Infill Partitions," by Yanev, B. and McNiven, H.D., December 1985.

UCB/EERC-86/01 "A Study of Seismically Resistant Eccentrically Braced Steel Frame Systems," by Kasai, K. and Popov, E.P., January 1986, (PB87 124 178/AS)A14.

UCB/EERC-86/02 "Design Problems in Soil Liquefaction," by Seed, H.B., February 1986, (PB87 124 186/AS)A03.

UCB/EERC-86/03 "Implications of Recent Earthquakes and Research on Earthquake-Resistant Design and Construction of Buildings," by Bertero, V.V., March 1986, (PB87 124 194/AS)A05.

UCB/EERC-86/04 "The Use of Load Dependent Vectors for Dynamic and Earthquake Analyses," by Leger, P., Wilson, E.L. and Clough, R.W., March 1986, (PB87 124 202/AS)A12.

UCB/EERC-86/05 "Two Beam-To-Column Web Connections," by Tsai, K.-C. and Popov, E.P., April 1986, (PB87 124 301/AS)A04.

UCB/EERC-86/06 "Determination of Penetration Resistance for Coarse-Grained Soils using the Becker Hammer Drill," by Harder, L.F. and Seed, H.B., May 1986, (PB87 124 210/AS)A07.

UCB/EERC-86/07 "A Mathematical Model for Predicting the Nonlinear Response of Unreinforced Masonry Walls to In-Plane Earthquake Excitations," by Mengi, Y. and McNiven, H.D., May 1986, (PB87 124 780/AS)A06.

UCB/EERC-86/08 "The 19 September 1985 Mexico Earthquake: Building Behavior," by Bertero, V.V., July 1986.

UCB/EERC-86/09 "EACD-3D: A Computer Program for Three-Dimensional Earthquake Analysis of Concrete Dams," by Fok, K.-L., Hall, J.F. and Chopra, A.K., July 1986, (PB87 124 228/AS)A08.

UCB/EERC-86/10 "Earthquake Simulation Tests and Associated Studies of a 0.3-Scale Model of a Six-Story Concentrically Braced Steel Structure," by Uang, C.-M. and Bertero, V.V., December 1986, (PB87 163 564/AS)A17.

UCB/EERC-86/11 "Mechanical Characteristics of Base Isolation Bearings for a Bridge Deck Model Test," by Kelly, J.M., Buckle, I.G. and Koh, C.-G., 1987.

UCB/EERC-86/12 "Effects of Axial Load on Elastomeric Isolation Bearings," by Koh, C.-G. and Kelly, J.M., 1987.

UCB/EERC-87/01 "The FPS Earthquake Resisting System: Experimental Report," by Zayas, V.A., Low, S.S. and Mahin, S.A., June 1987.

UCB/EERC-87/02 "Earthquake Simulator Tests and Associated Studies of a 0.3-Scale Model of a Six-Story Eccentrically Braced Steel Structure," by Whittaker, A., Uang, C.-M. and Bertero, V.V., July 1987.

UCB/EERC-87/03 "A Displacement Control and Uplift Restraint Device for Base-Isolated Structures," by Kelly, J.M., Griffith, M.C. and Aiken, I.G., April 1987.

UCB/EERC-87/04 "Earthquake Simulator Testing of a Combined Sliding Bearing and Rubber Bearing Isolation System," by Kelly, J.M. and Chalhoub, M.S., 1987.

UCB/EERC-87/05 "Three-Dimensional Inelastic Analysis of Reinforced Concrete Frame-Wall Structures," by Moazzami, S. and Bertero, V.V., May 1987.

UCB/EERC-87/06 "Experiments on Eccentrically Braced Frames with Composite Floors," by Ricles, J. and Popov, E., June 1987.

UCB/EERC-87/07 "Dynamic Analysis of Seismically Resistant Eccentrically Braced Frames," by Ricles, J. and Popov, E., June 1987.

UCB/EERC-87/08 "Undrained Cyclic Triaxial Testing of Gravels-The Effect of Membrane Compliance," by Evans, M.D. and Seed, H.B., July 1987.

UCB/EERC-87/09 "Hybrid Solution Techniques for Generalized Pseudo-Dynamic Testing," by Thewalt, C. and Mahin, S.A., July 1987.

UCB/EERC-87/10 "Investigation of Ultimate Behavior of AISC Group 4 and 5 Heavy Steel Rolled-Section Splices with Full and Partial Penetration Butt Welds," by Bruneau, M. and Mahin, S.A., July 1987.

UCB/EERC-87/11 "Residual Strength of Sand from Dam Failures in the Chilean Earthquake of March 3, 1985," by De Alba, P., Seed, H.B., Retamal, E. and Seed, R.B., September 1987.

UCB/EERC-87/12 "Inelastic Seismic Response of Structures with Mass or Stiffness Eccentricities in Plan," by Bruneau, M. and Mahin, S.A., September 1987.

UCB/EERC-87/13 "CSTRUCT: An Interactive Computer Environment for the Design and Analysis of Earthquake Resistant Steel Structures," by Austin, M.A., Mahin, S.A. and Pister, K.S., September 1987.

UCB/EERC-87/14 "Experimental Study of Reinforced Concrete Columns Subjected to Multi-Axial Loading," by Low, S.S. and Moehle, J.P., September 1987.

UCB/EERC-87/15 "Relationships between Soil Conditions and Earthquake Ground Motions in Mexico City in the Earthquake of Sept. 19, 1985," by Seed, H.B., Romo, M.P., Sun, J., Jaime, A. and Lysmer, J., October 1987.

UCB/EERC-87/16 "Experimental Study of Seismic Response of R. C. Setback Buildings," by Shahrooz, B.M. and Moehle, J.P., October 1987.

UCB/EERC-87/17 "Three Dimensional Aspects of the Behavior of R. C. Structures Subjected to Earthquakes," by Pantazopoulou, S.J. and Moehle, J.P., October 1987.

UCB/EERC-87/18 "Design Procedures for R-FBI Bearings," by Mostaghel, N. and Kelly, J.M., November 1987.

UCB/EERC-87/19 "Analytical Models for Predicting the Lateral Response of R C Shear Walls: Evaluation of their Reliability," by Vulcano, A. and Bertero, V.V., November 1987.

UCB/EERC-87/20 "Earthquake Response of Torsionally-Coupled Buildings," by Hejal, R. and Chopra, A.K., December 1987.

UCB/EERC-87/21 "Dynamic Reservoir Interaction with Monticello Dam," by Clough, R.W., Ghanaat, Y. and Qiu, X-F., December 1987.